

# **SOLSTICE:** An Electronic Journal of Geography and Mathematics.

(Major articles are refereed; full electronic archives linked)

Congratulations to all *Solstice* contributors:

*Solstice* was a SemiFinalist (top 80 in the world out of over 1000 entries), Pirelli  
INTERNETional Award, 2001.

## **CURRENT ISSUE** **SOLSTICE, VOLUME XV, NUMBER 1;** **JUNE, 2004.**

Cover

**Front matter: Summer, 2004.**  
**Editorial Board, Advice to Authors, Mission Statement.**

Awards to Solstice Authors

**Articles (reviewed):**

**Sandra Lach Arlinghaus and William Charles Arlinghaus**  
**Spatial Synthesis Sampler.**  
**Geometric Visualization of Hexagonal Hierarchies: Animation**  
**and Virtual Reality**

**Klaus-Peter Beier**  
**One Optimization of an Earlier Model of Virtual Downtown**  
**Ann Arbor**

**Frank J. A. Witlox, Aloys W. J. Borgers, Harry J. P. Timmermans**  
**Modelling Locational Decision Making of Firms Using Multidimensional Fuzzy Decision Tables: An Illustration**

**Sandra L. Arlinghaus, Fred J. Beal, and Douglas S. Kelbaugh**  
**The View from the Top: Visualizing Downtown Ann Arbor in Three Dimensions**

**Marc Schlossberg**  
**Visualizing Accessibility II: Access to Food**

***Summer in the Northern Hemisphere is Winter in the Southern Hemisphere...***

**Peter A. Martin**  
**Energy Flow: Spatial and Temporal Patterns**

**Alma S. Lach**  
**Winter Windows: Ice Largo**

**Seung-Hoon Han**  
**Spatial Analysis of Subway Zones in Boston, Massachusetts**

**Andrew Walton**  
**A Golfer's Resource: Huron Hills Golf Course, Ann Arbor, Michigan**

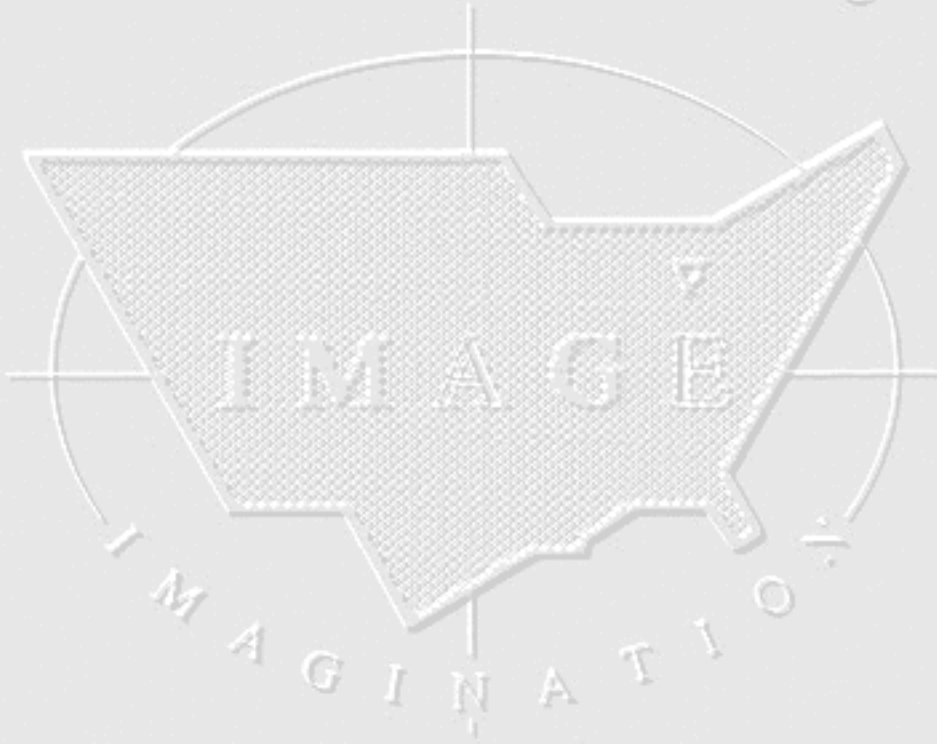
**Thana Chirapiwat ([link to his server, unreviewed material](#))**  
**Visualization of Geographic Information with VRML**

**Mail**

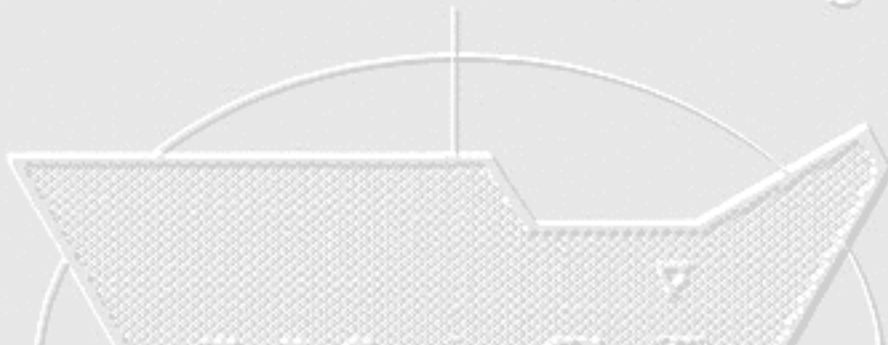
1964 Boulder Drive  
Ann Arbor, MI 48104

734.975.0246  
[image@imagenet.org](mailto:image@imagenet.org)

Institute of Mathematical Geography

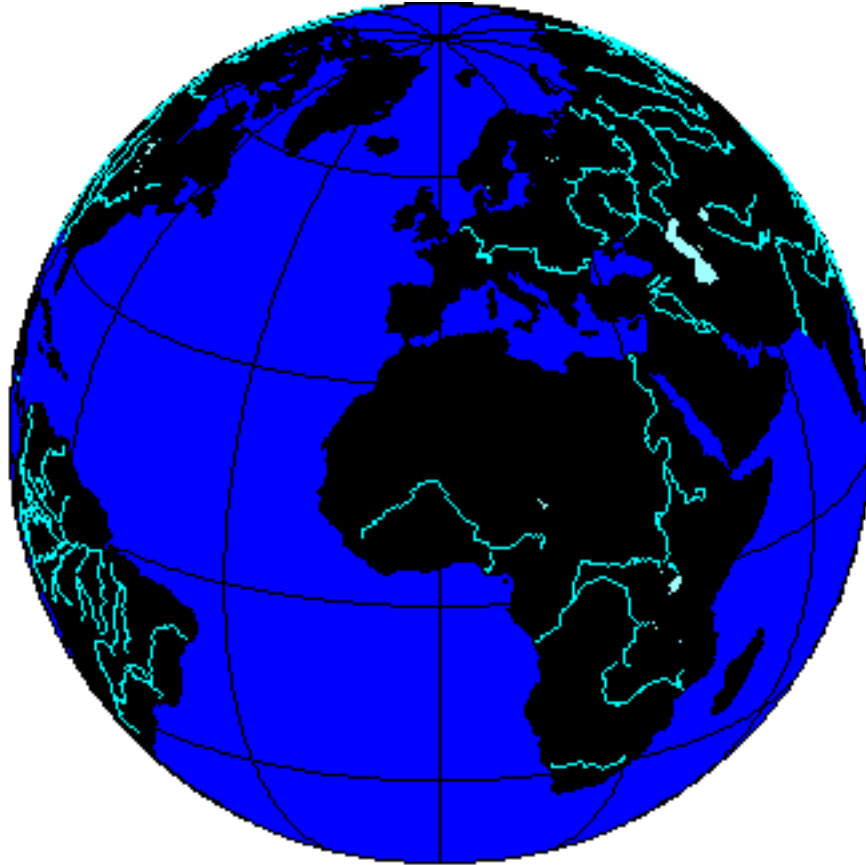


Institute of Mathematical Geography



# Solstice:

An Electronic Journal of Geography and Mathematics



Earth: with 23.5 degrees north latitude as the central parallel.

Volume XV  
Number 1  
June, 2004

Institute of Mathematical Geography (IMaGe)

**SOLSTICE: AN ELECTRONIC JOURNAL OF GEOGRAPHY AND MATHEMATICS**

<http://www.imagenet.org>

**SUMMER, 2004**

VOLUME XV, NUMBER 1

ANN ARBOR, MICHIGAN

---

**Founding Editor-in-Chief:**

Sandra Lach Arlinghaus, University of Michigan;  
Institute of Mathematical Geography (independent)

**Editorial Advisory Board:**

Geography.

Michael F. Goodchild, University of California, Santa Barbara  
Daniel A. Griffith, Syracuse University  
Jonathan D. Mayer, University of Washington (also School of Medicine)  
John D. Nystuen, University of Michigan

Mathematics.

William C. Arlinghaus, Lawrence Technological University  
Neal Brand, University of North Texas  
Kenneth H. Rosen, A. T. & T. Bell Laboratories

Engineering Applications.

William D. Drake, (deceased), University of Michigan

Education.

Frederick L. Goodman, University of Michigan

Business.

Robert F. Austin, Austin Communications Education Services.

**Book Review Editors:**

Richard Wallace, University of Michigan.  
Kameshwari Pothukuchi, Wayne State University

**Web Design:**

Sandra L. Arlinghaus  
(with early input from William E. Arlinghaus).

**Educational Technology:**

Marc Schlossberg, University of Oregon  
Ming-Hui Hsieh, Taiwan

**WebSite:** <http://www.imagenet.org>

**Electronic address:** [sarhaus@umich.edu](mailto:sarhaus@umich.edu)

## MISSION STATEMENT

The purpose of Solstice is to promote interaction between geography and mathematics. Articles in which elements of one discipline are used to shed light on the other are particularly sought. Also welcome are original contributions that are purely geographical or purely mathematical. These may be prefaced (by editor or author) with commentary suggesting directions that might lead toward the desired interactions. Individuals wishing to submit articles or other material should contact an editor, or send e-mail directly to sarhaus@umich.edu.

---

---

## SOLSTICE ARCHIVES

Back issues of Solstice are available on the WebSite of the Institute of Mathematical Geography, <http://www.imagenet.org> and at various sites that can be found by searching under "Solstice" on the World Wide Web. Thanks to Bruce Long (Arizona State University, Department of Mathematics) for taking an early initiative in archiving Solstice using GOPHER.

---

---

## PUBLICATION INFORMATION

The electronic files are issued yearly as copyrighted hardcopy in the Monograph Series of the Institute of Mathematical Geography. This material will appear in a Volume in that series, ISBN to be announced.

To cite the electronic copy, note the exact time of transmission from Ann Arbor, and cite all the transmission matter as facts of publication. Any copy that does not superimpose precisely upon the original as transmitted from Ann Arbor should be presumed to be an altered, bogus copy of *Solstice*. The oriental rug, with errors, serves as the model for creating this weaving of words and graphics.

---

---

## Awards and Recognition

(See [Press Clippings](#) page for other.)

---

- Sandra Lach Arlinghaus, recipient, The President's Volunteer Service Award, March 11, 2004.
  - [Jeffrey A. Nystuen](#), won the 2003 Medwin Prize in Acoustical Oceanography given by the [Acoustical Society of America](#). The citation was "for the innovative use of sound to measure rainfall rate and type at sea". It is awarded to a young/mid-career scientist whose work demonstrates the effective use of sound in the discovery and understanding of physical and biological parameters and processes in the sea.
  - [Sandra L. Arlinghaus](#), William C. Arlinghaus, and Frank Harary. *Graph Theory and Geography: an Interactive View (eBook)*, published by John [Wiley](#) and Sons, New York, April 2002. Finished as a Finalist in the 2002 Pirelli INTERNETional Award Competition (in the top 20 of over 1200 entries worldwide). [Link](#) to Pirelli website and to downloaded pages concerning this particular competition: [1](#), [2](#), [3](#).
  - *Solstice*, Semi-Finalist, Pirelli 2001 INTERNETional Award Competition in the Environmental Publishing category.
  - *Solstice*, article about it by Ivars Peterson in *Science News*, 25 January, 1992..
  - *Solstice*, article about it by Joe Palca, *Science* (AAAS), 29 November, 1991.
-

## Geometric Visualization of Hexagonal Hierarchies: Animation and Virtual Reality\*

---

**Requires browser plug-ins for viewing virtual reality (.wrl files) and for hearing sound (.midi files)**

---

**Sandra Lach Arlinghaus**

The University of Michigan, Ann Arbor, Michigan

**William C. Arlinghaus**

Lawrence Technological University, Southfield, Michigan

---

### Hexagonal Hierarchies and Close Packing of the Plane: Overview

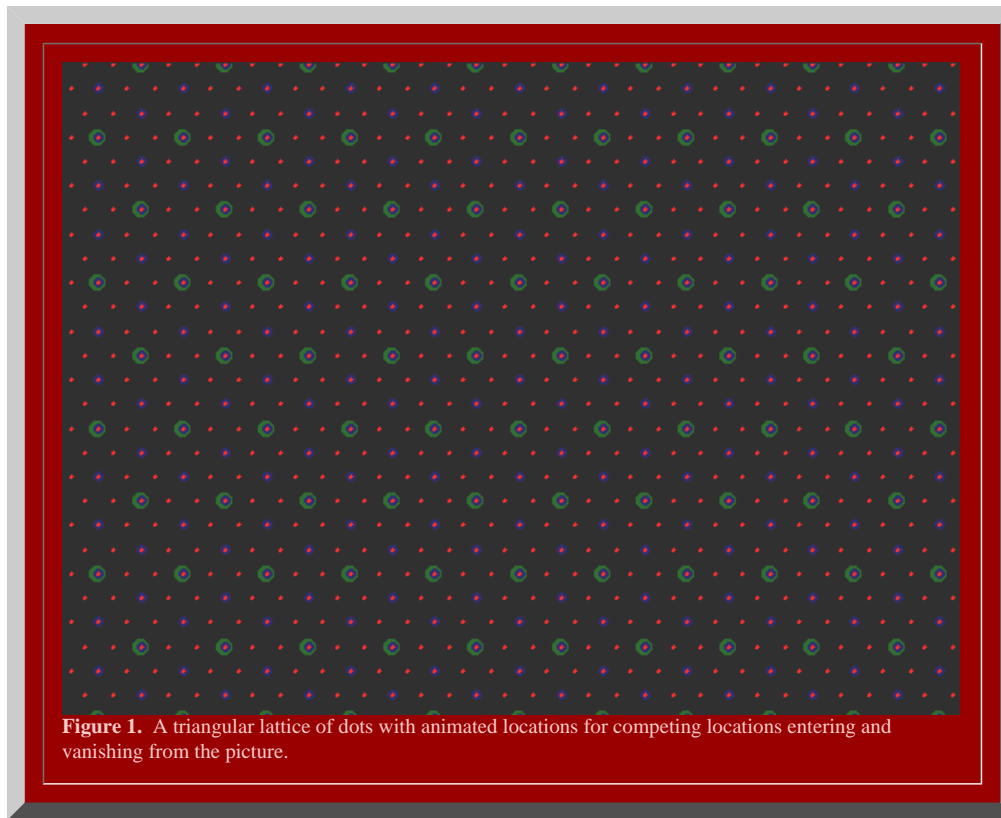
A scatter of points, spread evenly across the plane, may take on a variety of configurations: two simple regular lattices involve points that suggest squares or equilateral triangles. If one wishes to consider circular buffers around each point, then these buffers may overlap or be widely spaced. A natural issue to consider is to provide some sort of maximal coverage of the plane by the buffers: to provide a "close packing" of the plane by circles. Gauss (1831/40) proved that the densest lattice packing of the plane is the one based on the triangular lattice. In 1968 (and earlier), Fejes-Toth proved that that same packing is not only the densest lattice packing of the plane but is also the densest of all possible plane packings. If one thinks, then, of the circles as if they were bubble foam, the circles centered on a square grid pattern expand and collide to form a grid of squares (Boys). The circles centered on a triangular grid pattern expand and collide to form a mesh of regular hexagons, like the cells in a slice of the honeycomb of bees (de Vries). The theoretical issues surrounding tiling in the plane are complex; even deeper are those issues involving packings in three dimensional space. The reader interested in probing this topic further is referred to the Bibliography at the end of this document. Interpretation of the simple triangular grid has range sufficient to fill this document and far more.

### Classical Urban Hexagonal Hierarchies

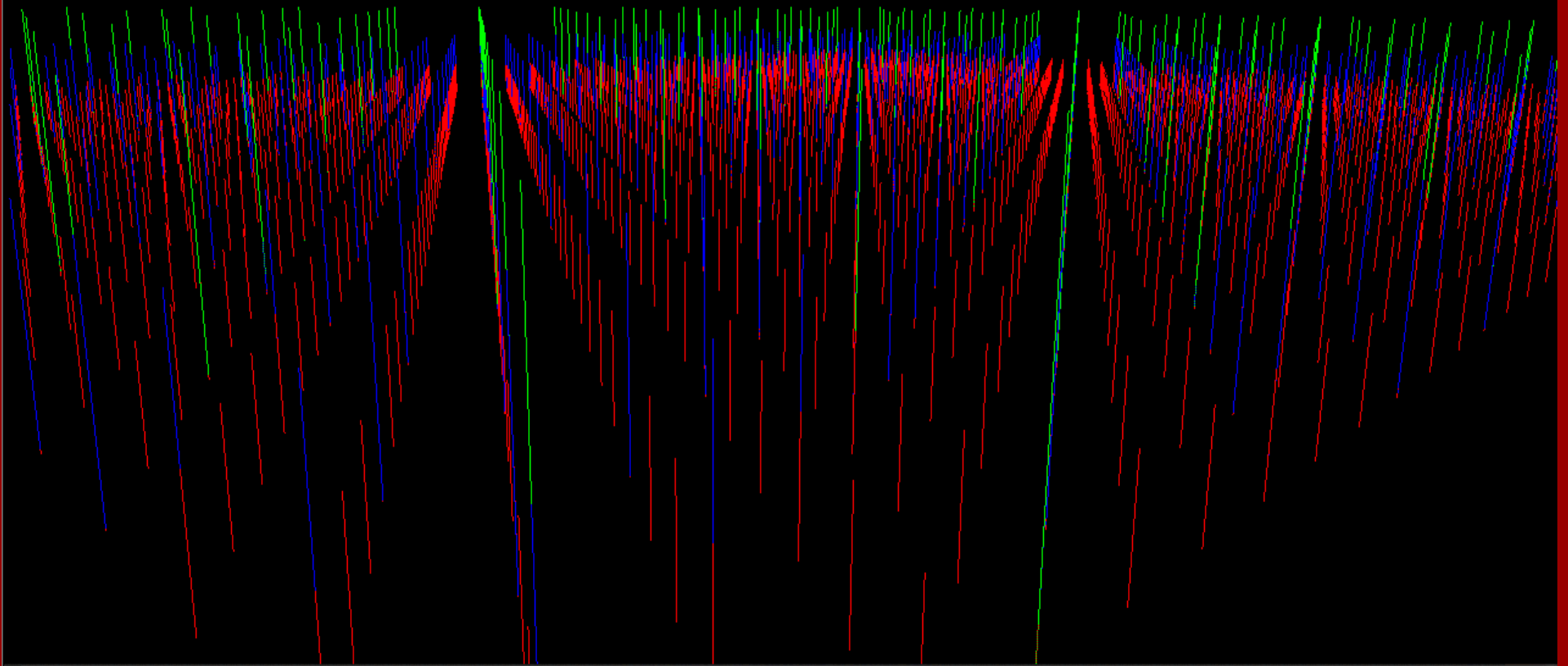
One classical interpretation of what dots on a lattice might represent is found in the geometry of "central place theory" (Christaller, Lösch). This idea takes the complex human process of urbanization and attempts to look at it in an abstract theoretical form in order to uncover any principles which might endure despite changes over time, situation, cultural tradition, and all the various human elements that are truly the hallmarks of urbanization. Simplicity helps to reveal form: models are not precise representations of reality. They do, however, offer a way to look at some structural elements of complexity. Thus, dots on a triangular lattice are populated places (often, villages). Circles, expanding into hexagons, are areas that are tributary to the populated places. In the traditional formulation (described after Kolars and Nystuen) one considers four basic postulates (no one of which is "real" but each of which is simple):

- The backdrop of land supports uniform population density
- There is a maximum distance that residents can easily penetrate into the tributary area.
- There is slow, steady population growth
- Village residents who move, as a result of growth (or for other reasons), attempt to remain in close contact with their previous location (to maintain social or other networks).

Suppose, in a triangular lattice of villages, that one village adds to its retailing activities. After some time, growth occurs elsewhere. How might other villages compete to serve tributary areas: how will the larger, new villages share the tributary area? The answers lead to a surprising number of possible scenarios. Figure 1 shows the first in an infinite number of possibilities. Animated locations, for competing larger villages, are shown in Figure 1. The smallest villages are represented as small red dots; next nearest neighbors competing for intervening red dots are represented in blue; and, next nearest neighbors competing for intervening blue dots are represented in green. Of course, one is usually only willing to travel so far to go to a place only slightly larger, so the fact that the animated pattern could be extended to an infinite number of levels, beyond green, may not mirror the second postulate. Over time, however, one might suppose further growth and an entire hierarchy of populated places.



Virtual reality is an exciting form of visualizing three dimensional objects. Figure VR01 has a link on to a virtual reality view of that figure: click on that figure to move into the virtual environment. Imagine the dots are holes in a pasta machine through which the pasta dough is to be extruded as spaghetti: the view in Figure 1 is the template and the linked virtual reality is the extruded pasta pulled through the red, blue, and green holes. Drive through this landscape; think of the view as a skyline of cell towers or some other tall thin structures (Arlinghaus, 1993). The placement of these towers is at vertices of equilateral triangles of various sizes forming an hexagonal hierarchy.



Default view

**Figure VR01.** A screen shot from the virtual world linked to this image. Click on the image to enter that world!

The pattern in Figure 1 suggests one arrangement for villages, towns, and cities. We offer systematic visualization schemes for a variety of such arrangements: first, following the classical approaches to this issue found in the works of Walter Christaller and August Lösch and, second, following the contemporary approach presented in previous conventional publications by the authors of this submission.

### CLASSICAL GEOMETRIC APPROACH TO HEXAGONAL HIERARCHIES

### Visualization of Hexagonal Hierarchies using Animated Geometric Figures

Marketing principle:  $K=3$

Consider a central place point,  $A$ , in a triangular lattice. Unit hexagons (fundamental cells) surround each of the points in the lattice and represent the small tributary area of each village (Figure 2). Growth at  $A$  has distinguished it from other villages in the system. It will now serve a tributary area larger than will the unit hexagon. There are six villages directly adjacent to  $A$ . The unit hexagons represent a partition of area based on even sharing of area between  $A$  and these six villages. When  $A$  expands its central place activities, others may also desire to do so as well. Figure 2 shows the locations for the next nearest competitors to enter the system. Given that they, too, will share area evenly, a set of larger hexagons emerges. Figure 3a shows the unit hexagons and the larger hexagons based on expansion of goods

and services. The competitors that enter are spaced at a distance, in terms of lattice points spaced one unit apart, of  $\sqrt{3}$  units (Figure 2). The position of the competitors that enter the system in this scenario are as close as possible to  $A$ ; expansion of goods and services at any of the six closest neighbors would constitute no change in basic pattern. One might imagine, therefore, that emphasis on distance minimization optimizes marketing capability--distance to market is at a minimum.

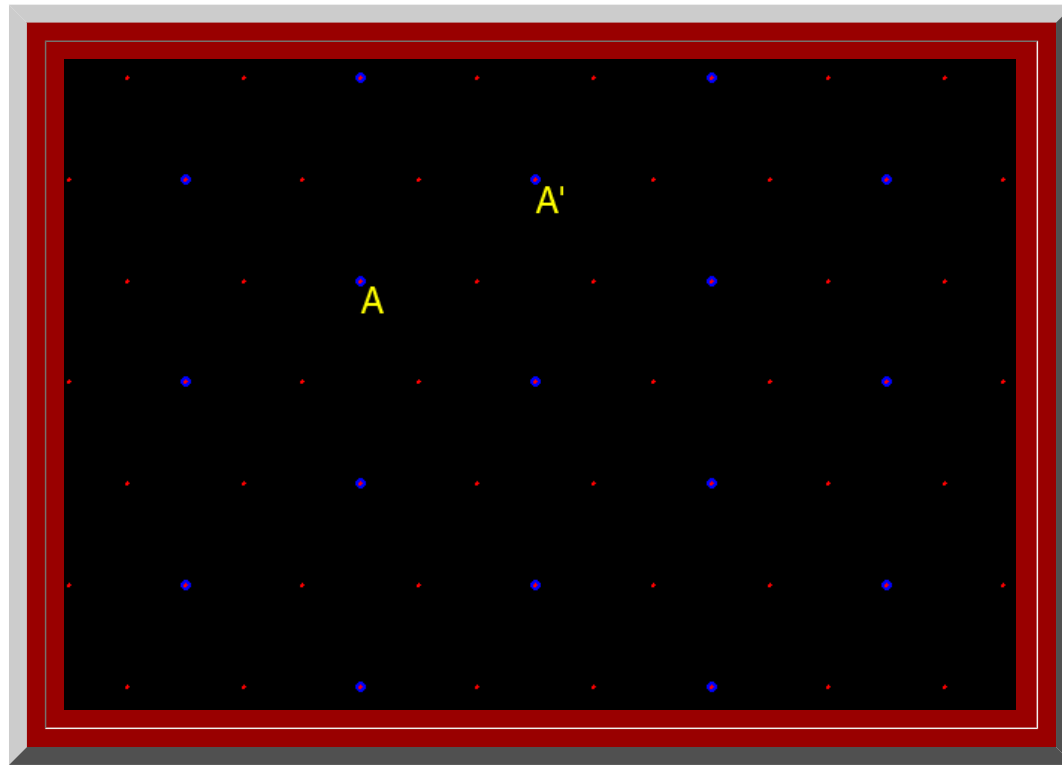


**Figure 2.**  $K=3$ : Marketing. Distance measurement between adjacent competing new centers,  $A$  and  $A'$ : in this case, competing centers, blue dots, are spaced  $\sqrt{3}$  units apart, assuming a distance of one unit between adjacent red dots.

Thus, when competitors are chosen in this manner, the pattern of one layer of hexagons, in relation to another, has become known as a hierarchy arranged according to a "marketing principle" (Figure 3a). Notationally, it is captured by the square of the distance between competing centers: as a " $K=3$ " hierarchy (Figure 2). Each large hexagon contains the equivalent of three smaller hexagons. One large hexagon = 1 small hexagon + six copies of  $1/3$  of a small hexagon = 3 small hexagons (Figure 3b, c, and d). Thus, the value  $K=3$  is not only related to distance between competing centers but also to size of tributary areas generated by competition: as a constant of the hierarchy.

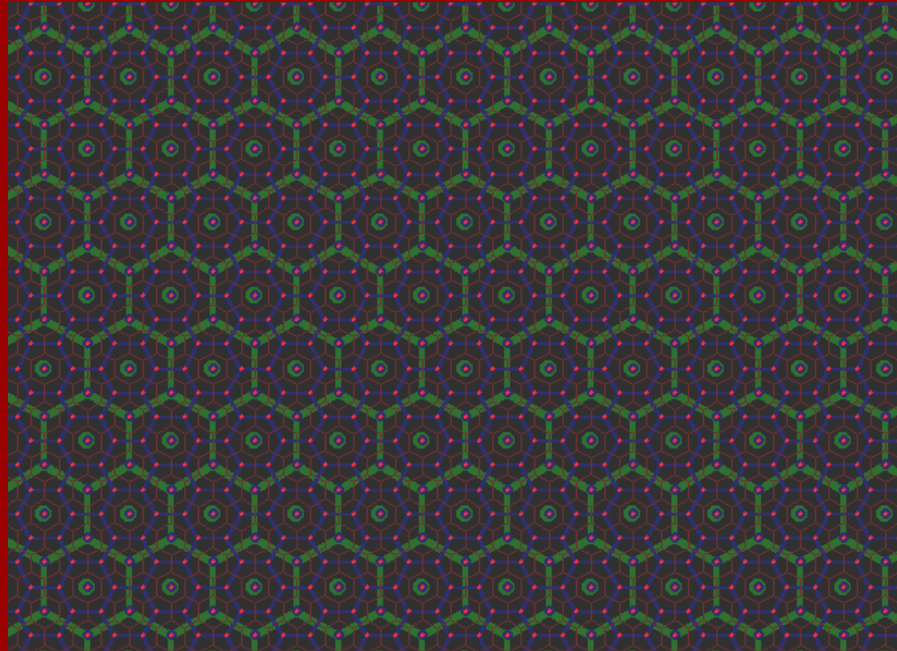


**Figure 3a.**  $K=3$  hierarchy showing three layers of a nested hierarchy of hexagons of various sizes oriented with respect to one another according to the distance principle illustrated in Figure 2.

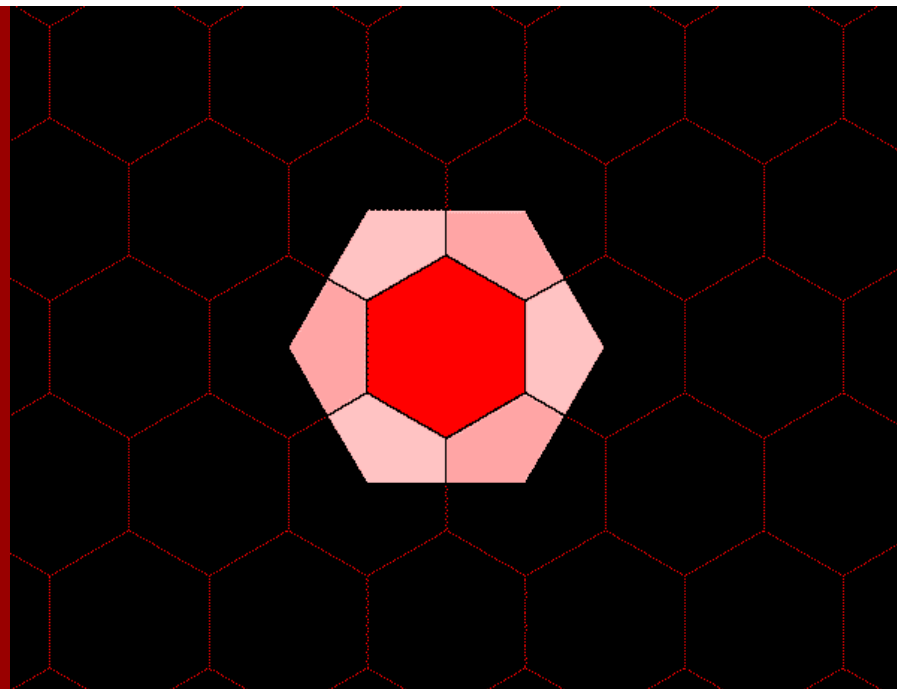


**Figure 3b.** Each blue hexagon contains the equivalent of three red hexagons: one entire red hexagon surrounded by six copies of  $1/3$  of a red hexagon.

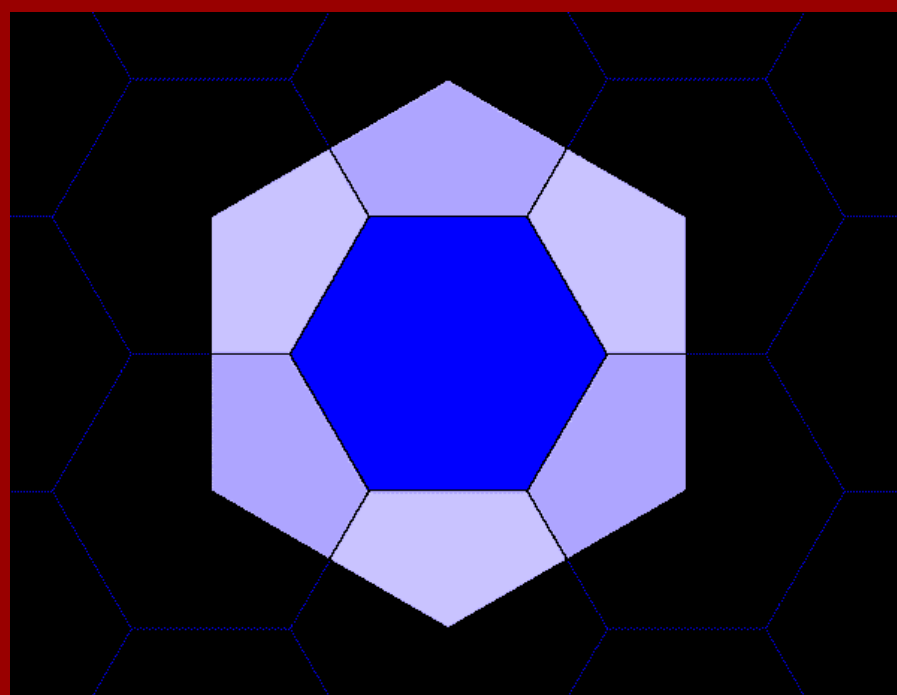


**Figure 3c.** Each green hexagon contains the equivalent of three blue hexagons: one entire blue hexagon surrounded by six copies of  $1/3$  of a blue hexagon.

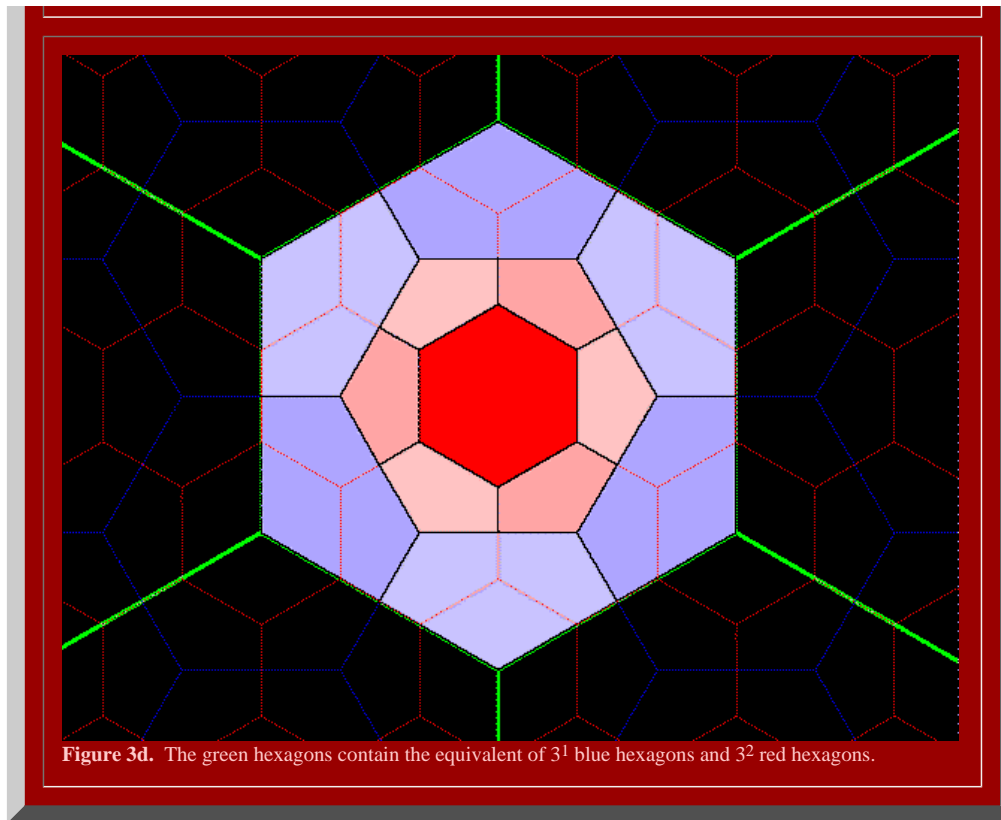


**Figure 3d.** The green hexagons contain the equivalent of  $3^1$  blue hexagons and  $3^2$  red hexagons.

[Back to fractal  \$K=3\$](#)

*Transportation principle:  $K=4$*

Figure 4 shows the locations for the next nearest competitors, next beyond those from  $K=3$ , to enter the system. Given that they, too, will share area evenly, a set of even larger hexagons emerges. Figure 5a shows the unit hexagons and the larger hexagons based on expansion of goods and services. The competitors that enter are spaced at a distance, in terms of lattice points spaced one unit apart, of 2 units (Figure 4). The position of the competitors that enter the system in this scenario lie along radials that fan outward from  $A$  and pass along existing boundaries to tributary areas. One might imagine, therefore, that emphasis on market penetration, or transportation, is the focus here.



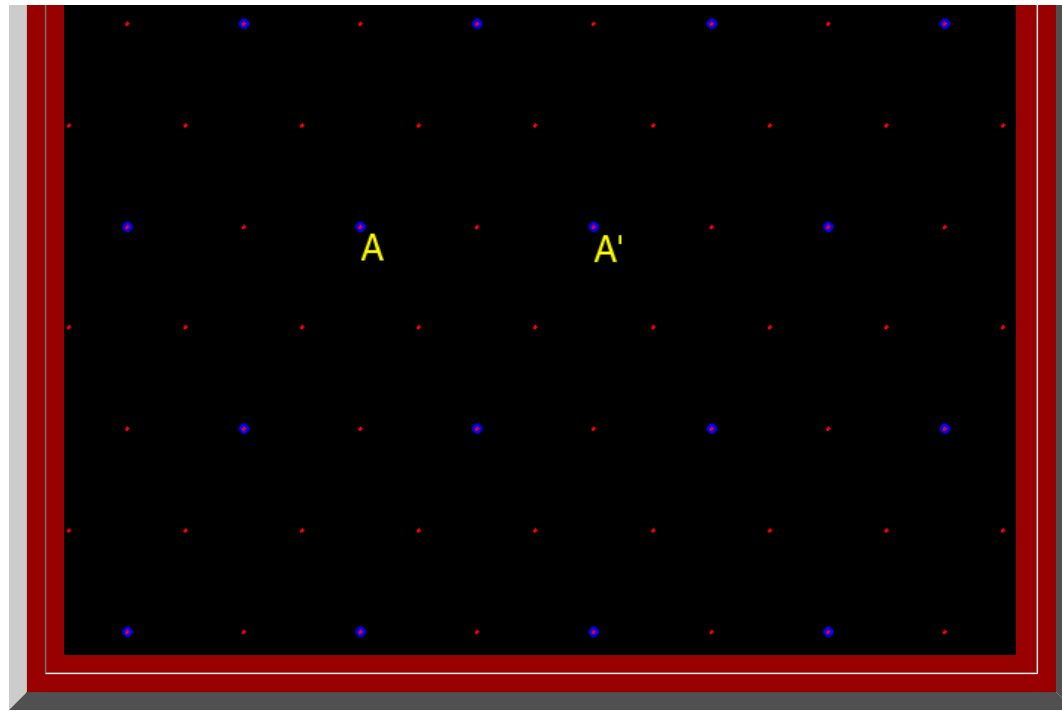


**Figure 4.**  $K=4$ : Transportation. Distance measurement between adjacent competing new centers,  $A$  and  $A'$  is 2 units, in this case (assuming a distance of 1 unit between adjacent red dots).

Thus, when competitors are chosen in this manner, the pattern of one layer of hexagons, in relation to another, has become known as a hierarchy arranged according to a "transportation principle" (Figure 5a). Notationally, it is captured by the square of the distance between competing centers: as a " $K=4$ " hierarchy (Figure 4). Each large hexagon contains the equivalent of four smaller hexagons. One large hexagon = 1 small hexagon + six copies of  $1/2$  of a small hexagon = 4 small hexagons (Figure 5b, c, d). Thus, the value  $K=4$  is not only related to distance between competing centers but also to size of tributary areas generated by competition--as a constant of the hierarchy.



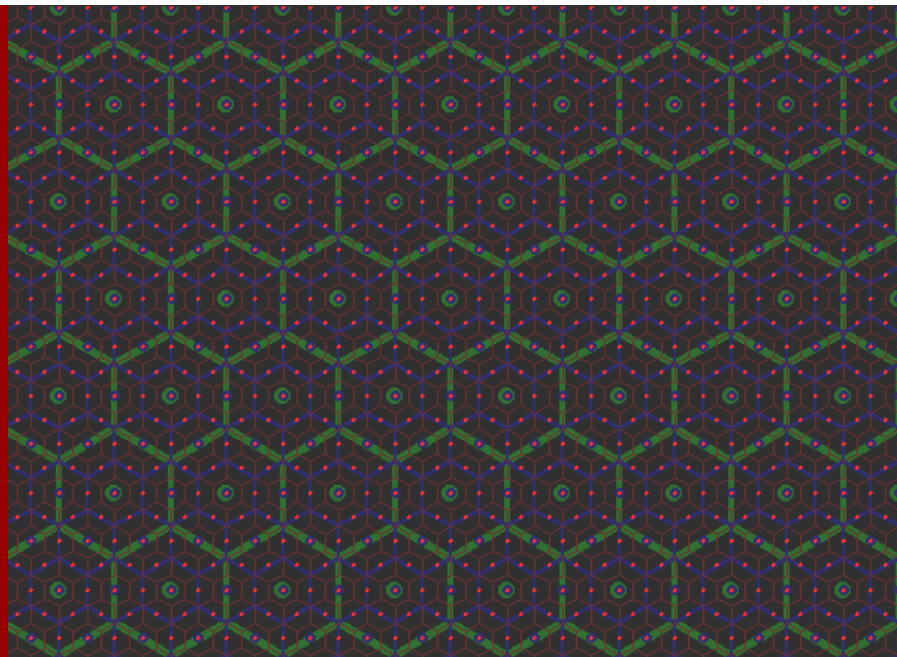


**Figure 5a.**  $K=4$  hierarchy showing three layers of a nested hierarchy of hexagons of various sizes oriented with respect to one another according to the distance principle illustrated in Figure 4.

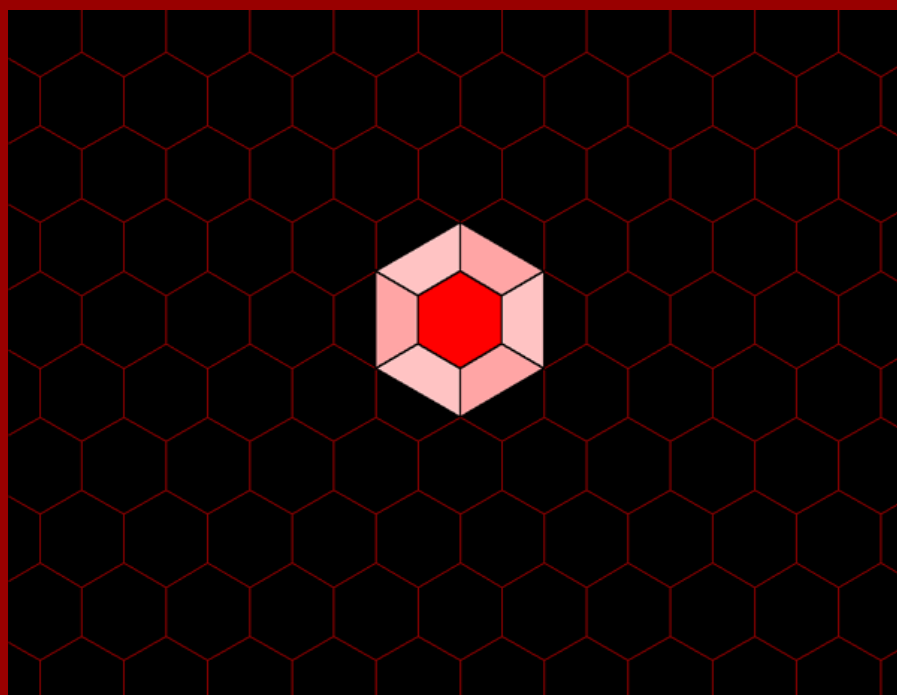


**Figure 5b.** Each blue hexagon contains the equivalent of four red hexagons: one entire red hexagon surrounded by six copies of  $1/2$  of a red hexagon.

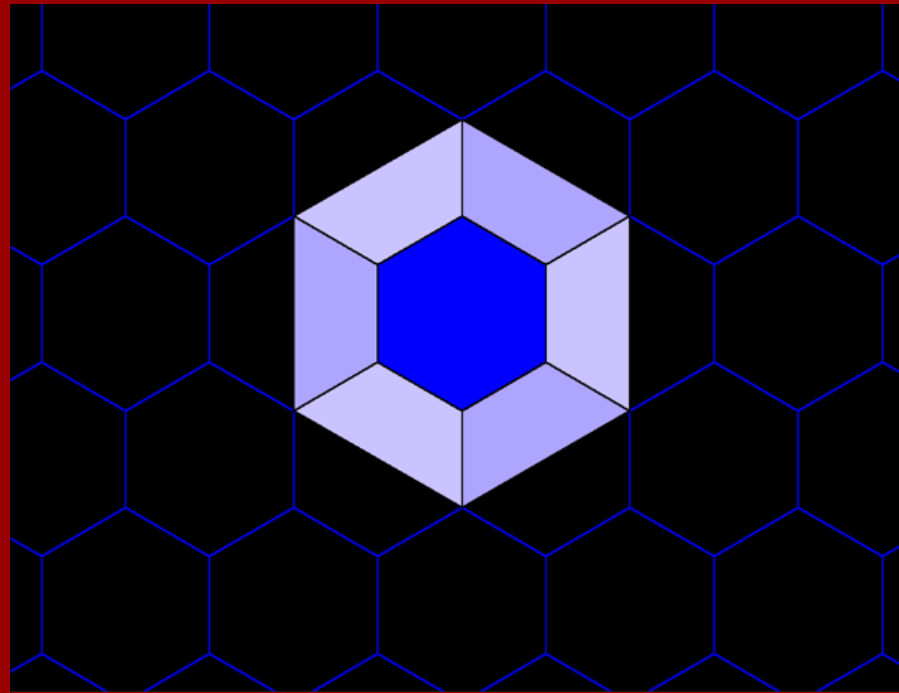


**Figure 5c.** Each green hexagon contains the equivalent of four blue hexagons: one entire blue hexagon surrounded by six copies of 1/2 of a blue hexagon.

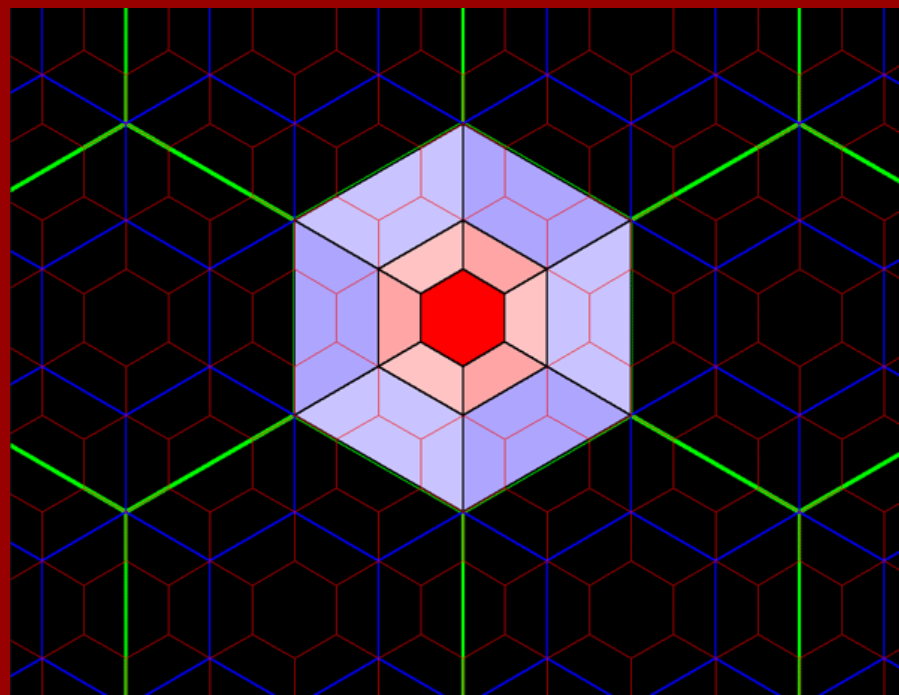


**Figure 5d.** The green hexagons contain the equivalent of  $4^1$  blue hexagons and  $4^2$  red hexagons.

[Back to fractal  \$K=4\$ .](#)

*Administrative principle:  $K=7$*

Figure 6 shows the locations for the next nearest competitors, next beyond those from  $K=4$ , to enter the system. Given that they, too, will share area evenly, a set of even larger hexagons emerges. Figure 7a shows the unit hexagons and the larger hexagons based on expansion of goods and services. The competitors that enter are spaced at a distance, in terms

of lattice points spaced one unit apart, of  $\sqrt{7}$  units (Figure 6). The position of the competitors that enter in this scenario create larger hexagons whose boundaries pass through very few other populated places: hence, top-down control, or rule from the center is emphasized. One might imagine, therefore, an emphasis on administrative control here.

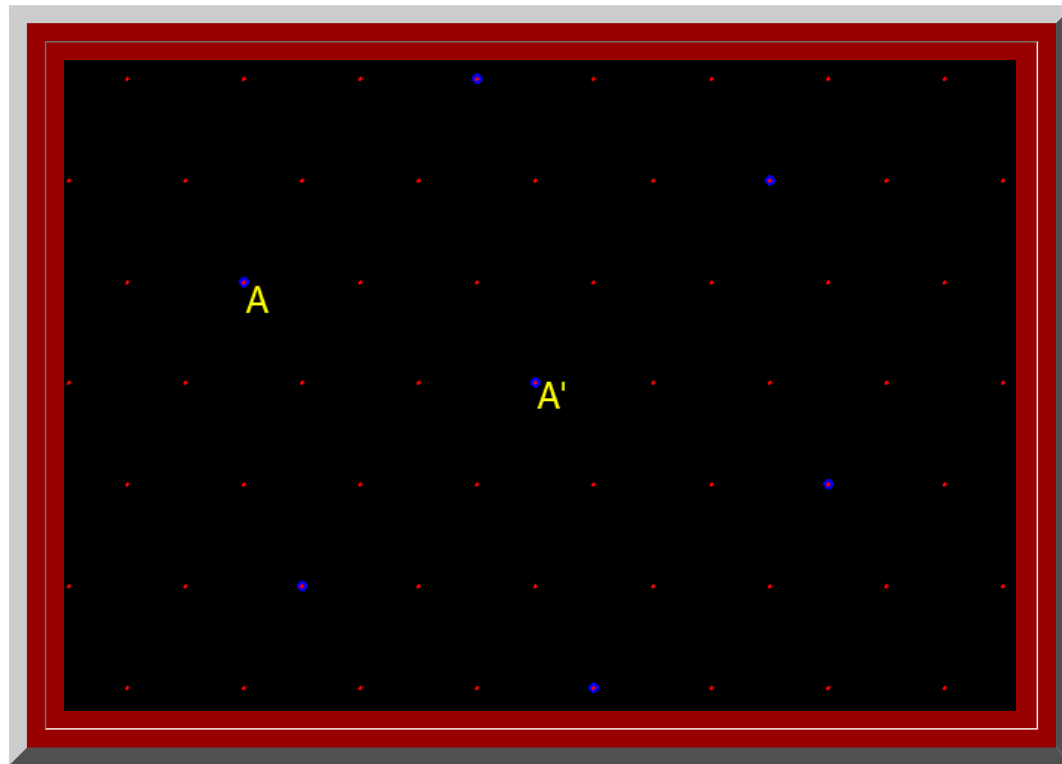


**Figure 6.**  $K=7$ : Administrative. Distance measurement between adjacent competing new centers, A and A' is  $\sqrt{7}$  (assuming a distance of 1 unit between adjacent red dots).

Thus, when competitors are chosen in this manner, the pattern of one layer of hexagons, in relation to another, has become known as a hierarchy arranged according to an "administration principle" (Figure 7a). Notationally, it is captured by the square of the distance between competing centers: as a " $K=7$ " hierarchy (Figure 6). Each large hexagon contains the equivalent of seven smaller hexagons. One large hexagon = 1 small hexagon + six copies of a small hexagon (underfit and overfit regions balance) = 7 small hexagons (Figure 7b, c, d). Thus, the value  $K=7$  is not only related to distance between competing centers but also to size of tributary areas generated by competition—as a constant of the hierarchy.

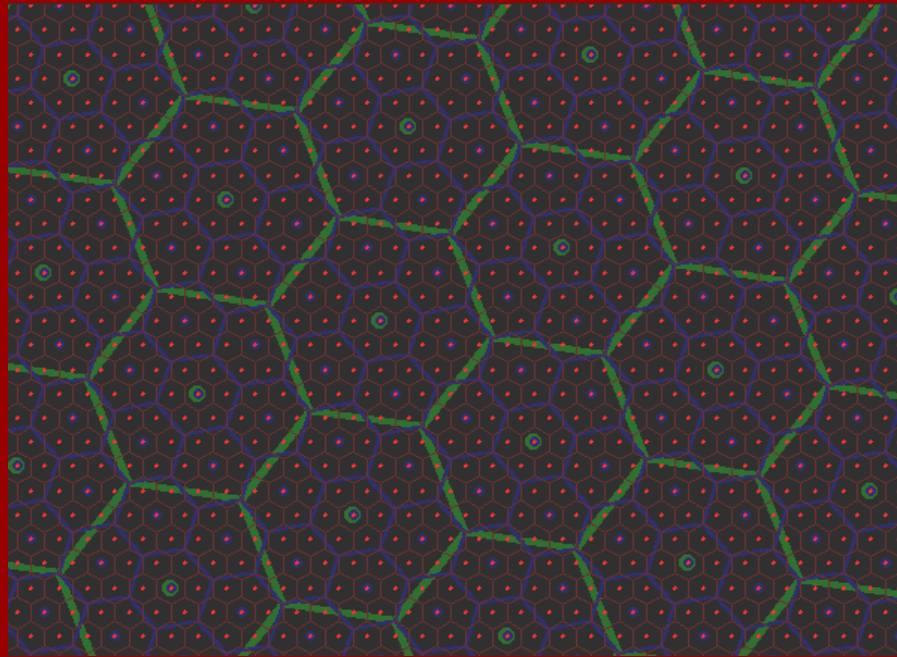


**Figure 7a.**  $K=7$  hierarchy showing three layers of a nested hierarchy of hexagons of various sizes oriented with respect to one another according to the distance principle illustrated in Figure 6.

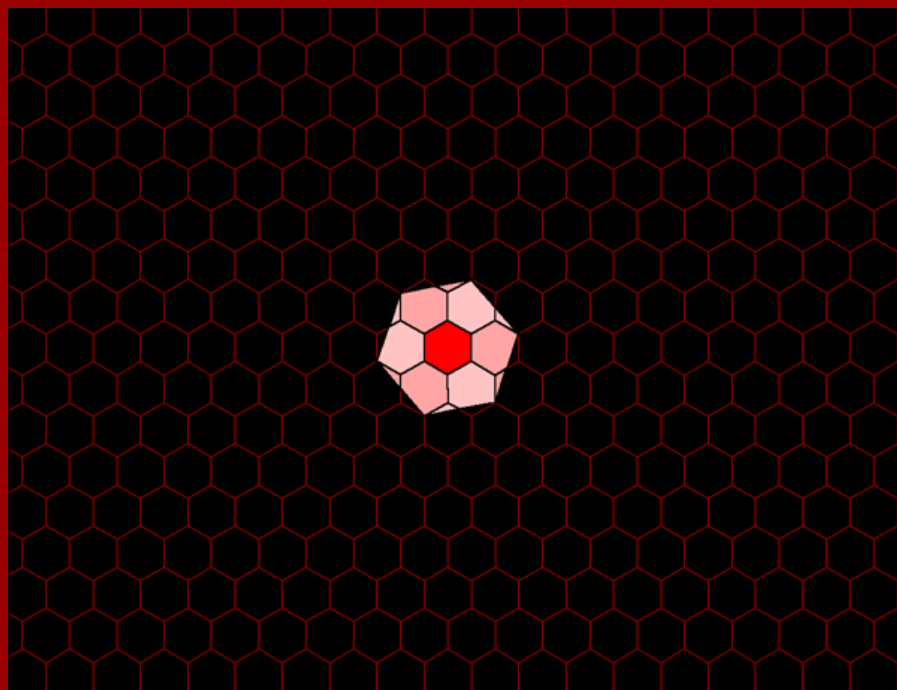


**Figure 7b.** Each blue hexagon contains the equivalent of seven red hexagons: one entire red hexagon

surrounded by six copies equivalent to a single red hexagon. Each of the perimeter red hexagons is composed of  $11/12$  of a single red hexagonal cell plus  $1/12$  of an adjacent red cell: in an underfit/overfit pattern.

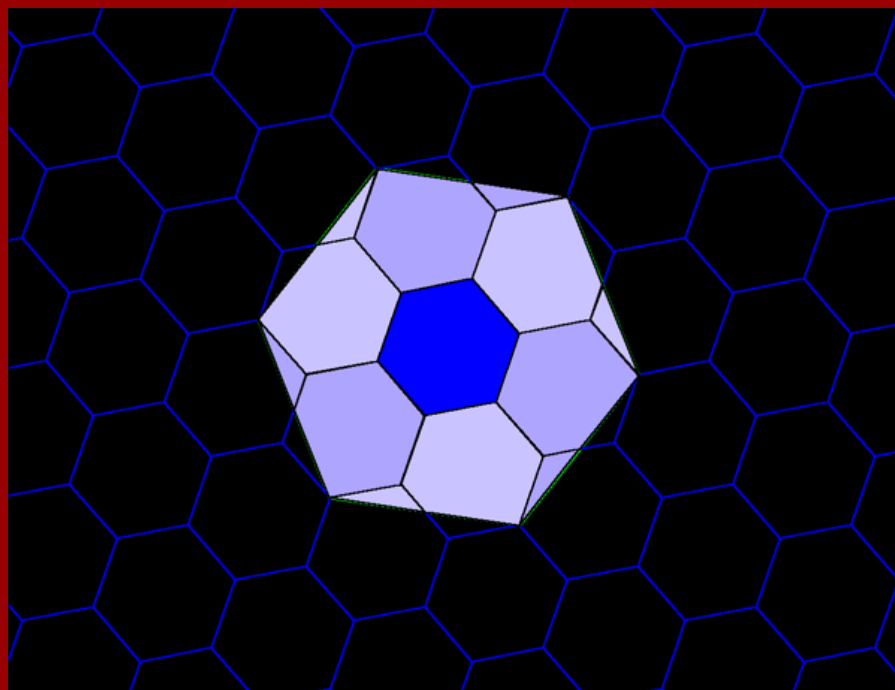
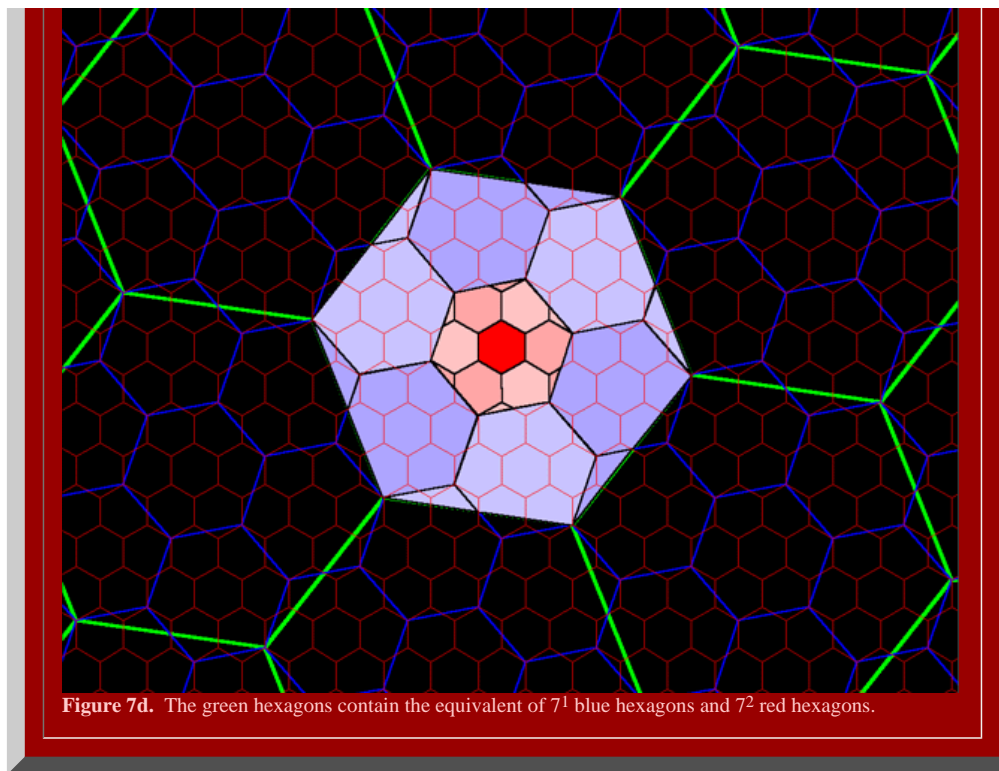


**Figure 7c.** Each green hexagon contains the equivalent of seven blue hexagons: one entire blue hexagon surrounded by six copies equivalent to a single blue hexagon. Each of the perimeter blue hexagons is composed of  $11/12$  of a single blue hexagonal cell plus  $1/12$  of an adjacent blue cell: in an underfit/overfit pattern.



[Back to fractal  \$K=7\$ .](#)

One difficulty in constructing these geometric visualizations is that slight errors in placement of points get magnified in overlay alignments. To create a meshed hierarchy in which overlays are aligned is a drafting task of substantial proportions, when done by hand. Geographic Information System software, however, offers an easy and accurate method of constructing central place landscapes at almost any level of complexity (up to the limits of hardware and software capability). Figures 2-7 were created using ArcView GIS (v. 3.2, ESRI). The method for creating GIS-generated central place landscapes employed the following steps:

- obtain as a base map a triangular lattice shape file; such a file may be created in ArcView using EdTools extension to precisely translate a point.
- ensure that each record in the underlying database has a unique code entered in "number" format (using the "add record number" feature of Animal Movement extension, if need be).
- if desired, create in a separate layer, a bounded region to serve as limits within which to calculate the landscape--a rectangle, for example. One way to create such a region is to calculate the minimum convex polygon (convex hull) of the distribution of red dots using Home Range extension.
- load Spatial Analyst extension (ESRI) to ArcView and calculate Thiessen polygons using the Analysis|Assign Proximity command; choose the rectangle layer as the region within which to calculate the Thiessen polygons. Alternately, employ the same strategy using Home Range extension and calculate Dirichlet regions.
- The result will appear as a set of small hexagons surrounding the dots, as in the red layers in Figures 2-7.
- Repeat the procedure on other triangular lattices, with broader spacing of lattice points as in the blue and green points above, derived from the base lattice. The result will produce landscapes such as those in Figures 2-7 depending on how the broader spacing pattern is selected.

The process of creating larger hexagons, as larger tributary areas representing expanded central place activities, can be carried out indefinitely. The set of figures above (3, 5, and 7) shows the general patterns that emerge and underscores, particularly, the importance of the constant of the hierarchy. Large hexagons in one layer contain the equivalent of  $K^1$  hexagons of the next smallest size within them; they contain the equivalent of  $K^2$  hexagons from the level two layers down in the hierarchy, and so forth. The  $K$  value is an invariant of each geometric hierarchy that uniquely characterizes it. The mathematical search for invariants as bench marks against which to view abstract structure is equivalent to the geographical search for bench marks in the field (physical or human) against which to view mapped,

spatial structure.

### Visualization of Hexagonal Hierarchies using Mapplets

Another method of visualizing hexagonal hierarchies, that is available only in current technology, looks simultaneously at connection patterns between multiple hierarchical layers of urban location maps and captures them as Java (TM) Applets: as "Mapplets." This process suggests a measure of visual stability of the geometric connectivity pattern that is related to the dimensions of the bounding box. Figures 8, 9, and 10 show Mapplets for the  $K=3$ ,  $K=4$ , and  $K=7$  hierarchies, respectively.



Figure 8.  $K=3$  Mapplet



Figure 9.  $K=4$  Mapplet



Figure 10.  $K=7$  Mapplet

Mapplets focus on connection patterns between successive hierarchical layers and, when  $K$  values are loaded as distances between hierarchies, they also suggest some elusive form of structural stability of geometric form. Animated maps of the central place geometry of the plane, coupled with mapplets showing animated hierarchical pattern alone, suggest a three dimensional view of central place geometry. A broader 3D view is suggested in the next section.

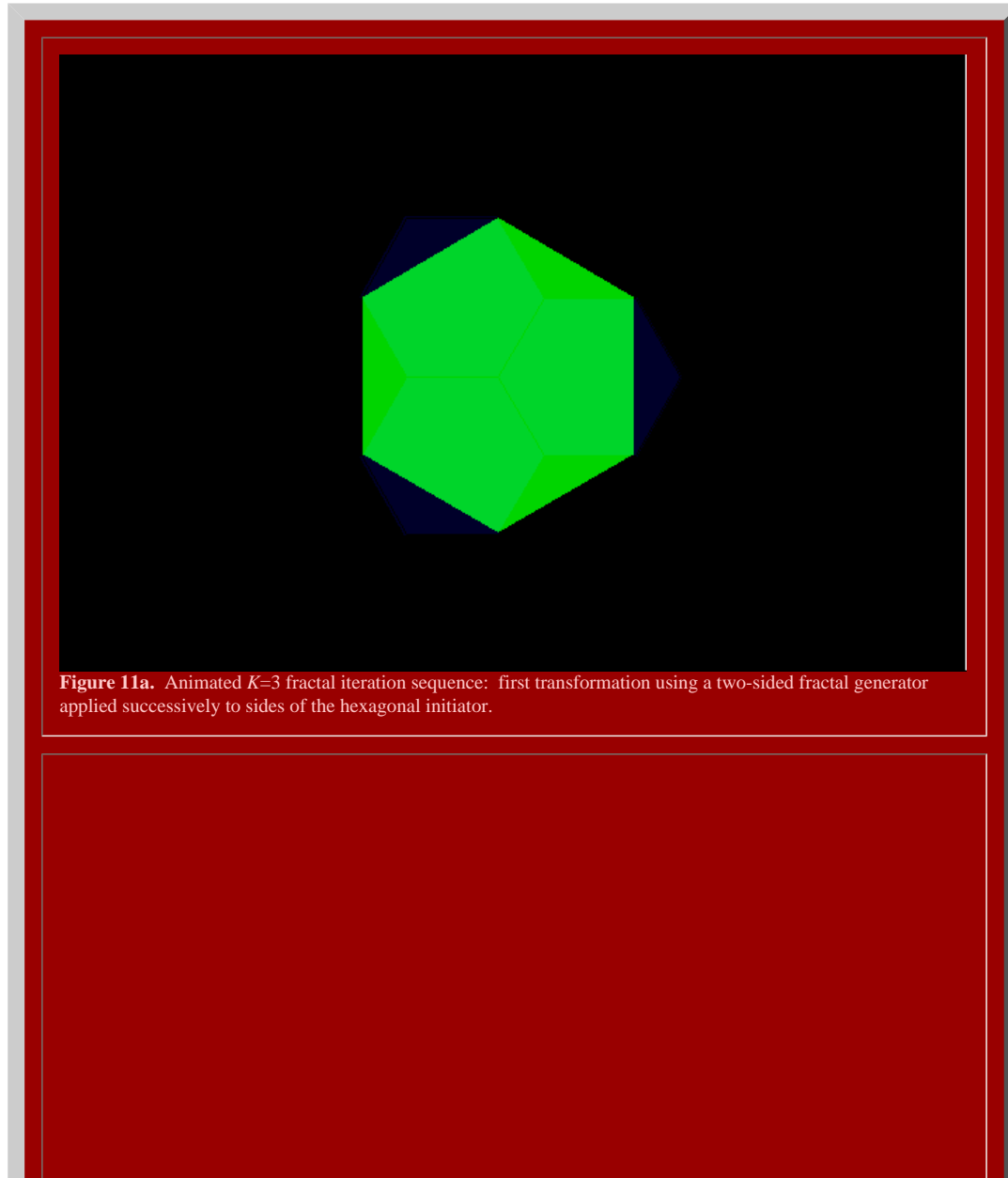
## CONTEMPORARY GEOMETRIC APPROACH TO HEXAGONAL HIERARCHIES

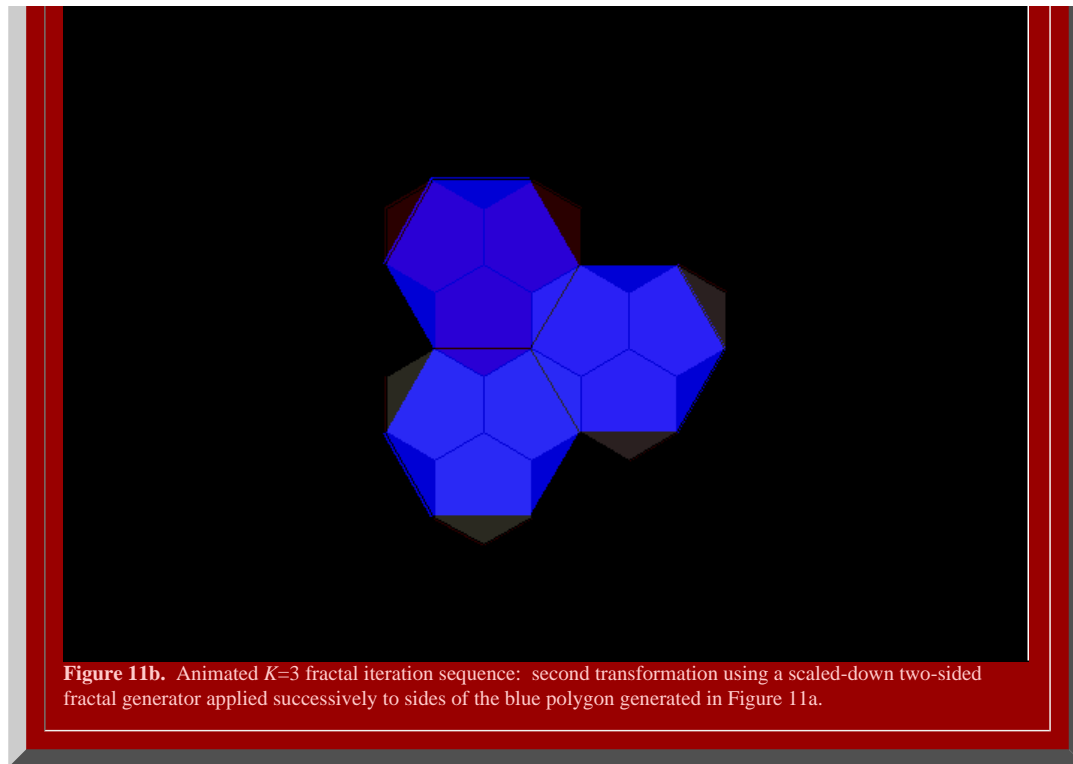
### Visualization of Hexagonal Hierarchies using Animated Geometric Figures and Virtual Reality

In the material below, we illustrate the use of the fractal concept of self-similarity to generate hexagonal hierarchies equivalent to those above. We use a hexagon as an initiator, and apply to it different selections of generators, to produce the different hexagonal hierarchies of classical central place theory (based on original concept and work of S. Arlinghaus). In the previous sections we formed central place hexagonal hierarchies by moving from small hexagons to large ones; here, we reverse the process and dissect, using the self-similarity transformation, a large hexagon to create the smaller ones. In both processes, the results correspond exactly. The art is in generator selection, and it is simply that art that is presented in this chapter. Later work delves into the mathematical foundations of that art.

#### *The $K=3$ Hierarchy*

When an hexagonal initiator is chosen and a two-sided generator, with included angle of 120 degrees, is used to make successive replacement of the sides of the hexagon (as in the animated Figure 11a), the outline of the next layer of the  $K=3$  central place hierarchy is generated (the black lines in Figure 11a suggest interior connections). The replacement sequence applies the generator in an alternating pattern to the outside and then to the inside of the initiator. When the original generator is scaled down, with shape preserved, and applied in the outside/inside sequence to the newly formed blue polygon, the next lower level central place  $K=3$  hierarchy is formed (as in the animated Figure 11b). The second, blue polygon contains three scaled-down hexagons, self-similar to the first hexagon (Figure 11a); the red polygon in the animation sequence contains three shapes self-similar to the blue polygon (Figure 11b), and 27 (or 3 cubed) hexagons self-similar to the original hexagon (Figure 11b). The invariant of 3, in the  $K=3$  hierarchy, is replicated in this particular fractal iteration sequence.





It remains to determine if the polygons generated in Figure 11 will in fact fit together to form the broad central place landscape of arbitrary size suggested in [Figure 3](#). To that end, we stack the layers generated above using the fractal iteration sequence to form a tile of layers centered on the single polygonal initiator (Figure 12). Click [here](#), or on the screen shot in Figure VR02 below, to see a virtual solid model of the tile with which the reader can interact. Click [here](#), or on the screen shot in Figure VR03 below, to see a virtual translucent model of the tile with which the reader can interact.

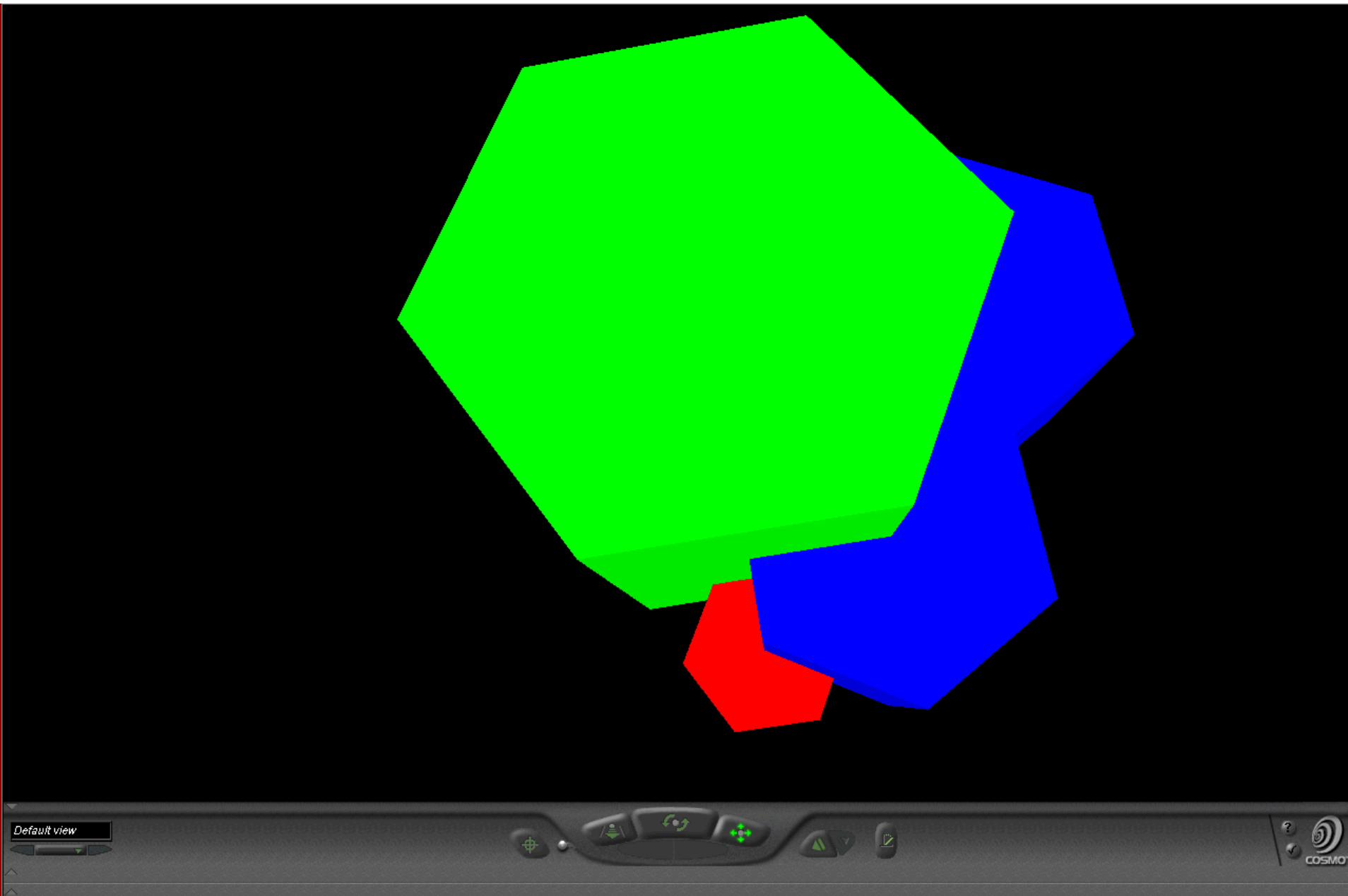


**Figure VR02.** A screen shot from the virtual world linked to this image. Click on the image to enter that world!

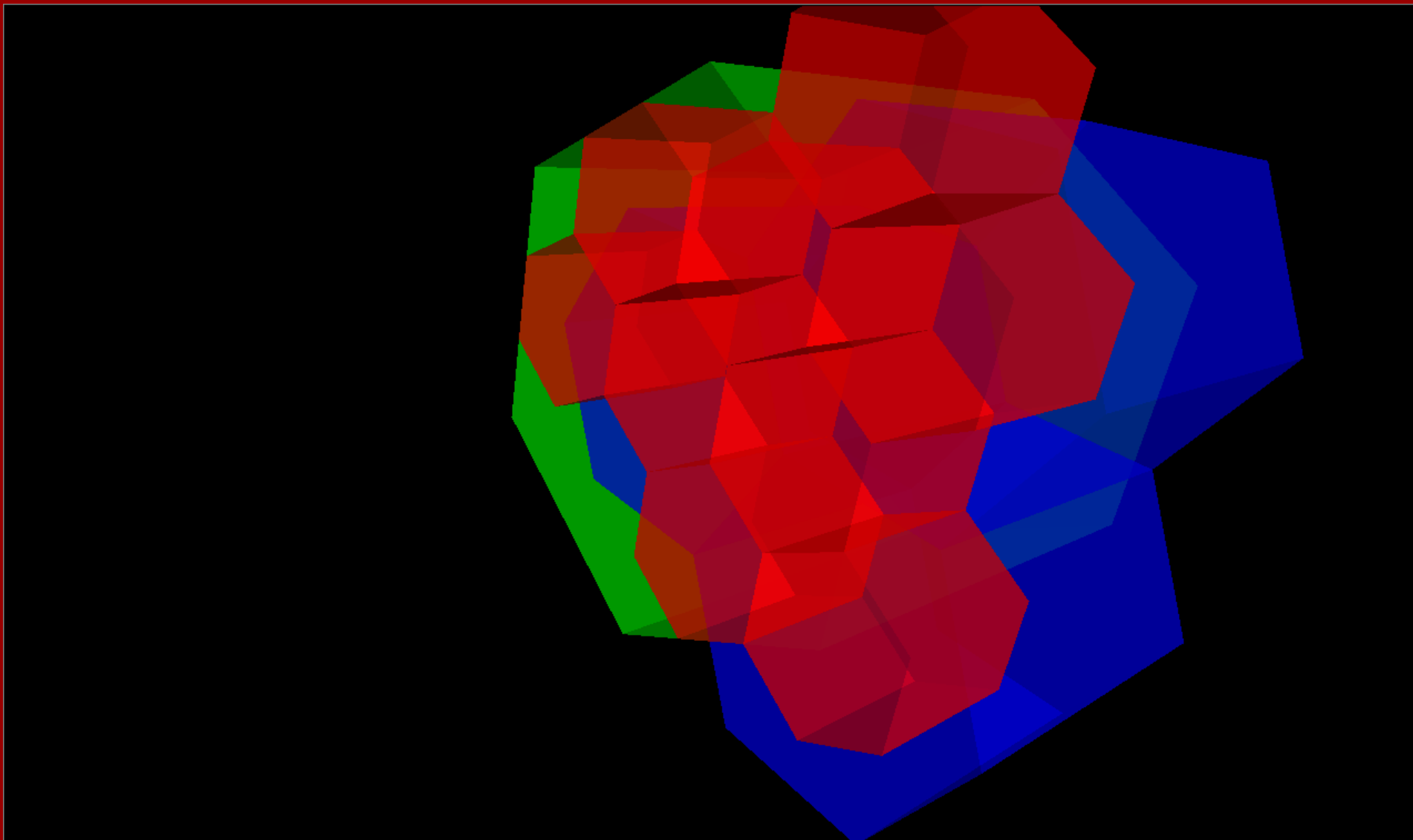
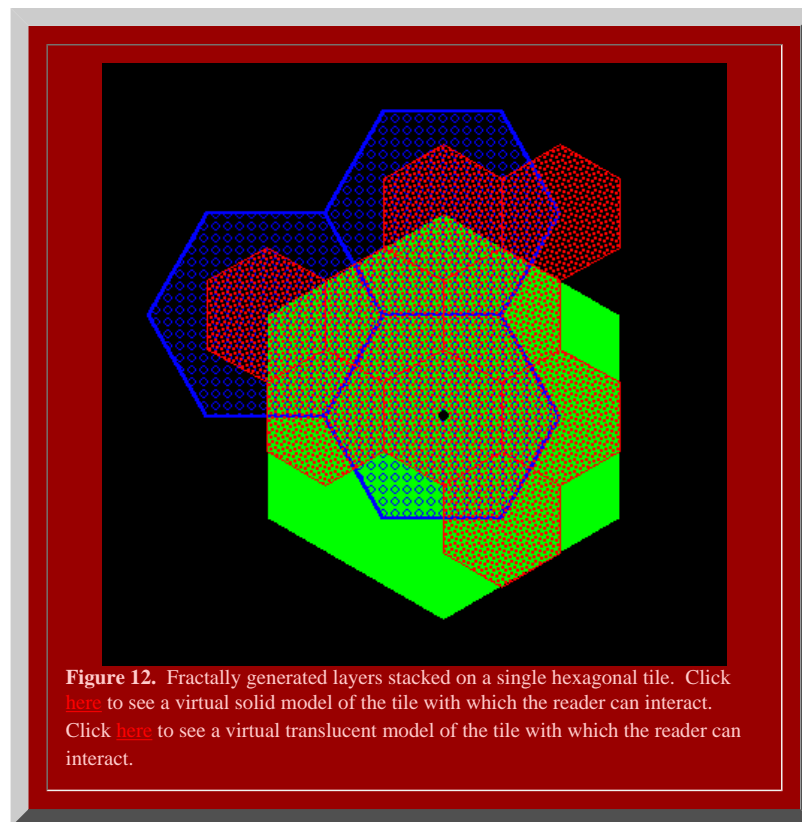


**Figure VR03.** A screen shot from the virtual world linked to this image. Click on the image to enter that world!  
Translucent solids permit one to see relationships among layers of the hexagonal hierarchy while travelling through the solids.



Finally, we tile the plane using the hexagonal initiators to discover if the superimposed structure also fits together perfectly (Figure 13). Hexagonal tiles are used to cover the plane without gaps, as is the case with the sample of green hexagons in Figure 13a. The hexagons mesh perfectly to cover the plane (Theorem of Gauss). In Figure 13b, the green outline of the hexagons remains. Each of the solid green hexagons has had the fractal generator above applied and the consequent superimposed blue tiles come into view sequentially in this animation. Again, the fit is exact, as we had hoped it might be. Finally, in Figure 13c, the blue outline only is retained from Figure 13b (along with the green outline from Figure 13a). The final fractally generated layer derived from the blue polygons of Figure 13b comes into view in shades of red (or yellow/gold for contrast). The final layer of hexagonal base of unit hexagons appears last. The fit is perfect: each green hexagon contains the equivalent of four blue hexagons and each blue hexagon contains the equivalent of four red hexagons. The fractal generation procedure created exactly the classical central place landscape of [Figure 3](#). As the animation proceeds in Figure 13, further layers of the fractally generated hierarchy, attached to the tile in Figure 12, come into view illustrating an exact meshing of tiles at all levels to form a  $K=3$  hierarchy.



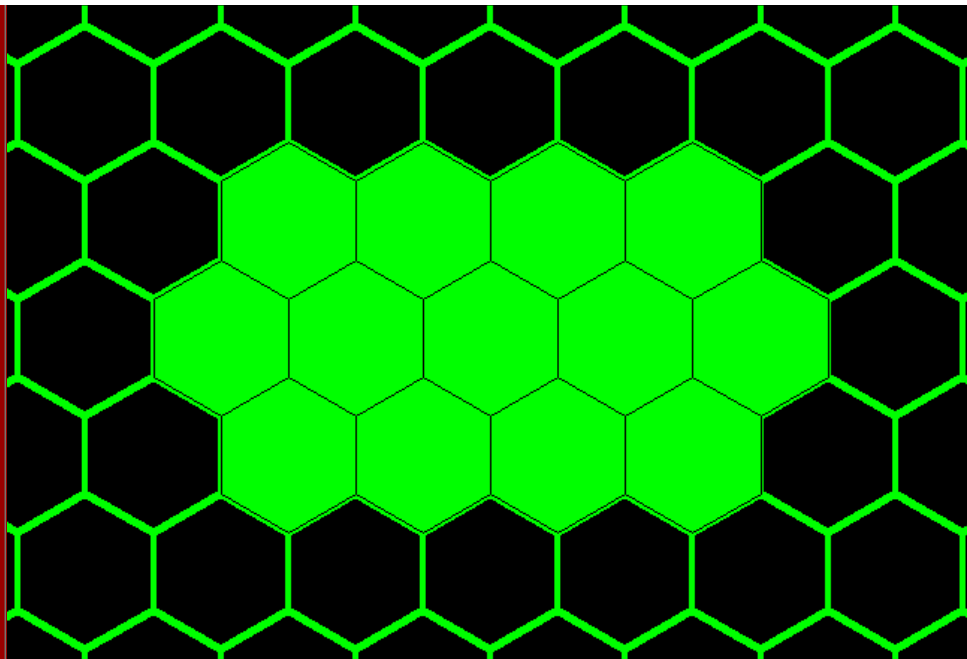


Figure 13a. Green layer on tile from Figure 12 fits exactly to tile the plane (Theorem of Gauss).

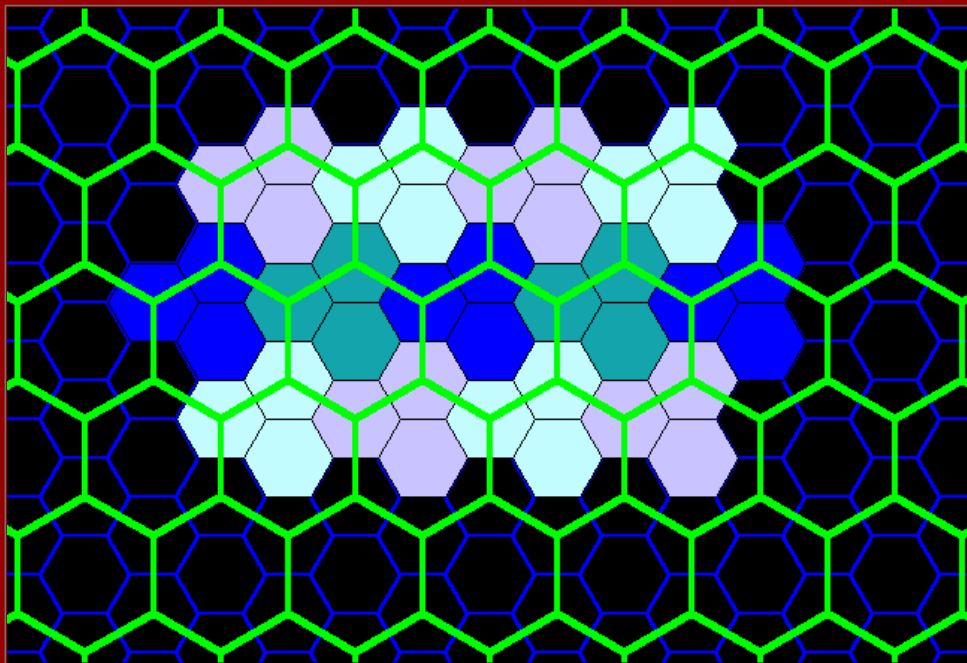
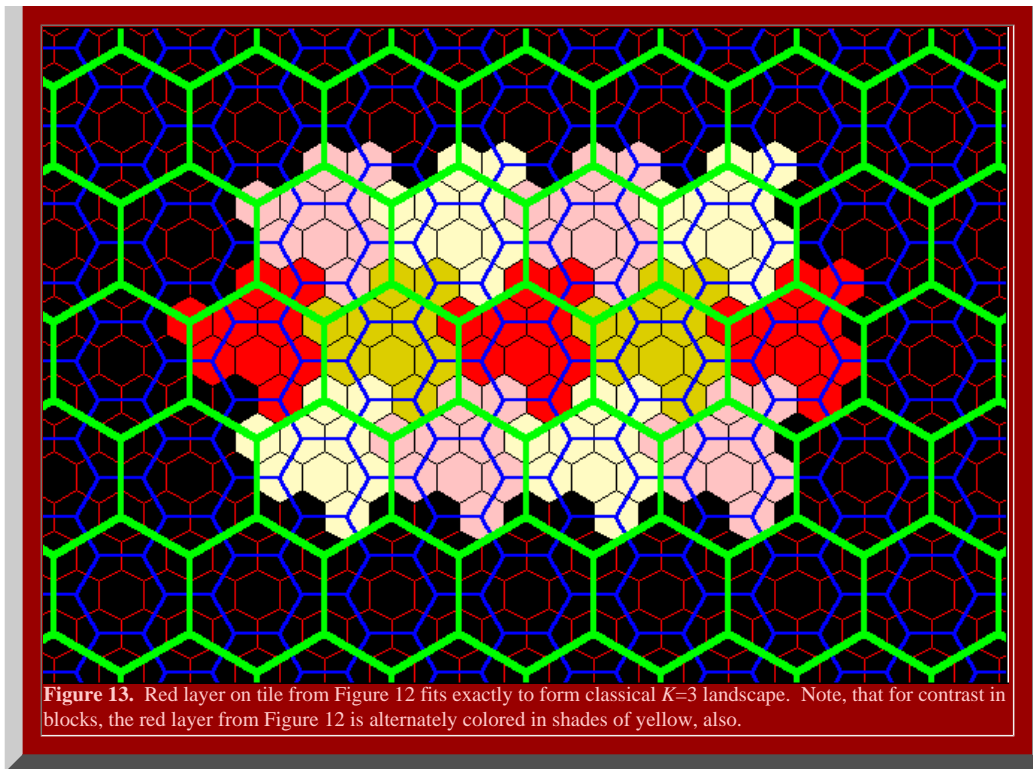


Figure 13b. Blue layer on tile from Figure 12 fits exactly to form classical  $K=3$  landscape.



#### *The $K=4$ Hierarchy*

When an hexagonal initiator is chosen and a three-sided generator, with included angles of 120 degrees and shaped in the form of an isosceles trapezoid, is used to make successive replacement of the sides of the hexagon (as in the animated Figure 14a), the outline of the next layer of the  $K=4$  central place hierarchy is generated (the black lines in Figure 14a suggest interior connections). The replacement sequence applies the generator in an alternating pattern to the outside and then to the inside of the initiator. When the original generator is scaled down, with shape preserved, and applied in the outside/inside sequence to the newly formed blue polygon, the next lower level central place  $K=4$  hierarchy is formed (as in the animated Figure 14b). The second, blue polygon contains four scaled-down hexagons, self-similar to the first hexagon (Figure 14a); the red polygon in the animation sequence contains four shapes self-similar to the blue polygon (Figure 14b), and 64 (or 4 cubed) hexagons self-similar to the original hexagon (Figure 14b). The invariant of 4, in the  $K=4$  hierarchy, is replicated in this particular fractal iteration sequence.



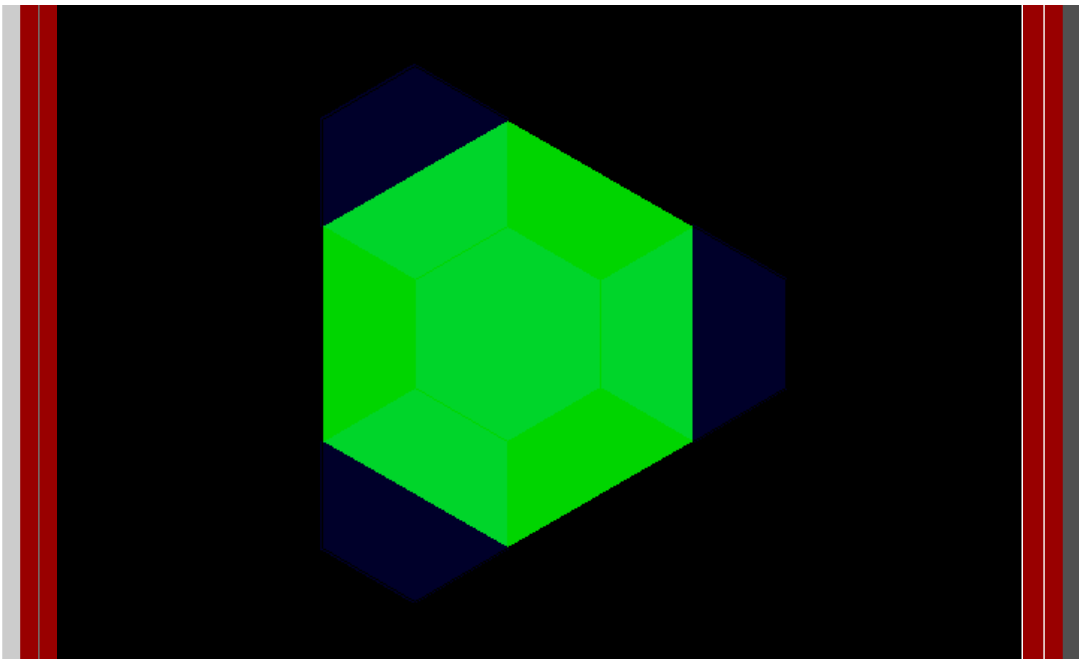


**Figure 14a.** Animated  $K=4$  fractal iteration sequence: first transformation using a three-sided fractal generator applied successively to sides of the hexagonal initiator.

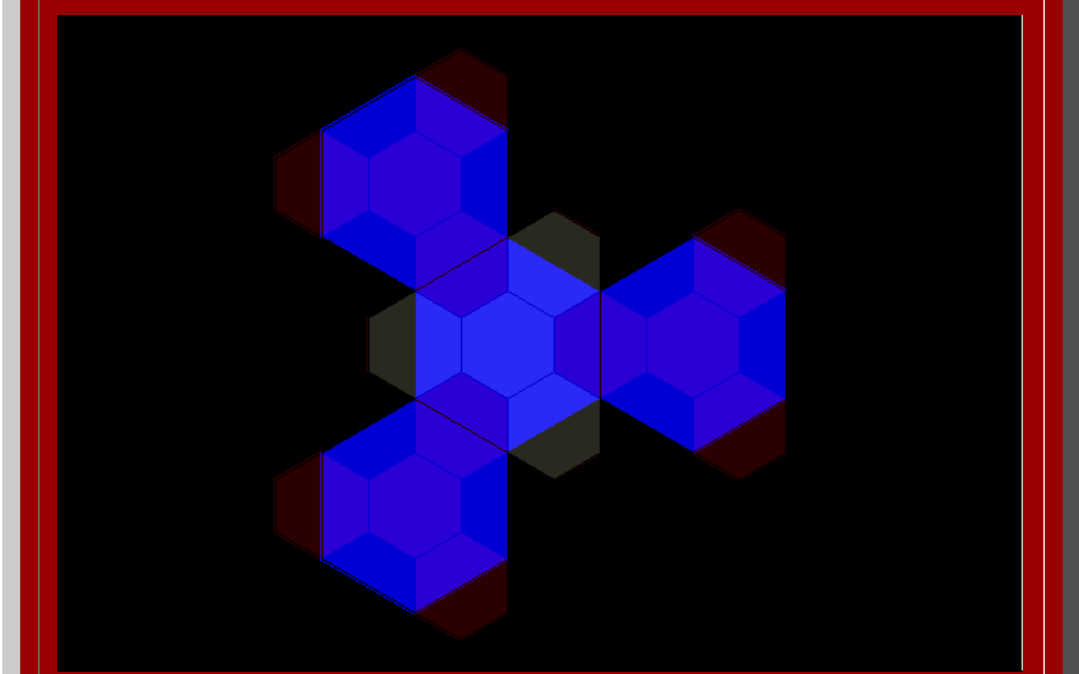


**Figure 14b.** Animated  $K=4$  fractal iteration sequence: second transformation using a scaled-down three-sided fractal generator applied successively to sides of the blue polygon generated in Figure 14a.

It remains to determine if the polygons generated in Figure 14 will in fact fit together to form the broad central place landscape of arbitrary size suggested in Figure 5. To that end, we stack the layers generated above using the fractal iteration sequence to form a tile of layers centered on the single polygonal initiator (Figure 15). Click [here](#), or on the screen shot in Figure VR04 below, to see a virtual solid model of the tile with which the reader can interact. Click [here](#), or on the screen shot in Figure VR05 below, to see a virtual translucent model of the tile with which the reader can interact.

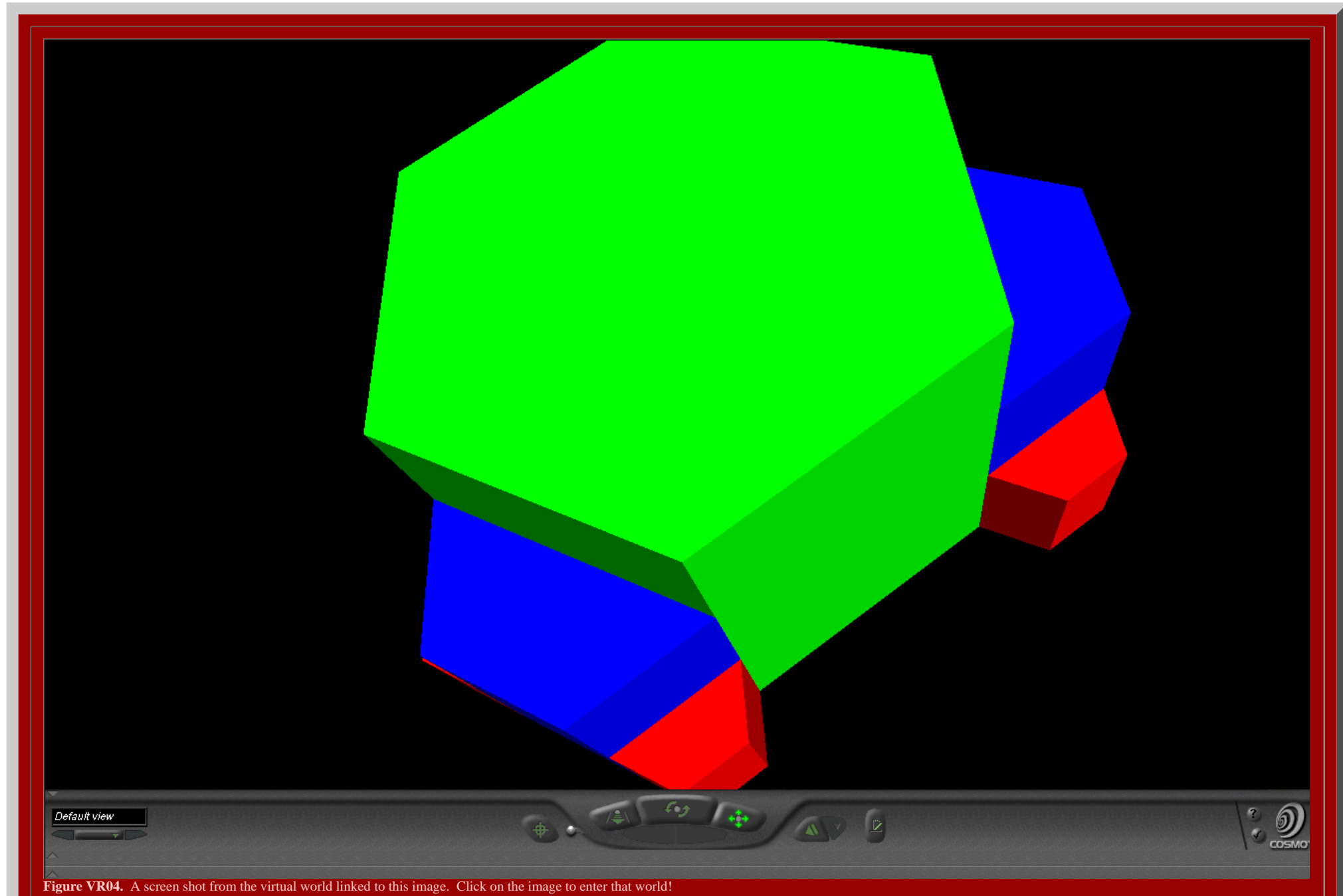


**Figure VR04.** A screen shot from the virtual world linked to this image. Click on the image to enter that world!

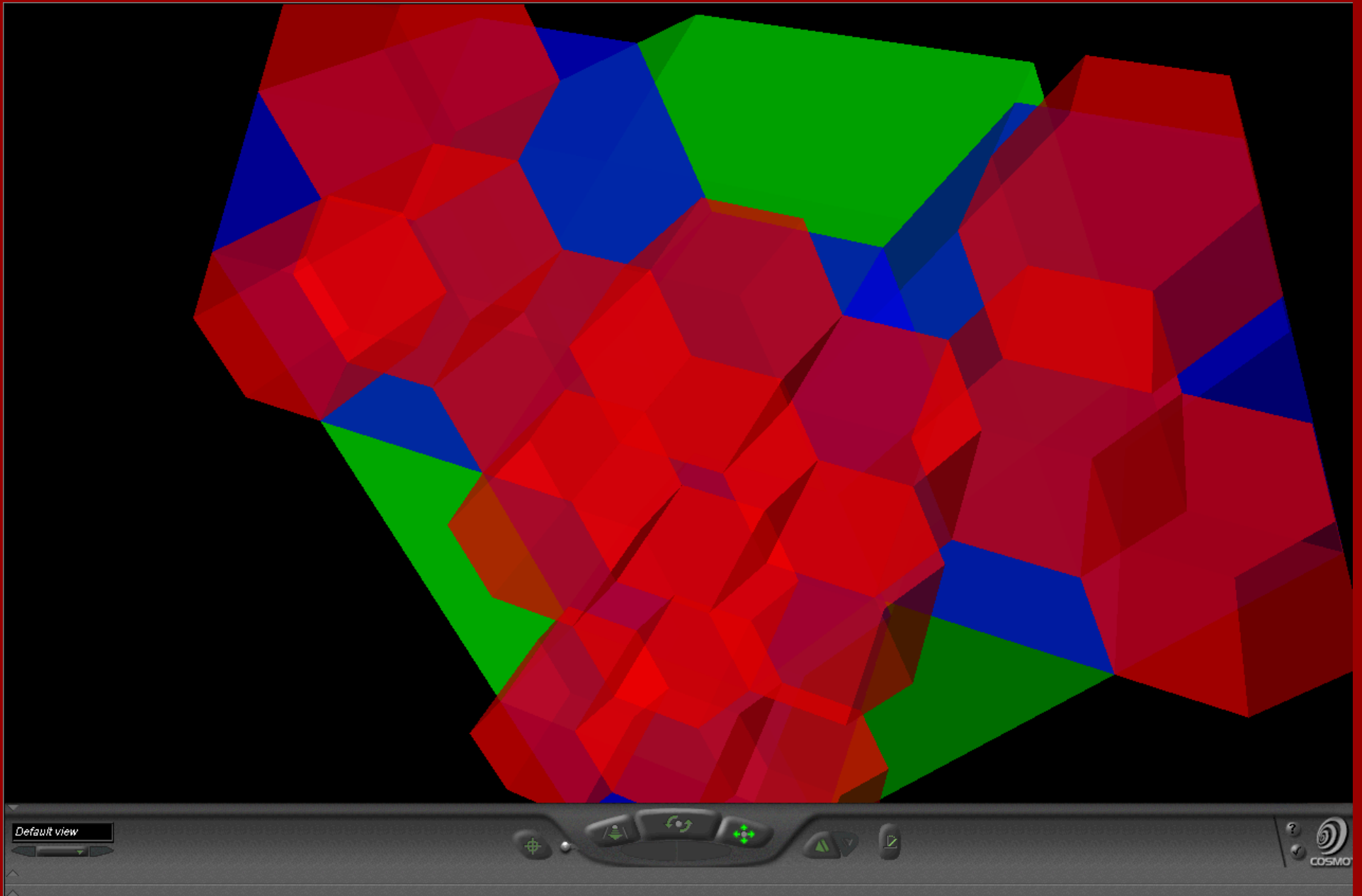
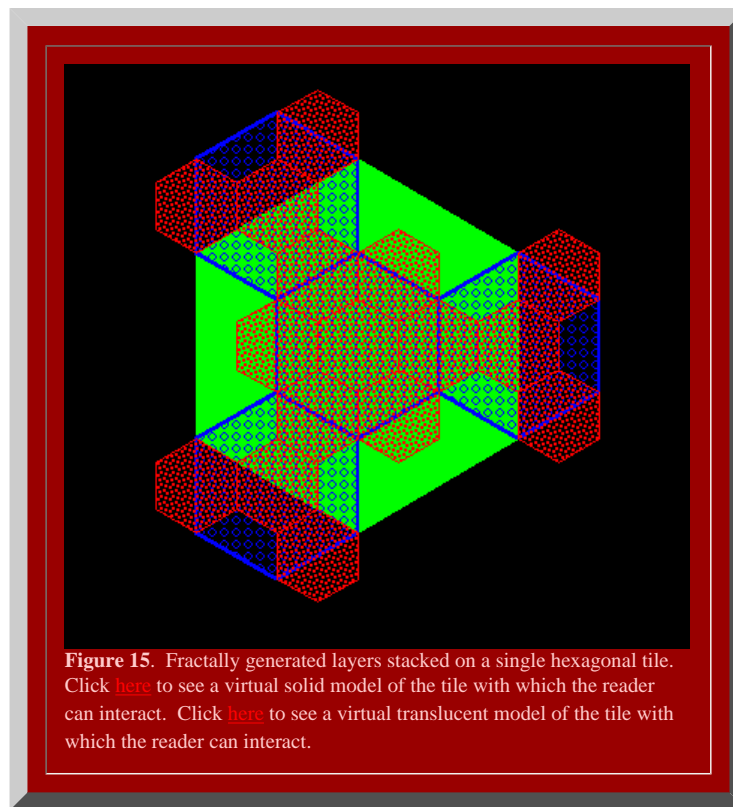


**Figure VR05.** A screen shot from the virtual world linked to this image. Click on the image to enter that world!  
Translucent solids permit one to see relationships among layers of the hexagonal hierarchy while travelling through the solids.



Finally, we tile the plane using the hexagonal initiators to discover if the superimposed structure also fits together perfectly (Figure 16). Hexagonal tiles are used to cover the plane without gaps, as is the case with the sample of green hexagons in Figure 16a. The hexagons mesh perfectly to cover the plane (Theorem of Gauss). In Figure 16b, the green outline of the hexagons remains. Each of the solid green hexagons has had the fractal generator above applied and the consequent superimposed blue tiles come into view sequentially in this animation. Again, the fit is exact, as we had hoped it might be. Finally, in Figure 16c, the blue outline only is retained from Figure 16b (along with the green outline from Figure 16a). The final fractally generated layer derived from the blue polygons of Figure 16b comes into view in shades of red (or yellow/gold for contrast). The final layer of hexagonal base of unit hexagons appears last. The fit is perfect: each green hexagon contains the equivalent of four blue hexagons and each blue hexagon contains the equivalent of four red hexagons. The fractal generation procedure created exactly the classical central place landscape of [Figure 5](#). As the animation proceeds in Figure 16, further layers of the fractally generated hierarchy, attached to the tile in Figure 15, come into view illustrating an exact meshing of tiles at all levels to form a  $K=4$  hierarchy.



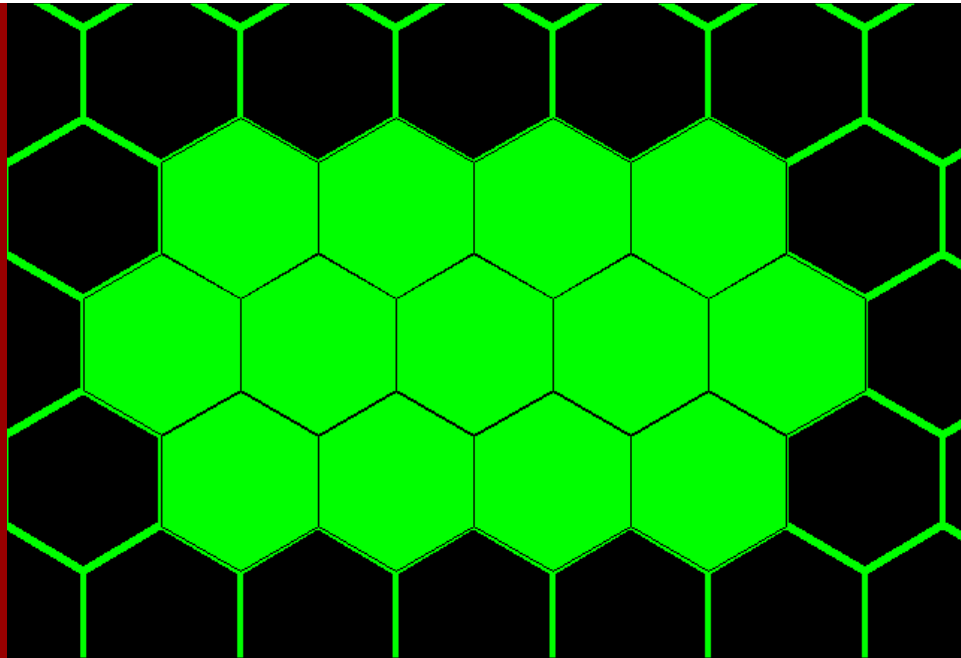


Figure 16a. Green layer on tile from Figure 15 fits exactly to tile the plane (Theorem of Gauss).

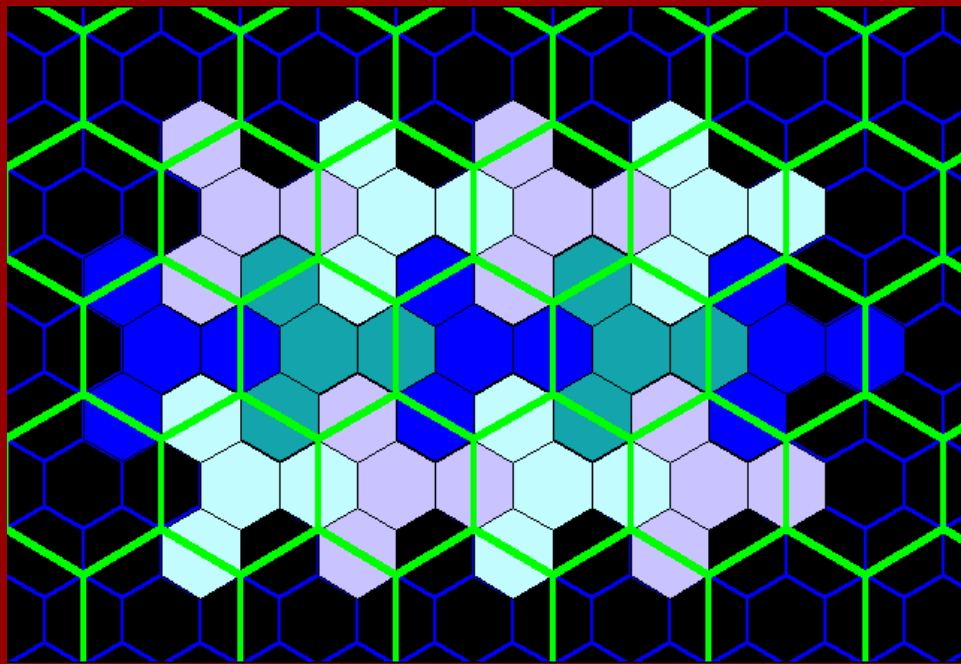
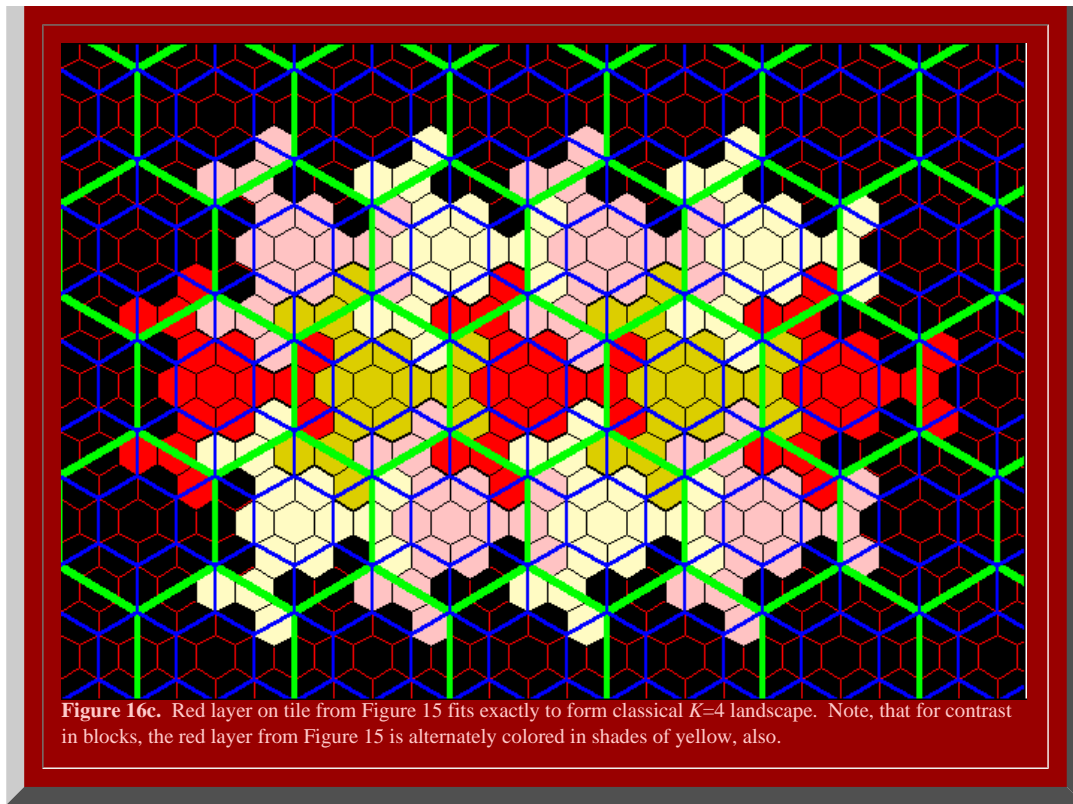


Figure 16b. Blue layer on tile from Figure 15 fits exactly to form classical  $K=4$  landscape.



### The $K=7$ Hierarchy

When an hexagonal initiator is chosen and a three-sided generator, with included angles of 120 degrees and shaped in a zig-zag form, is used to make successive replacement of the sides of the hexagon (as in the animated Figure 17a), the outline of the next layer of the  $K=7$  central place hierarchy is generated (the black lines in Figure 17a suggest interior connections). The replacement sequence applies the generator in an alternating pattern to the outside and then to the inside of the initiator. When the original generator is scaled down, with shape preserved, and applied in the outside/inside sequence to the newly formed blue polygon, the next lower level central place  $K=7$  hierarchy is formed (as in the animated Figure 17b). The second, blue polygon contains seven scaled-down hexagons, self-similar to the first hexagon (Figure 17a); the red polygon in the animation sequence contains seven shapes self-similar to the blue polygon (Figure 17b), and 343 (or 7 cubed) hexagons self-similar to the original hexagon (Figure 17b). The invariant of 7, in the  $K=7$  hierarchy, is replicated in this particular fractal iteration sequence.



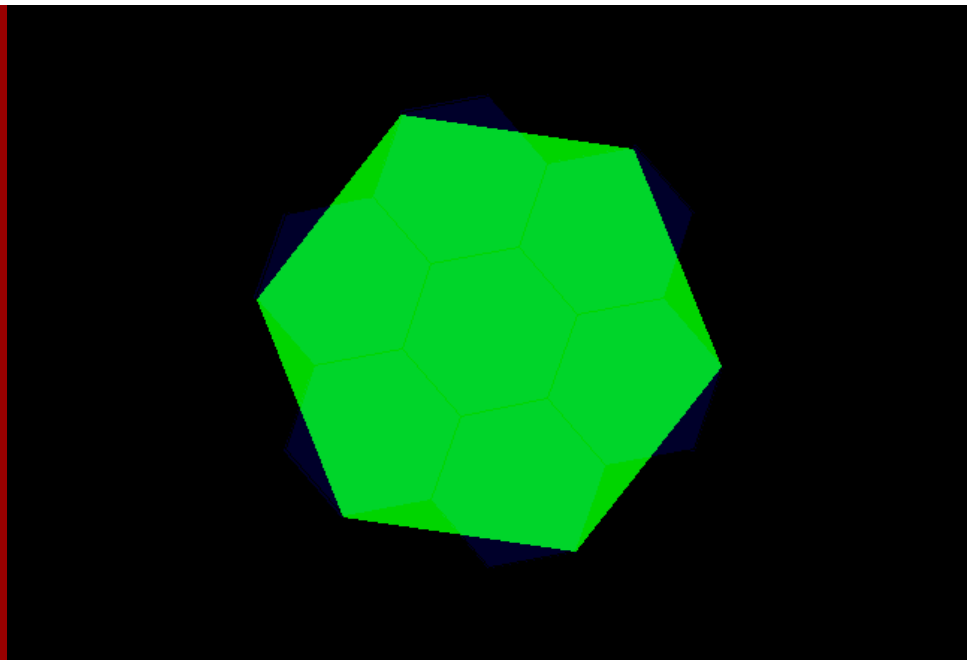


**Figure 17a.** Animated  $K=7$  fractal iteration sequence: first transformation using a three-sided fractal generator applied successively to sides of the hexagonal initiator.

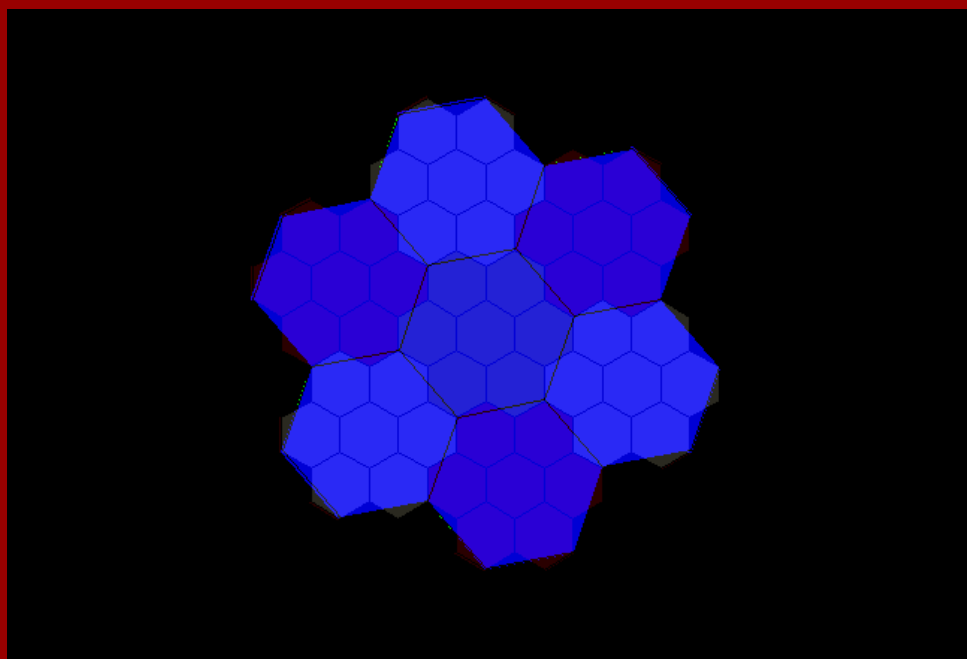


**Figure 17b.** Animated  $K=7$  fractal iteration sequence: second transformation using a scaled-down three-sided fractal generator applied successively to sides of the blue polygon generated in Figure 17a.

It remains to determine if the polygons generated in Figure 17 will in fact fit together to form the broad central place landscape of arbitrary size suggested in [Figure 7](#). To that end, we stack the layers generated above using the fractal iteration sequence to form a tile of layers centered on the single polygonal initiator (Figure 18). Click [here](#), or on the screen shot in Figure VR06 below, to see a virtual solid model of the tile with which the reader can interact. Click [here](#), or on the screen shot in Figure VR07 below, to see a virtual translucent model of the tile with which the reader can interact.

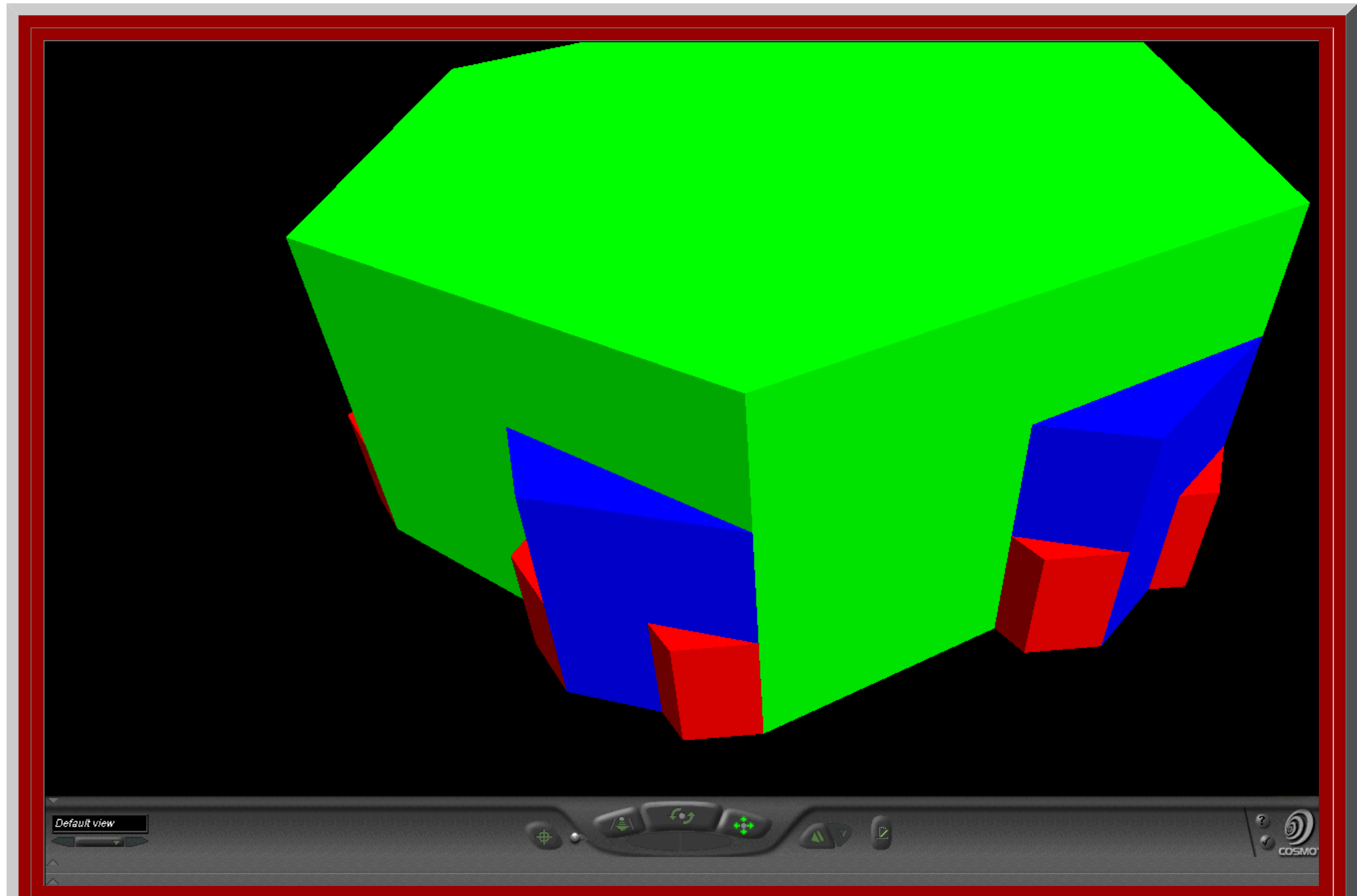


**Figure VR06.** A screen shot from the virtual world linked to this image. Click on the image to enter that world!

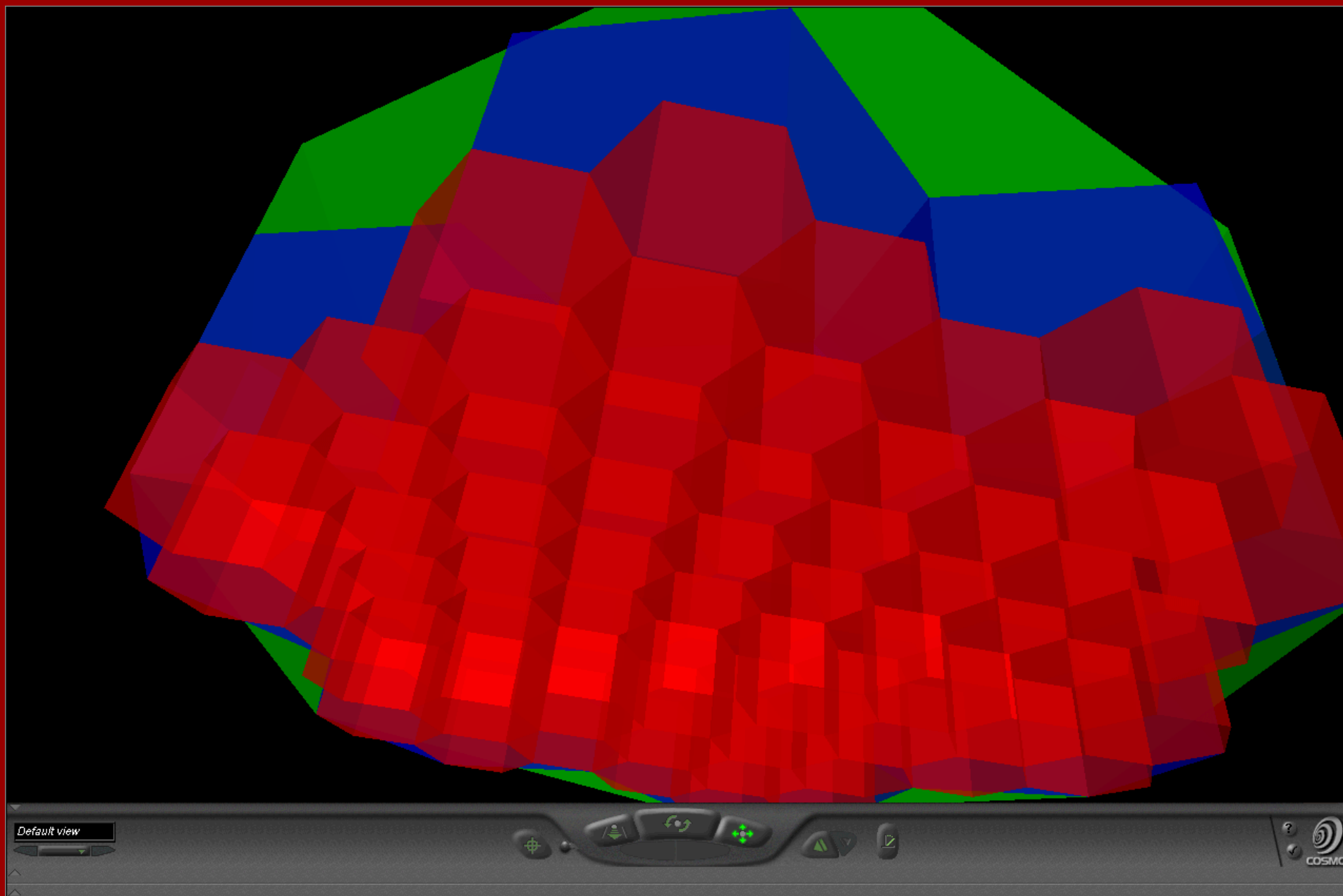
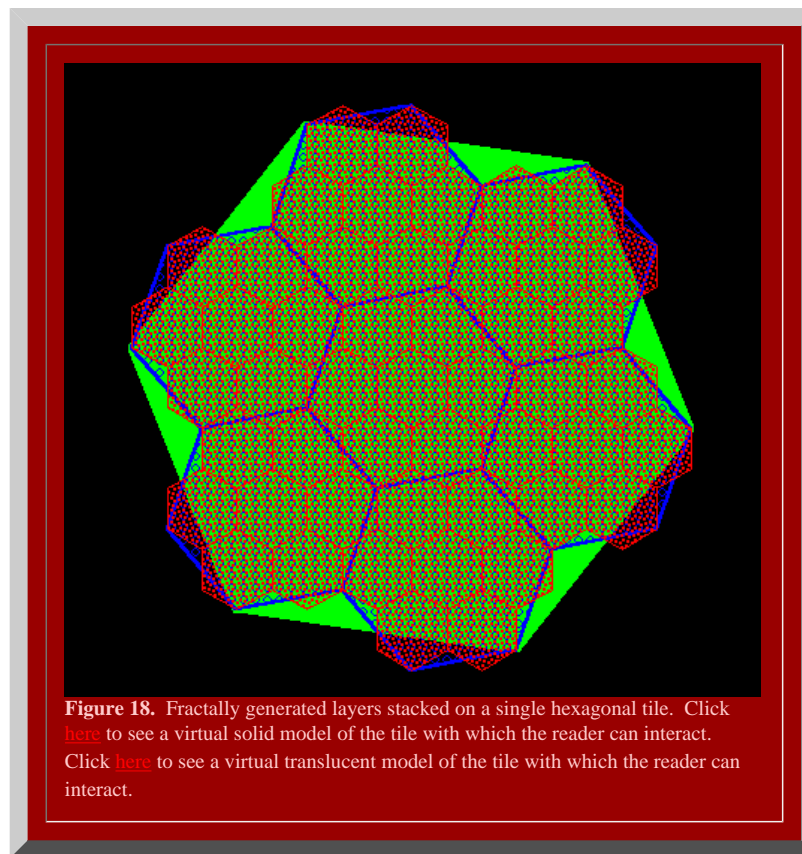


**Figure VR07.** A screen shot from the virtual world linked to this image. Translucent solids permit one to see relationships among layers of the hexagonal hierarchy while travelling through the solids. Click on the image to enter that world: blast off in this virtual hexagonal space ship!



Finally, we tile the plane using the hexagonal initiators to discover if the superimposed structure also fits together perfectly (Figure 19). Hexagonal tiles are used to cover the plane without gaps, as is the case with the sample of green hexagons in Figure 19a. The hexagons mesh perfectly to cover the plane (Theorem of Gauss). In Figure 19b, the green outline of the hexagons remains. Each of the solid green hexagons has had the fractal generator above applied and the consequent superimposed blue tiles come into view sequentially in this animation. Again, the fit is exact, as we had hoped it might be. Finally, in Figure 19c, the blue outline only is retained from Figure 19b (along with the green outline from Figure 19a). The final fractally generated layer derived from the blue polygons of Figure 19b comes into view in shades of red (or yellow/gold for contrast). The final layer of hexagonal base of unit hexagons appears last. The fit is perfect: each green hexagon contains the equivalent of four blue hexagons and each blue hexagon contains the equivalent of four red hexagons. The fractal generation procedure created exactly the classical central place landscape of [Figure 7](#). As the animation proceeds in Figure 19, further layers of the fractally generated hierarchy, attached to the tile in Figure 18, come into view illustrating an exact meshing of tiles at all levels to form a  $K=7$  hierarchy.



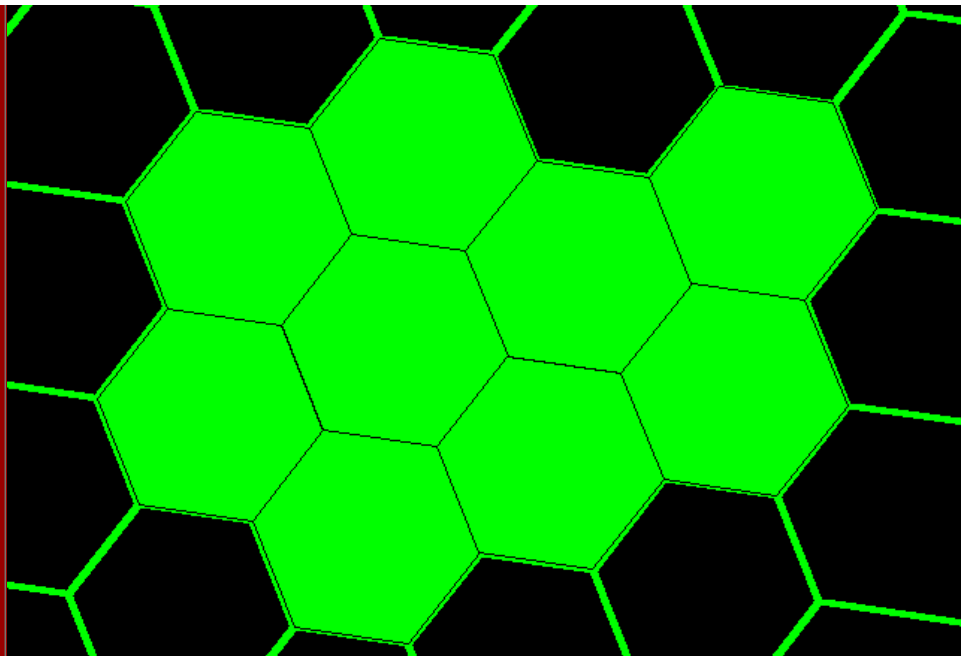


Figure 19a. Green layer on tile from Figure 18 fits exactly to tile the plane (Theorem of Gauss).

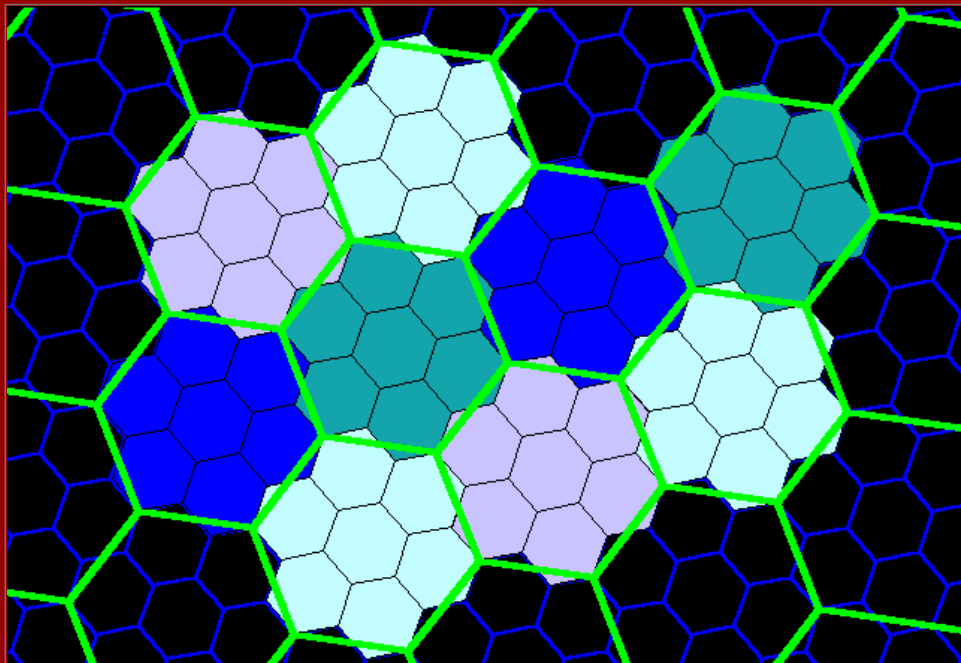
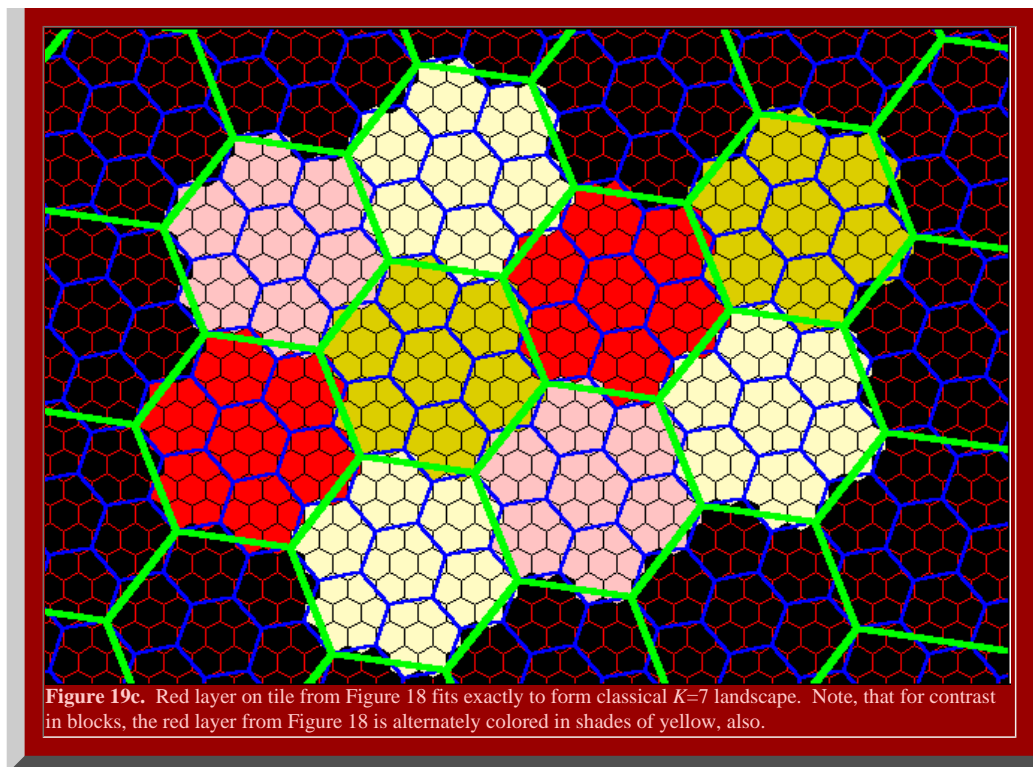


Figure 19b. Blue layer on tile from Figure 18 fits exactly to form classical  $K=7$  landscape.



Thus, the complex mechanics of classical central place theory come alive as a single dynamic system when viewed using fractal geometry. The fit is exact.

#### The Added Role of the Fractional Dimension

A fractal iteration sequence, such as those above but carried out infinitely, might be thought to increase the extent to which a line "fills" space. Both a single line segment and the letter "N" have Euclidean dimension 1; yet one of them fills more space than does the other. Mandelbrot (and others before him) captures this notion of space-filling with the concept of fractional dimension (hence "fractal"). He uses Hausdorff-Besicovitch dimension to measure the enduring mathematical concept of space-filling. We employ Mandelbrot's formulation for fractional dimension  $D$  as,  $D = \log(\text{number of generator sides}) / \log(\text{square root of } K)$ . Thus, the following values for fractally-generated central place hierarchies emerge:

- $K=3, D = \log 2 / \log \sqrt{3} = 1.2618595$
- $K=4, D = \log 3 / \log 2 = 1.5849625$
- $K=7, D = \log 3 / \log \sqrt{7} = 1.1291501$

The idea with the space-filling is to pick an arbitrary point in the bounded space containing the curve. Place a circle of arbitrarily small radius around that point. Does that circle contain a point on the curve as the fractal iteration sequence goes to infinity? If that is the case for any point, then the curve is said to fill space and have dimension 2. If not, then there are holes or gaps (perhaps of infinitesimal size) in the space and the curve fails to fill space completely and has fractional dimension between 1 and 2 (as a sort of Swiss cheese, Emmenthaler, with holes). Thus, the  $K=4$  fractal iteration sequence, if permitted to repeat infinitely, has the highest fractional dimension of these three: this curve gets "closer" to arbitrary points in space than do the lines of the other hierarchies, as one might hope a hierarchy interpreted as a "transportation" hierarchy would. The fractional dimension of the fractal iteration sequence corresponds to the intuitive notion of scholars over time as to interpretation: as another benchmark or field test of theory. The  $K=7$  fractal iteration sequence, if permitted to repeat infinitely, has the lowest fractional dimension of these three, keeping control from the center optimized and hence supporting the "administrative" interpretation often given to the classical  $K=7$  hierarchy. Finally, the  $K=3$  falls between: marketing needs greater spatial penetration than does administration but less than does transportation. Here, the fit between classical interpretation and fractal calculation is reasonable (one could never say "exact" because the terms "marketing," "transportation," and "administrative" are inexact terms themselves).

What is difficult with fractals is to visualize the infinite process. Graphic color display, including three dimensional display, offers exciting strategies for visualization. Very quickly, however, it becomes difficult to draw the fine lines required by repeating the process at more and more local scales: lines have width. Electronic lines can be controlled and made finer than can pen lines, but eventually the line-width limits the capability to produce graphic images. Eventually, the mind's eye must take over and extrapolate the visual infinite process.

Another possibility might be to draw on the other human senses to aid in that extrapolation. Thus, Figure 20 shows figures generated by Fractal Music 1.9; click on the images and hear the associated music. The left figure shows the cellular automata base generated by default--it is bilaterally symmetric about a central vertical line and was generated using a symmetrically arranged initiator string of 64 digits ranging in value from 0 to 7 (one for each tone). The next figure,  $K=3$ , shows the cellular automata diagram (another sort of "bubble foam" in appearance) generated using the value for the fractional dimension of the  $K=3$  hexagonal hierarchy carried out to 64 decimal places as the initiator string for the music. The next figure,  $K=4$ , shows the cellular automata diagram generated using the value for the fractional dimension of the  $K=4$  hexagonal hierarchy carried out to 64 decimal places as the initiator string for the music. The final figure,  $K=7$ , shows the cellular automata diagram generated using the value for the fractional dimension of the  $K=7$  hexagonal hierarchy carried out to 64 decimal places as the initiator string for the music. Click on each figure to hear the music. Each musical sequence, of over 1000 steps, was created from the default base, changing only the initiator string, so that the fractional dimension is what operates on a "seed" value of basic notes. The listener should hear the basic pattern in all characterizations: great symmetry in the base value; abrupt changes of state in the  $K=3$  value; a smoother filling of musical space in the  $K=4$  music; and, gaps in the  $K=7$  musical characterization derived from the  $K=7$  fractional dimension. Thus, we extend visualization from two dimensional graphical images to three dimensional graphical images to the mind's eye, and finally, to the mind's ear: capturing hierarchical pattern through 1000 steps or more is easy in the musical clips. Such characterization offers added capability to those of us with all of our senses that are functional: for those with limited visual sensory function, it offers a way to an auditory "visualization" of the beauty of geometry.

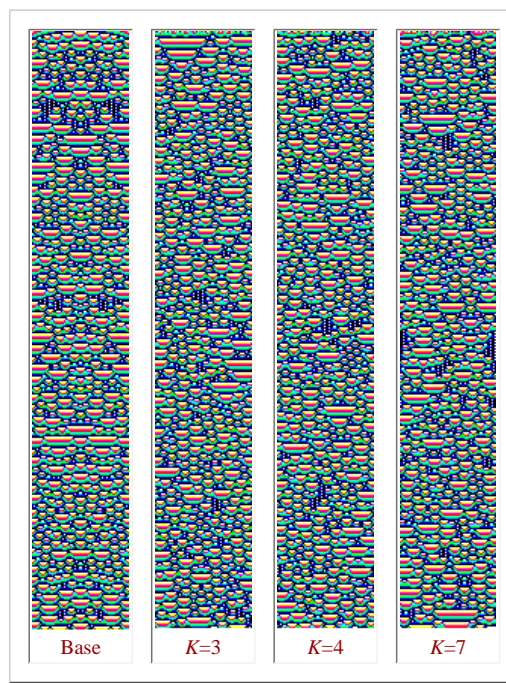


**Figure 20.** Fractal music connection. Click on the images generated by the fractional dimensions of the hexagonal hierarchies; compare these to the default base created by the software.

## Future Directions

The complex mechanics of the theory behind hexagonal hierarchies come alive as a single dynamic system when visualized through the lens of fractal geometry. The fit of the classical and fractal geometric hierarchies is exact. Thus, as one might use a carefully surveyed topographic map, with field-checked spot elevations, as a guide into dense jungle or other unsurveyed landscapes, so too we use our carefully surveyed alignment of the classical and the fractal hexagonal hierarchies as a guide into unseen or unproven areas of geometry and geography. The difference is that the "field" tests in one case occur "terrestrial space" while in the other the "field" tests occur in "geometry, number theory, and pure mathematics."

In the material above, we saw hexagonal hierarchies, of different orientation, cell size, and stacking characteristics, arise from the same base of unit hexagons. These were associated with three integers: 3, 4, and 7. The thoughtful reader might naturally ask a number of questions, such as:

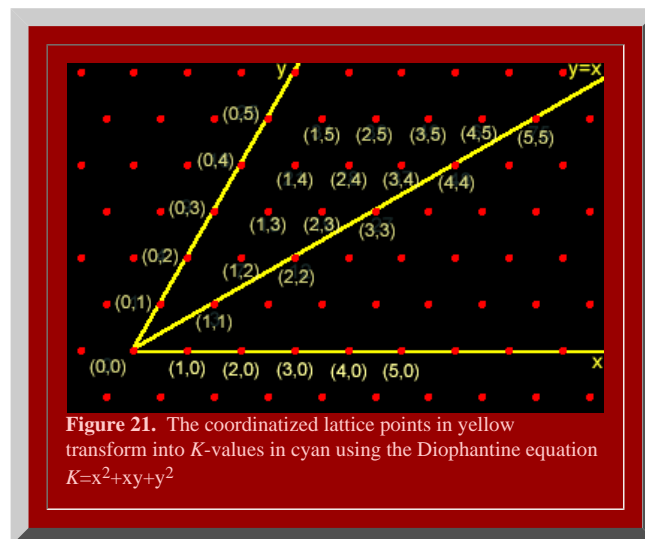
- are there other numbers that would serve as  $K$  values or are 3, 4, and 7 the only such values?
  - are 5 or 6 possible  $K$  values?
  - are there  $K$  values larger than 7?
  - how many  $K$  values are there?
- How does one determine the number of sides in a fractal generator that will generate a correct hierarchy for arbitrary  $K$  values?
- How does one determine fractal generator shape that will generate a correct hierarchy for arbitrary  $K$  values?

Earlier research, by August Lösch, Michael Dacey, and others shows illustrations of  $K$ -values greater than 7. Indeed, research by Arthur Loeb, in crystallography, and Dacey, in geography, led to independent discovery that the Diophantine equation,  $x^2+xy+y^2$  would generate all  $K$  values when pairs of positive integers were substituted for  $x$  and for  $y$ . Thus, when  $(x,y)=(1,1)$  the equation  $x^2+xy+y^2 = K$  yields a value of  $K=3$ ; when  $(x,y)=(0,2)$ , it follows that  $K=4$ ; and, when  $(x,y)=(1,2)$ , it follows that  $K=7$ . Pairs such as  $(0,0)$  and  $(1,0)$  yield only trivial results so that the values of 3, 4, and 7 are the three smallest  $K$ -values. There are no other  $K$  values less than 7.

The result of Loeb/Dacey is important because it shows

- that there are an infinite number of possible  $K$  values
- that this infinity of values is in one-to-one correspondence with the integral lattice points in the plane
- that one can give a numerical generating function to create  $K$  values

Thus, a graph of lattice points in the plane offers a convenient method of visualizing  $K$ -values (Figure 21). The animation shows the coordinate pairs in this oblique coordinate system with axes inclined at 60 degrees (instead of the conventional 90 degrees). The coordinate pairs are replaced in animated fashion by single numbers representing the  $K$  value that corresponds to that ordered pair.



Previous published research by the authors of this presentation has shown how to determine the number of sides in a fractal generator that will generate a correct hierarchy for arbitrary  $K$  values and how to determine fractal generator shape that will generate a correct hierarchy for arbitrary  $K$  values. Work in progress shows how to extend the three dimensional and other visualization schemes shown here to higher  $K$  values. In it, we offer mathematical proof of these ideas and extensions of them into new realms. The classical is used for alignment of new with the old: a strategy useful in a wide range of theoretical and applied research.

---

## BIBLIOGRAPHY

1. Arlinghaus, Sandra L. 1985. "Fractals take a central place," *Geografiska Annaler*, 67B, pp. 83-88. Journal of the Stockholm School of Economics.
2. Arlinghaus, Sandra Lach. 1990. "Fractal geometry of infinite pixel sequences: 'Super-definition' resolution?" *Solstice: An Electronic Journal of Geography and Mathematics*, Institute of Mathematical Geography (the journal *Solstice* was in the Pirelli top 80, semi-finalist, in 2001)
3. Arlinghaus, Sandra Lach. 1993. "Microcell Hex-nets?" *Solstice: An Electronic Journal of Geography and Mathematics*, Institute of Mathematical Geography
4. Arlinghaus, Sandra Lach. 1993. "Electronic Geometry," *The Geographical Review* April, Vol. 83, No. 2, pp. 160-169.
5. Arlinghaus, Sandra Lach. 1993. "Central Place Fractals"--Chapter 10 in *Fractals in Geography*, edited by Nina Lam and Lee DeCola, Prentice-Hall.
6. Arlinghaus, Sandra L. and Arlinghaus, William C. 1989. "The fractal theory of central place hierarchies: a Diophantine analysis of fractal generators for arbitrary Lösschian numbers," *Geographical Analysis: an International Journal of Theoretical Geography*. Ohio State University Press. Vol. 21, No. 2, April, pp. 103-121.
7. Arlinghaus, Sandra L. and Arlinghaus, William C. 2002. Spatial Synthesis: A Research Program, *Solstice: An Electronic Journal of Geography and Mathematics*, Volume XIII, Number 2.
8. Arlinghaus, Sandra L. and Arlinghaus, William C. 2003. *Spatial Synthesis*, Volume I, Book 1. Forthcoming.
9. Arlinghaus, Sandra L., Arlinghaus, William C., and Harary, Frank. Graph Theory and Geography: An Interactive View eBook (Pirelli top 20, finalist, 2002), John Wiley and Sons, New York, 2002.
10. Boys, C. Vernon. 1902. *Soap Bubbles and the Forces which Mould Them*. Society for Promoting Christian Knowledge.
11. Christaller, Walter. Struktur und Gestaltung der Zentralen Orte des Deutschen Ostens, Gemeinschaftswerk im Auftrage der Reichsarbeitsgemeinschaft für Raumforschung, Teil 1, Dr. Walter Christaller, *Die Zentralen Orte in den Ostgebieten und ihre Kultur- und Marktbereiche*, K. F. Koehler Verlag, Leipzig, 1941
12. Christaller, Walter. 1933. *Die zentralen Orte in Süddeutschland*. Jena: Gustav Fischer. (Translated (in part), by Carlisle W. Baskin, as *Central Places in Southern Germany*. Prentice Hall 1966).
13. Coxeter, H. S. M. 1961. *Introduction to Geometry*. New York: John Wiley & Sons, pp. 53-54.
14. Dacey, Michael F. The geometry of central place theory. *Geografiska Annaler*, B, 47, 1965, 111-124.
15. Fejes-Toth, Laszlo. 1968. Solid circle-packings and circle-coverings, *Studia Sci. Math. Hungar.* 3(1968).
16. Gauss, Carl Friedrich. 1840. Untersuchungen über die Eigenschaften der positiven ternären quadratischen Formen von Ludwig August Seber, Göttingische gelehrte Anzeigen, Juli 9 [J. Reine Angew. Math. 20 (1840), 312-320: Werke, Vol. 2 (Königliche Gesellschaft der Wissenschaften, Göttingen 1876), 188-196].
17. Kolars and Nystuen, 1974. *Human Geography*, New York: McGraw-Hill.
18. Loeb, Arthur L. 1976. *Space Structures: Their Harmony and Counterpoint*. Reading, MA: Addison-Wesley.
19. Lösch, August. 1954. *The Economics of Location*, translated by William H. Woglom. New Haven: Yale University Press.
20. Mandelbrot, Benoit. 1983. *The Fractal Geometry of Nature*. San Francisco: W. H. Freeman.
21. Nystuen, J., 1966. "Effects of boundary shape and the concept of local convexity;" Michigan Interuniversity Community of Mathematical Geographers (unpublished). Reprinted, Ann Arbor: [Institute of Mathematical Geography](#).
22. Singer, David H. 2003. Fractal Music, 1.9, [The Fractal Music Generator](#)
23. Tufte, E. R. (1990). *Envisioning Information*. Cheshire, CT. Graphics Press.
24. Vries, Hugo de. 1906. *Species and Varieties: Their Origin by Mutation* (second edition; Chicago: The Open Court Publishing Company), ed. by Daniel Trembly MacDougal (Gutenberg text)

---

Based on part of a book currently in progress, entitled *Spatial Synthesis*, by the authors of this document.

## One Optimization of an Earlier Model of Virtual Downtown Ann Arbor

Klaus-Peter Beier\*  
The University of Michigan

In *Ann Arbor, Michigan: Virtual Downtown Experiments, Part III*, *Solstice*, Vol. XIII, No. 2, the authors, Kwon, Lazzaro, Oppenheim, and Rosenblum, portray a useful virtual model of four blocks of downtown Ann Arbor. The file size of their model is, however, quite large: 40 MB. This article illustrates one way to reduce the size of that file and, consequently, load time. The newly optimized file is now 8 MB which is useful to a wider audience than is the previous file. The appearance of the two files does not differ greatly; what does differ is load time. Figure 1 below shows a screen capture from the 40 MB file set at High resolution; Figure 2 below shows a screen capture from the 8 MB file set at Medium resolution and modified as noted below. The optimization for improved load time does not make a noticeable difference in visual appearance. Figure 3 shows the edited 8 MB vrmf file embedded in the html (requires that Cosmo Player or Cortona be pre-loaded in the browser; both are free downloads).



**Figure 1.** Screen capture from the 40 MB file set at a viewpoint, zoomed in on, and lightened in Adobe Photoshop (trademark, Adobe). [Link](#) to VR file: requires Cosmo Player plug in to browser (IE or Netscape 4.x) or Cortona from Parallel Graphics (free download).



**Figure 2.** Screen capture from the 8 MB file set at a viewpoint, zoomed in on, and lightened in Adobe Photoshop (trademark Adobe). [Link](#) to VR file: requires Cosmo Player plug in to browser (IE or Netscape 4.x) or Cortona from Parallel Graphics. This linked file is also shown embedded in the html, below.

**Figure 3.** Edited file. Try looking at the model from different viewpoints or navigate, on your own, using the control panel.

Still, the application is big and runs slowly (low frame rate) if the most advanced graphics board is not available. The culprit is the artifacts file. The artifacts (trees, lamps, benches) are over-defined (too many polygons). Also, exhaustive field checking is a recommended future step to remove any error in detail in the scene as compared to reality. The appendix to this document, made from notes, shows the modifications made to the files.

#### APPENDIX

Removed option for low-res and high-res textures, using only med-res textures.  
This eliminates all jpg files for high and low res.

Changed all file types to lower case (e.g. WRL -> wrl)

Removed all instances of Lamp (43 lamps) from artifacts.wrl  
Created Inline file for lamp: LAMPUS.wrl  
Created prototype MyLamp using Inline file  
This reduced the size of artifacts.wrl

Same for 46 trees

Same for 7 benches

Removed all TimeSensors connected to trees (no need)

Modified many instances of "solid FALSE" to "solid TRUE"

Removed invalid color in Lamp

Removed reference to non-existing texture REKKANIG.BMP

Cleaned up ROUTING and Script

Set "collision FALSE" for all artifact.wrl objects

Improved navigation, added useful viewpoints

-----  
Professor Beier, Ph.D., is Director of the 3D Laboratory of The University of Michigan Media Union  
-----

---

*Solstice: An Electronic Journal of Geography and Mathematics, Institute of Mathematical Geography, Ann Arbor, Michigan.*

Volume XV, Number 1.

<http://www.InstituteOfMathematicalGeography.org/>

---

**MODELLING LOCATIONAL DECISION MAKING OF FIRMS USING  
MULTIDIMENSIONAL FUZZY DECISION TABLES:  
AN ILLUSTRATION**

**Frank J.A. WITLOX**

Ghent University  
Department of Geography  
Krijgslaan 281 (S8) – B-9000 Gent (Belgium)  
Email: frank.witlox@ugent.be

**Aloys W.J. BORGERS**

Eindhoven University of Technology  
Department of Architecture, Building and Planning,  
Urban Planning Group  
Email: a.w.j.borgers@bwk.tue.nl

**Harry J.P. TIMMERMANS**

Eindhoven University of Technology  
Department of Architecture, Building and Planning,  
Urban Planning Group  
Email: h.j.p.timmermans@bwk.tue.nl

## 1 INTRODUCTION

The locational decision making of firms can be modelled from different perspectives. Especially in economic research, several authors have suggested to use stated or revealed preference choice models to predict the probability that a particular location will be chosen as a function of its locational and non-locational attributes (Timmermans, 1986; Moore, 1988; Henley *et al.*, 1989; Friedman *et al.*, 1992). Such algebraic models do have the appeal of theoretical rigour, mathematical sophistication, and an associated error theory. However, the application of such models, in particular when revealed preference is used, is characterised by many problems, including high multi-collinearity among explanatory variables, complexity in the sense of a large number of influential attributes, and the fact that algebraic equations by definition cannot capture all theoretical notions. For example, the situation that at one level a locational requirement serves as a veto criterion, whereas at another level compensation is allowed, is difficult to represent using an algebraic equation.

A modelling approach that avoids these problems is qualitative modelling. The quintessence of this approach is to represent the locational decision-making process in terms of a set of IF, THEN ... ELSE expressions. These logical expressions have sufficient flexibility to represent a wider variety of decision rules. On the other hand, their “crisp” (or exact) nature implies the lack of an error theory, limiting in some cases the realism of such systems. In previous papers, Witlox *et al.* (1997) and Witlox and Timmermans (2000, 2002) therefore argued for the development of multidimensional *fuzzy* systems.

The current paper reports on the application of such a model to represent the locational decision making behaviour of firms, taking the petrochemical industry as an example. The article is organised as follows. In the second section, the problem of membership value measurement in a decision table environment is introduced. The aim is to introduce the technique that will enable us to estimate membership values of the fuzzy sets used in the condition part of a fuzzy decision table. The third section of this article discusses the process of membership value estimation. The fourth section reports on the application. Finally, in the fifth section, the results of this study are summarized and some issues for future research are discussed.

## 2 MEMBERSHIP VALUE MEASUREMENT IN A FUZZY DECISION TABLE

### 2.1 Fuzzy decision tables

A decision table (DT) consists of an exhaustive set of mutually exclusive conditions, leading to particular actions. Each DT consists of four quadrants: condition set  $[C_i]$ , action set  $[A_j]$ , condition space  $[\text{SPACE}(C_i)]$ , and action space  $[\text{SPACE}(A_j)]$ . The *condition set* consists of all the relevant conditions or attributes (inputs, premises or causes) that have an influence on the decision-making process. The *condition space* specifies all possible combinations of *condition states* of a condition. The *action set* contains all the possible actions (outputs, conclusions or consequences) a decision-maker is able to take. This is, the action set points to the possible choice outcome if (for instance) an existing location with a number of specific characteristics is processed through the DT. Finally, the *action space* contains the categorizations of all the possible *action states* of an action. Any vertical linking of an element from the condition space with an element from the action space produces a decision rule (Figure 1).

**Figure 1:** The general structure of a decision table

Problem area	
CONDITION SET	CONDITION SPACE
ACTION SET	ACTION SPACE

Traditionally, decision tables (DTs) are crisp, indicating that the conditions are specified in an exact manner. A potential problem of such DTs is that any measurement error is not taken into account. Fuzzy decision tables (FDTs) offer a solution to this problem. A fuzzy decision table (FDT) is an extended version of a crisp DT in order to deal with imprecise and vague decision situations (Francioni and Kandel, 1988; Vanthienen *et al.*, 1996). The extension amounts to the introduction of fuzzy sets in the condition and action space of the crisp DT; the crisp condition and action states are replaced with fuzzy conditions and actions. The latter two are a combination of fuzzy sets. A membership function needs to be specified which represents the extent to which a particular attribute level meets a particular condition

## 2.2 Membership value measurement

To discuss the issue of membership value measurement in a decision table environment, the problem is formally defined as follows. Assume that a decision table is characterised by  $I$  conditions ( $i = 1, 2, \dots, I$ ) with  $n_i$  states and  $A$  action states. In the case of a fuzzy table, the  $n_i$  states for each condition are fuzzy, and the table has  $M$  fuzzy action states,  $FAS_m$  ( $m = 1, 2, \dots, M$ ).  $FAS_m$  ( $m = 1, 2, \dots, M$ ) is carried out, if and only if, the fuzzy condition states  $FCS_{1?}$  &  $FCS_{2?}$  &  $FCS_{3?}$  &  $FCS_{4?}$  &  $FCS_{5?}$  & ... &  $FCS_{I?}$  are simultaneously satisfied. The question marks in the indices refer to the fuzzy condition states associated with each particular condition that, simultaneously combined, will result in the execution of fuzzy action state  $FAS_m$ . Note that  $FAS_m$  may be carried out by means of various combinations of fuzzy condition states. An important point is that in an FDT all interpretations should be made at the individual decision rule level (Wets, 1998). This point implies that we need to formalize our problem at the level of rules. To this end, three new notations are introduced:  $S_r$ ,  $x_{ir}$ , and  $\mu_{RULE_r}$ . Let  $S_r$  define the crisp set of all combinations  $(x_{1r}, x_{2r}, \dots, x_{Ir})$  resulting in the execution of  $RULE_r$  ( $r = 1, 2, \dots, R$ ). Let  $x_{ir}$  define the identifier or index (one of the numbers  $1, 2, \dots, n_i$ ) of the fuzzy condition state of  $C_i$ , in a way that  $RULE_r$  is carried out, if fuzzy condition states  $FCS_{ix_{ir}}$  for all  $i$  ( $i = 1, 2, \dots, I$ ) are satisfied. More formally: if  $\exists r \in \{1, \dots, R\}$  and  $\forall i \in \{1, \dots, I\}$ :  $FCS_{ix_{ir}}$  is satisfied, then  $RULE_r$  is carried out. Finally,  $\mu_{RULE_r}$  represents the membership value for  $RULE_r$ . The membership value for a single fuzzy action state (i.e.  $\mu_{FAS_m}$ ) can be achieved by adding the membership values for the corresponding rules. From now on, it is assumed that when action  $RULE_r$  ( $r = 1, 2, \dots, R$ ) is executed, all indexes  $x_{ir}$  ( $i = 1, 2, \dots, I$ ;  $r = 1, 2, \dots, R$ ) are known.

The finite set of fuzzy decision rules may then be defined as follows:

$$\text{if } FCS_{1x_{1r}} \text{ and } FCS_{2x_{2r}} \text{ and } \dots \text{ and } FCS_{Ix_{Ir}} \rightarrow RULE_r; \forall r \in \{1, \dots, R\}. \quad [1]$$

Assume further that for  $I$  conditions with  $n_i$  fuzzy condition states for each  $i$ , there exists a membership value (or truth value)  $\mu \in [0,1]$ . The problem then is to estimate these membership values according to the following model specification:

$$\mu_{RULE_1} = \mu_{1x_{11}}(C_1) \mu_{2x_{21}}(C_2) \dots \mu_{Ix_{I1}}(C_I) \quad [2a]$$

$$\mu_{RULE_2} = \mu_{1x_{12}}(C_1) \mu_{2x_{22}}(C_2) \dots \mu_{Ix_{I2}}(C_I) \quad [2b]$$

$$\dots \quad \dots$$

$$\mu_{RULE_R} = \mu_{1x_{1R}}(C_1) \mu_{2x_{2R}}(C_2) \dots \mu_{Ix_{IR}}(C_I) \quad [2c]$$

Or, equivalently,

$$\mu_{RULE_r} = \mu_{1x_{1r}}(C_1) \mu_{2x_{2r}}(C_2) \dots \mu_{Ix_{Ir}}(C_I); \forall r \in \{1, \dots, R\}. \quad [2d]$$

Subject to:

$$\sum_{k=1}^{n_i} \mu_{ik}(C_i) = 1; \forall i \in \{1, \dots, I\}. \quad [3]$$

Relation [3] is called the fuzzy condition state partition constraint. It states that the membership function values associated with the fuzzy condition states of a particular condition in the FDT need to sum up to unity. Hence, a probabilistic approach to fuzzy set theory is advocated here.

Suppose that an estimate of  $\mu_{ix_r}(C_i)$  can be represented by the parameters,  $\alpha_{ix_r}$ , leading to an estimate of  $\hat{\mu}_{RULE_r}$ , the model to be estimated then becomes:

$$\hat{\mu}_{RULE_r} = \alpha_{1x_{1r}} \alpha_{2x_{2r}} \alpha_{3x_{3r}} \dots \alpha_{Ix_{Ir}}; \forall r \in \{1, \dots, R\} \quad [4]$$

Subject to

$$0 \leq \alpha_{ix_r} \leq 1; \forall r \in \{1, \dots, R\}; \forall i \in \{1, \dots, I\}. \quad [5a]$$

$$\sum_{k=1}^{n_i} \alpha_{ik} = 1; \forall i \in \{1, \dots, I\}. \quad [5b]$$

For the model to be consistent, the following relation should also be satisfied:

$$\sum_{r=1}^R \hat{\mu}_{RULE_r} = 1. \quad [6]$$

Finally, the number of parameters to be estimated can be derived from the number of conditions and the number of associated fuzzy condition states. For instance, to estimate  $C_1$  with  $n_1$  fuzzy condition states,  $(n_1-1)$  parameters are required. This complies with the imposed constraints on the model specification. Thus, generalizing for  $I$  conditions with  $n_i$  ( $i = 1, 2, \dots, I$ ) fuzzy condition states, the number of parameters, denoted by  $J$ , to estimate is equal to:

$$\sum_{j=1}^I (n_j-1), \text{ or rearranged: } \left( \sum_{j=1}^I n_j \right) - I. \quad [7]$$

### 3 MEMBERSHIP VALUE ESTIMATION

The goal of the membership estimation is to find parameters that lie within the  $[0,1]$  interval. Calibration is done using maximum-likelihood (ML) estimation. To briefly describe the ML procedure, a likelihood function,  $L: \mathbf{Q} \rightarrow \mathbb{R}^+$  is introduced. This is a function of the unknown parameters that is denoted  $L(\mathbf{Q})$ , where  $\mathbf{Q}$  denotes the collection of unknown parameters being estimated in the model. The basic principle of the ML estimation is to find the value that maximises the likelihood of the observed sample. The maximum likelihood function for  $I$  independent conditions can then be written as follows:

$$L(\mathbf{Q}) = (\hat{\mu}_{RULE_1})^{f_{RULE_1}} (\hat{\mu}_{RULE_2})^{f_{RULE_2}} \dots (\hat{\mu}_{RULE_Z})^{f_{RULE_Z}} \quad [8]$$

which is equal to,

$$L(\mathbf{Q}) = \prod_{z=1}^Z (\hat{\mu}_{RULE_z})^{f_{RULE_z}} \quad [9]$$

where  $f_{RULE_z}$  denotes the number of observations (or frequencies) for each of the  $z \in \{1, \dots, Z\}$  associated fuzzy decision rules  $RULE_z$ .

The log-likelihood function may then be written as:

$$L^*(\mathbf{Q}) = \sum_{z=1}^Z f_{RULE_z} \ln (\hat{\mu}_{RULE_z}). \quad [10]$$

By substituting  $\hat{\mu}_{RULE_z}$  with their associated, expanded fuzzy condition state paths, the result is the following:

$$L^*(\mathbf{Q}) = \sum_{z=1}^Z f_{RULE_z} \ln \left[ \sum_{S_z} \alpha_{1x_{1z}} \alpha_{2x_{2z}} \alpha_{3x_{3z}} \dots \alpha_{ix_{iz}} \right]; \forall z \in \{1, \dots, Z\} \quad [11]$$

The log-likelihood function  $L^*(\mathbf{Q})$  is maximized with respect to the parameters  $\alpha_{ix_{iz}}$  subject to the imposed constraints stated in relations [5a] and [5b] and [6].

## 4 APPLICATION

### 4.1 The case

In this sub-section, we will illustrate the use of the multi-dimensional membership value estimation procedure applied to the data collected. In particular, we intend to create a fuzzy equivalent of the following DT representing locational requirements.

**Table 1:** DT representing the locational requirements

$C_1$ Site within port zone?	yes					no
$C_2$ Site <i>near</i> residential area?	yes	no				-
$C_3$ Site <i>near</i> school/hospital?	-	yes	no			-
$C_4$ Site <i>near</i> recreational area?	-	-	yes	no		-
$C_5$ Site <i>near</i> scenic area?	-	-	-	yes	no	-
$A_1$ Suitable	.	.	.	.	x	.
$A_2$ Non-suitable	x	x	x	x	.	x
	$RULE_1$	$RULE_2$	$RULE_3$	$RULE_4$	$RULE_5$	$RULE_6$

Table 1 depicts a decision table that specifies a number of essential locational requirements that have to be fulfilled to consider a particular site suitable for the economic activity under investigation. Only if a site meets all five conditions, is it classified as being suitable (i.e. rule  $RULE_5$ ). In all other cases, a site is evaluated as "non-suitable". Note that condition  $C_1$  is a strictly crisp condition. It deals with the issue of whether or not a site is situated somewhere within the legal boundaries demarcating the port region. Given that a site is either located within this zone or is not, only a crisp evaluation is possible. In contrast, the remaining four conditions all contain the notion of *nearness*, which is fuzzy and context-related. One way to avoid this type of vagueness is to redefine the conditions in the table in

non-fuzzy, crisp terms. For example, instead of asking a decision-maker whether or not a potential site is "near" a residential area, school/hospital, recreational area and scenic area, the decision-maker can be asked to indicate minimum separating distances. By way of illustration, Table 2 displays the resulting values.

**Table 2:** DT representing the locational redefined requirements

$C_1$ Site within port zone?	yes				no	
$C_2$ Distance to residential area (km)?	$X \leq 5$ (short)	$X > 5$ (long)			-	
$C_3$ Distance to school or hospital (km)?	-	$X \leq 8$ (short)	$X > 8$ (long)		-	
$C_4$ Distance to recreational area (km)?	-	-	$X \leq 10$ (short)	$X > 10$ (long)		-
$C_5$ Distance to scenic area (km)?	-	-	-	$X \leq 15$ (short)	$X > 15$ (long)	-
$A_1$ Suitable	.	.	.	.	x	.
$A_2$ Not satisfied	x	x	x	x	.	x
	$RULE_1$	$RULE_2$	$RULE_3$	$RULE_4$	$RULE_5$	$RULE_6$

An alternative approach would be to construct a fuzzy decision table by replacing all crisp condition states that have to be fuzzified with associated fuzzy membership values. In the present context, only condition  $C_1$  remains crisp which implies that its two states are each assigned a crisp value: i.e.  $CS_{11} = 1$  (denoting "yes") and  $CS_{12} = 0$  (denoting "no"). The condition states of the four remaining conditions are each assigned an unknown fuzzy value (denoted by  $\alpha$ ). In what follows, we assume that  $\alpha$  refers to the fuzzy set "long", whereas  $(1 - \alpha)$  points to the fuzzy set "short". Note that the degree of accepting the alternative increases as distance increases. Consequently, we are concerned with the estimation of the membership values of the fuzzy set "long", and deduce from it the membership values of the fuzzy set "short". Hence,  $FCS_{22} = \alpha_1$ ,  $FCS_{32} = \alpha_2$ ,  $FCS_{42} = \alpha_3$  and  $FCS_{52} = \alpha_4$ . Because the membership function values over the domain of a fuzzy set need to add to one, the corresponding fuzzy condition state values for the notion "short" are equal to  $FCS_{21} = (1-\alpha_1)$ ,  $FCS_{31} = (1-\alpha_2)$ ,  $FCS_{41} = (1-\alpha_3)$  and  $FCS_{51} = (1-\alpha_4)$ . The result is shown in Table 3.

**Table 3:** Contracted FDT representing the locational prerequisites

$C_1$ Site within port zone?	1					0	crisp
$C_2$ Distance to residential area?	$(1-\alpha_1)$	$\alpha_1$				-	fuzzy
$C_3$ Distance to school or hospital?	-	$(1-\alpha_2)$	$\alpha_2$			-	fuzzy
$C_4$ Distance to recreational area?	-	-	$(1-\alpha_3)$	$\alpha_3$		-	fuzzy
$C_5$ Distance to scenic area?	-	-	-	$(1-\alpha_4)$	$\alpha_4$	-	fuzzy
$FAS_1$ Suitable	.	.	.	.	x	.	fuzzy
$FAS_2$ Non-suitable	x	x	x	x	.	x	fuzzy
	$RULE_1$	$RULE_2$	$RULE_3$	$RULE_4$	$RULE_5$	$RULE_6$	

With the exception of condition  $C_1$ , all conditions in Table 3 have been assigned an unknown membership value that needs to be estimated. As a result of this membership value substitution, the action states of the table (i.e.  $FAS_1$  and  $FAS_2$ ) also become fuzzy since they combine different fuzzy condition states. The fuzziness in the table is visualised by the shades in the table.

In order to obtain valid parameter estimates, the estimation should take place at the individual decision rule level of the expanded FDT. Hence, the log-likelihood function,  $L^*(\mathbf{Q})$  with  $\mathbf{Q} = (\alpha_1, \alpha_2, \alpha_3, \alpha_4)$ , for the expanded FDT requirements is:

$$L^*(\mathbf{Q}) = \sum_{z=1}^{16} f_{RULE_z} \ln(\hat{\mu}_{RULE_z}) \quad [12]$$

The value of  $f_{RULE_z}$  referring to the number of observations for  $RULE_z$  ( $z = 1, 2, \dots, I$ ), should then be maximised with respect to the four unknown  $\alpha$ -values, subject to the constraint:  $0 \leq \alpha_1, \alpha_2, \alpha_3, \alpha_4 \leq 1$ . Note again that all interpretations are done on the expanded version of the FDT. Thus, all columns of the table contain only simple states (no combination of states). The relation between the expanded (with  $I = 16$ ) and contracted (with  $I = 5$ ) FDT is as follows:

Decision rules expanded FDT	Corresponding decision rule contracted FDT (Table 3)
$RULE_1 = (1 - \alpha_1) (1 - \alpha_2) (1 - \alpha_3) (1 - \alpha_4);$ $RULE_2 = (1 - \alpha_1) (1 - \alpha_2) (1 - \alpha_3) \alpha_4;$ $RULE_3 = (1 - \alpha_1) (1 - \alpha_2) \alpha_3 (1 - \alpha_4);$ $RULE_4 = (1 - \alpha_1) (1 - \alpha_2) \alpha_3 \alpha_4;$ $RULE_5 = (1 - \alpha_1) \alpha_2 (1 - \alpha_3) (1 - \alpha_4);$ $RULE_6 = (1 - \alpha_1) \alpha_2 (1 - \alpha_3) \alpha_4;$ $RULE_7 = (1 - \alpha_1) \alpha_2 \alpha_3 (1 - \alpha_4);$ $RULE_8 = (1 - \alpha_1) \alpha_2 \alpha_3 \alpha_4;$	→ $RULE_1;$
$RULE_9 = \alpha_1 (1 - \alpha_2) (1 - \alpha_3) (1 - \alpha_4);$ $RULE_{10} = \alpha_1 (1 - \alpha_2) (1 - \alpha_3) \alpha_4;$ $RULE_{11} = \alpha_1 (1 - \alpha_2) \alpha_3 (1 - \alpha_4);$ $RULE_{12} = \alpha_1 (1 - \alpha_2) \alpha_3 \alpha_4;$	→ $RULE_2;$
$RULE_{13} = \alpha_1 \alpha_2 (1 - \alpha_3) (1 - \alpha_4);$ $RULE_{14} = \alpha_1 \alpha_2 (1 - \alpha_3) \alpha_4;$	→ $RULE_3;$
$RULE_{15} = \alpha_1 \alpha_2 \alpha_3 (1 - \alpha_4);$	→ $RULE_4;$
$RULE_{16} = \alpha_1 \alpha_2 \alpha_3 \alpha_4;$	→ $RULE_5.$

The expanded part of the FDT contains 16 decision rules. In the crisp case, only one decision rule would match, namely that rule where all ones are found for a particular combination of  $\alpha_i$  and  $(1 - \alpha_i)$ . In all other rules, at least one zero-value would be found which, using the product operator, results in a zero match. In the fuzzy case, however, more than one decision rule can match a given combination of condition values. Hence, each of the 16 decision rules will influence the decision to be made. The possibility of accepting a rule is found again by applying the product operator.

#### 4.2 Data collection

To estimate the different membership values of the FDT, data on the relationship between actual distances and their classifications into long versus short are required. We propose to obtain these data by conducting an experiment in which the experts are presented with a number of profiles (combinations of conditions) and asked to evaluate these profiles in terms of the action states of the table. The profiles are derived from the expanded DT. The total number of profiles in the design is a function of the number of conditions to be fuzzified and the number of associated condition states making up the DT.

The DT shown in Table 2 contains four conditions, each having only two associated condition states. These two different states reflect the fact that only one crisp assessment point is used as a limiting value. For example, in the case of condition  $C_2$ , this single measurement point is equal to 5

km. The use of only one measurement point implies that no distinction can be made between values that fall within the same condition state. Hence, if the aim is to fuzzify a specified measurement point so that a gradual transition between crisp states becomes possible, it is necessary to introduce additional evaluation points. These additional measurement values should be centred on the initial crisp boundary point resulting in a fuzzy range.

Note that, if we do not introduce additional measurement points and simply present the experts with different profiles in which conditions can only take on two different values (e.g.  $X \leq 5$  and  $X > 5$ ), then this would not lead to a fuzzification of the initial measurement point in question. Instead, we would be measuring the degree of heterogeneity present in the sample. By contrast, the introduction of additional measurement points, subdividing the domain of the condition in more condition states, allows for subtler decision-making and is also indicative of the degree of crispness of the different boundary values.

The introduction of additional measurement points implies that the specified log-likelihood function,  $L^*(\mathbf{Q})$  with  $\mathbf{Q} = (\alpha_1, \alpha_2, \alpha_3, \alpha_4)$ , or in short,  $\mathbf{Q} = (\alpha_i)$  needs to be respecified. Hence, the following substitution is made:

$$\mathbf{Q} \rightarrow \mathbf{Q}^*, \text{ with } \mathbf{Q}^* = (\alpha_i^*), \text{ where } \alpha_i^* = \text{mp}_i^0 \pm c_i. \quad [13]$$

where  $\text{mp}_i^0$  is the initial boundary measurement point.

As a result of this substitution, the following log-likelihood function specification,  $L^*(\mathbf{Q}^*)$ , is obtained which should be maximised subject to  $0 \leq \alpha_i^* \leq 1$ . Note that  $c_i$  determines the spread of the fuzzy interval around the initial crisp measurement point. It specifies a lower (i.e.  $\text{mp}_i^0 - c_i = \text{mp}_i^-$ ) and an upper (i.e.  $\text{mp}_i^0 + c_i = \text{mp}_i^+$ ) measurement point. The membership values for each introduced measurement point for each condition are represented by  $\alpha_i^*$ . Consequently, depending on the value of  $c_i$ ,  $\alpha_i^*$  denotes the estimated membership value for the:

- (i) lower mp ( $\text{mp}_i^0 - c_i = \text{mp}_i^-$ ) :  $\alpha_i^* = \alpha_i^-$  subject to  $0 \leq \alpha_i^- \leq 1$ ;
- (ii) initial mp ( $\text{mp}_i^0$ ) :  $\alpha_i^* = \alpha_i^0$  subject to  $0 \leq \alpha_i^0 \leq 1$ ;
- (iii) upper mp ( $\text{mp}_i^0 + c_i = \text{mp}_i^+$ ) :  $\alpha_i^* = \alpha_i^+$  subject to  $0 \leq \alpha_i^+ \leq 1$ .

It logically follows from the interpretation given to the estimated membership values that the following relation should also hold:  $0 \leq \alpha_i^- \leq \alpha_i^0 \leq \alpha_i^+ \leq 1$  for the results to have face validity. When the distance increases, the membership function should increase as well.

In the present paper,  $c_i$  was taken as 2 km. Thus, for condition  $C_2$  representing the distance to a

residential area the three measurement points with their associated to be estimated membership values are equivalent to:

$$\begin{aligned} \text{mp}^-_1 &= 5 - 2 = "3" && \rightarrow \alpha^-_1; \\ \text{mp}^0_1 &= "5" && \rightarrow \alpha^0_1; \\ \text{mp}^+_1 &= 5 + 2 = "7" && \rightarrow \alpha^+_1. \end{aligned}$$

The specification of the measurement points used for each of the four conditions that need to be fuzzified can be found in Table 4.

**Table 4:** Specification and encoding of the measurement points

Condition	Specified crisp condition states	Measurement points (mp) used
$C_1$	"yes", "no"	—
$C_2$	" $X \leq 5$ ", " $X > 5$ "	$\text{mp}^-_1 = "3"$ $\text{mp}^0_1 = "5"$ $\text{mp}^+_1 = "7"$
$C_3$	" $X \leq 8$ ", " $X > 8$ "	$\text{mp}^-_2 = "6"$ $\text{mp}^0_2 = "8"$ $\text{mp}^+_2 = "10"$
$C_4$	" $X \leq 10$ ", " $X > 10$ "	$\text{mp}^-_3 = "8"$ $\text{mp}^0_3 = "10"$ $\text{mp}^+_3 = "12"$
$C_5$	" $X \leq 15$ ", " $X > 15$ "	$\text{mp}^-_4 = "13"$ $\text{mp}^0_4 = "15"$ $\text{mp}^+_4 = "17"$

Combining these 12 different measurement points in all possible ways would yield  $3^4 = 81$  experimental profiles (Addelman, 1962). Obviously, evaluation of this number of profiles would be too demanding a task for the experts and hence it was decided to use an orthogonal fractional factorial design. There are several possible basic plans that can be used to construct such a design, whereby the number of profiles ranges from 9 to 32. In the present paper, it was decided to use a plan involving 16 profiles, to construct the orthogonal fractional factorial design. Each profile consists of a combination of distances on the four conditions.

### 4.3 Tasks

Next, experts were asked to evaluate each profile in terms of the decision table's action states. By way of an example, Table 5 illustrates how the first profile specified in Table 4 is transformed in a DT (split in two parts to fit the size of the page). This DT, depicting 16 different rules, was written on an option card and presented to the respondents. The respondents were then asked to appraise each individual decision rule by filling in the action part of the DT ( $FAS_1 = \text{'satisfied'}$ ;  $FAS_2 = \text{'not satisfied'}$ ). Clearly, an identical approach was followed with respect to the remaining 15 profiles in the experiment. Note that condition  $C_1$  is not included in the option card, given its non-fuzzy character.

Table 5: Illustration of an option card (profile 0 0 0 0)

1. C2 Dist. to residential area?	$X \leq 3$							
2. C3 Dist. to school/hospital?	$X \leq 6$				$X > 6$			
3. C4 Dist. to recreational area?	$X \leq 8$		$X > 8$		$X \leq 8$		$X > 8$	
4. C5 Dist. to scenic area?	$X \leq 13$	$X > 13$						
1. FAS1 Satisfied	.	.	.	.	.	.	.	.
2. FAS2 Not satisfied	.	.	.	.	.	.	.	.
	1	2	3	4	5	6	7	8

1. C2 Dist. to residential area?	$X > 3$							
2. C3 Dist. to school/hospital?	$X \leq 6$				$X > 6$			
3. C4 Dist. to recreational area?	$X \leq 8$		$X > 8$		$X \leq 8$		$X > 8$	
4. C5 Dist. to scenic area?	$X \leq 13$	$X > 13$						
1. FAS1 Satisfied	.	.	.	.	.	.	.	.
2. FAS2 Not satisfied	.	.	.	.	.	.	.	.
	9	10	11	12	13	14	15	16

In total, useful answers of 16 experts were obtained. These experts were all CEO's of the companies included in the sample and had experience in site selection. The obtained answers are in fact frequency data for each action state of each decision rule of each DT in the experiment. In total, 4,096 observations (i.e. 16 profiles or DTs, each consisting of 16 decision rules evaluated by 16 different respondents) were obtained. These observations were placed in a matrix in the form of aggregated frequency data. This data matrix was used as input file to estimate the membership values for the 12 measurement points.

The membership values were estimated using an optimisation routine that was especially

developed for our estimation problem. The threshold value suggests that the iterations ended if the goodness-of-fit of the model did not improve more than 0.0001. The minimum and maximum values for the estimates were set — logically — at 0.0 and 1.0, respectively. The starting values were all set equal to 0.5; but these values were later changed in order ensure that no local optimum was found (ML estimation implies having a unimodal function). The results of the optimisation routine are shown in Table 6.

Table 6 depicts the membership value estimation results for the 12 measurement points (lower, initial and upper measurement points) for the four conditions in the FDT that were fuzzified. In addition, the increment in these estimated membership values is also given. Note that convergence was achieved after 4 iterations.

**Table 6:** Estimation results

	membership value estimation results			Increment in membership values		
	lower mp <sub>i</sub>	initial mp <sub>i</sub>	upper mp <sub>i</sub>	$\alpha_i^- \rightarrow \alpha_i^0$	$\alpha_i^0 \rightarrow \alpha_i^+$	$\alpha_i^- \rightarrow \alpha_i^+$
$C_2$	.088	.145	.241	.057	.096	.153
$C_3$	.285	.318	.410	.033	.092	.125
$C_4$	.353	.392	.416	.039	.024	.063
$C_5$	.412	.438	.461	.026	.023	.049
Log-likelihood: - 3605.43400 (4 iterations); $N = 4096$						

The overall estimation results of the different membership values may be considered very satisfactory. First, the estimation results are consistent with theoretical and logical expectations giving face validity to the results. The membership values increase as a higher measurement point is used. Fulfilling this property of *monotonicity* in the present context is important since the following relation,  $0 \leq \alpha_i^- \leq \alpha_i^0 \leq \alpha_i^+ \leq 1$ , should hold.

Second, the model produces identical estimation results if other starting values are used, suggesting that the true optimum was reached. This means that our optimum found is stable and independent from the selection of the starting values. In each case, the model returned our initial optimum found; only the number of iterations needed differed.

Third, our approach demonstrates that a multi-dimensional approach to estimate membership values and functions is possible and also desirable. Instead of selecting *ad hoc* four separate membership functions, they are now estimated simultaneously from the input data.

Analysed in more detail, a number of additional interesting conclusions can be drawn. First, it can be noted that for condition  $C_2$  (representing the distance to a residential area), a distance of 3 km (i.e. lower measurement,  $mp^-_1$ ) results in an almost zero membership value ( $\alpha^-_1 = 0.088$ ). Hence, all potential industrial locations that are situated at less than 3 km from a residential area will be evaluated as not satisfactory. In the data matrix used as input file, it can also be seen that nearly all decision rules that have  $X \leq 3$  result in a rejection of the alternative. Given that the associated membership value in the fuzzy set "long distance to a residential area" is (almost) equal to zero, the possibility of accepting this choice alternative will, as a result of the use of the product operator, also be (almost) equal to zero. Consequently, 3 km is considered (almost) a full member of the fuzzy set "short distance to a residential area" which implies that the possibility of *not* accepting this choice alternative will be (almost) equal to one. As the distance between a location site and a residential area increases (use of  $mp^0_1$  and  $mp^+_1$ ), the membership values to the fuzzy set "long distance to a residential area" also increase to .145 and .241, respectively. The increase is not strictly linear since the increments are .057 and .096. If the membership values found are set out against the three measurement points in a two-dimensional plane, and a curve is fitted through it, then the corresponding membership function for condition  $C_2$  is found. Once this function has been determined, it is also possible to calculate the corresponding membership values of other distances than those used as measurement points.

Second, the results found for condition  $C_3$  (distance to school or hospital) are equally satisfactory. Note, however, that the lower measurement point used does not result in an almost zero membership value. It is equal to .285. As one moves along the distance domain, the membership values increase.

Third, the membership value estimates for the measurement point of the remaining two conditions  $C_4$  and  $C_5$  show only little variation. The increment in membership value with changing distances is very small. Hence, their influence on the choice problem may be considered of minor importance. In particular, condition  $C_5$  (distance to a scenic area) has little influence on the choice outcome. The experts' behaviour was little influenced by altering distances to a scenic area. Besides showing little variation, it can be seen that the membership values found are also close to 0.5, which may point to a situation of indecision.

## 5 CONCLUSION AND DISCUSSION

In this paper, a method proposed to estimate membership values of the fuzzy sets used in the condition and action part of a fuzzy decision table (FDT) was applied to the locational preference of decision makers in the petro-chemical industry. Although, only 16 valuable results from 19 respondents were

obtained for the purpose of fuzzification, it can be stated that the constrained maximum likelihood estimation procedure performs adequately with real data. The model produces valid estimation results that fulfil all desired properties (face validity, unimodality, partition constraint). Furthermore, the approach is multi-dimensional and the method is also direct. The latter characteristic refers to the fact that the membership functions can be directly deduced from the input data. The developed approach also concurs very well with the introduced concept of an FDT.

A (more or less disadvantageous) point of the modelling approach that should also be stressed is the problem of data collection. It is no coincidence that this particular problem is closely linked with the table contraction-expansion problem in an FDT. It is only when an FDT is specified and estimated in its expanded form (i.e. at the individual decision rule level) that valuable estimation results can be obtained. To a certain extent, this problem restricts the application of our approach in that the multidimensional fuzzification of large FDTs is rather problematic. Working with expanded FDTs has an effect on the data that are needed to estimate the model; these data should be collected at the individual decision rule level. Hence, the more condition and action states in the FDT, the larger the set of fuzzy decision rules, and thus the more difficult the task will be for the participating respondents.

## 6 REFERENCES

- ADDELMAN, S. (1962) "Orthogonal main-effect plans for asymmetrical factorial experiments". *Technometrics*. Vol. 4 (1), pp. 21-46.
- FRANCIONI, J.M. & A. KANDEL (1988) "A software engineering tool for expert system design". *IEEE Expert*. Vol. 3 (1), pp. 33-41.
- FRIEDMAN, J., D.A. GERLOWSKI & J. SILBERMAN (1992) "What attracts foreign multinational corporations? Evidence from branch plant location in the United States". *Journal of Regional Science*. Vol. 32 (4), pp. 403-418.
- HENLEY, A., A. CARRUTH, A. THOMAS & R. VICKERMAN (1989) "Location choice and labour market perceptions: a discrete choice study". *Regional Studies*. Vol. 23 (5), pp. 431-445.
- MOORE, L. (1988) "Stated preference analysis and new store location". In: N. WRIGLEY Ed. (1988) *Store Choice, Store Location and Market Analysis*. London, Routledge, pp. 203-224.
- TIMMERMANS, H. (1986) "Locational choice behaviour of entrepreneurs: an experimental analysis". *Urban Studies*. Vol. 23 (3), pp. 231-240.
- VANTHIENEN, J., G. WETS & G. CHEN (1996) "Incorporating fuzziness in the classical decision table formalism". *International Journal of Intelligent Systems*. Vol. 11 (11), pp. 879-891.
- WETS, G. (1998) *Decision Tables in Knowledge-Based Systems: Adding knowledge discovery and fuzzy concepts to the decision table formalism*. Leuven. Acco, Ph.D. thesis.

WITLOX, F. & H. TIMMERMANS (2000) "MATISSE: A knowledge-based system for industrial site selection and evaluation". *Computers, Environment and Urban Systems*. Vol. **24** (1), pp. 23-43.

WITLOX, F. & H.J.P. TIMMERMANS (2002) "Representing locational requirements using conventional decision tables: theory and illustration". *Geographical & Environmental Modelling*. Vol. **6** (1), pp. 59-79.

WITLOX, F., T. ARENTZE & H. TIMMERMANS (1997) "Constructing and consulting fuzzy decision tables". In: H. TIMMERMANS (Ed.) *Decision Support Systems in Urban Planning*. London, E & FN Spon, pp. 156-174.

## The View from the Top: Visualizing Downtown Ann Arbor in Three Dimensions

Sandra L. Arlinghaus, Fred J. Beal, Douglas S. Kelbaugh  
Download [Cortona](#) to see virtual reality

### 2004:

#### Meeting materials:

[June 7](#), [May 29](#), [May 27](#),  
[May 12](#), [May 10](#), [April 27](#),  
[April 26](#), [April 14](#), [April 7](#),  
[April 1](#), [March 18](#), [March](#)  
[12](#), [February 16](#), [February](#)  
[7](#), [February 2](#)

- Arlinghaus: Adjunct Professor, School of Natural Resources and Environment and Taubman College of Architecture and Urban Planning, The University of Michigan; Community Systems Foundation; IMAge; Arlinghaus Enterprises, L.L.C. [sarhaus@umich.edu](mailto:sarhaus@umich.edu)
- Beal: President JC Beal Construction Inc.; Downtown Development Authority; Downtown Residential Taskforce Member
- Kelbaugh: Professor and Dean, Taubman College of Architecture and Urban Planning, The University of Michigan; Downtown Residential Taskforce Member

### 2003:

#### Publications in

##### Solstice:

[December 21a](#), [December](#)  
[21b](#), [June 21](#)

[Handout:November 11](#),

**Links are provided to the complete set of virtual reality files created (about 3 gigabytes); due to server issues with the thousands of files involved, it may be that not all links will function all the time. Please contact the first author if VR files are desired that do not come up; at the very least, files will be rotated in and out of server space in response to reader demand (initially, the most recent VR files are placed on the server). All images, many derived from VR files, should appear all the time.**

[2D Images](#)

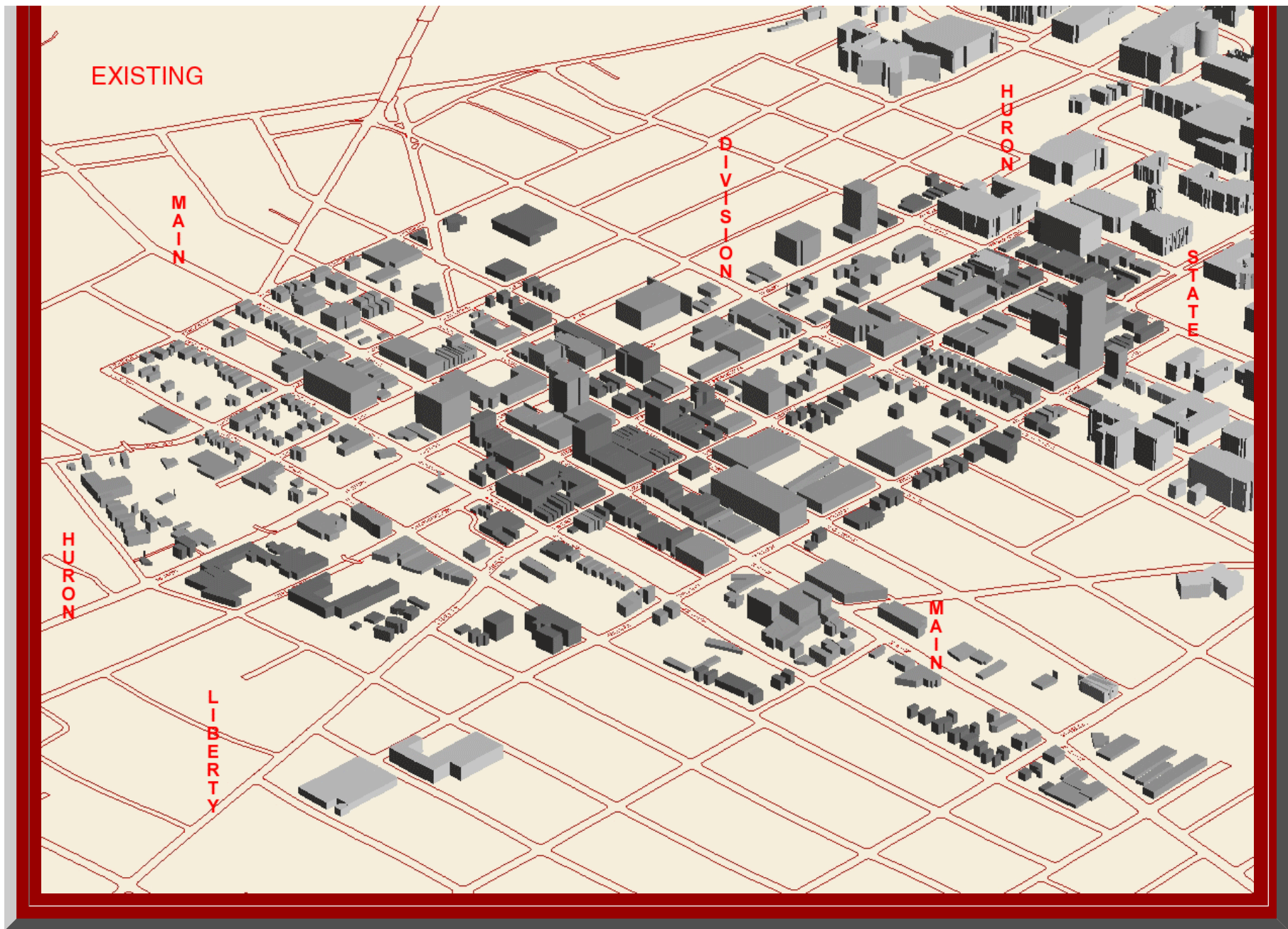
[Interactive Images](#)

[3D Images](#)

On June 7, 2004, the Downtown Residential Taskforce presented recommendations for increasing residential land use in the downtown to the City Council of the City of Ann Arbor. Some of the policy statements in that document derived support from earlier three-dimensional analysis, using virtual reality models and derivative animations. This article displays the complete chronological unfolding of the models behind a part of this document. Broadly stated, it synthesizes theory and practice: from the academic realm of model creation and the mathematical geography behind that activity, to the real-world arena of policy and decision makers. The maps and models we make can influence the decisions that are made; conversely, the decisions we make can shape the maps and models that are built. This interactive process between maps and decisions was in full force in this study. Follow the links on the left, in the "Archive" section, to watch the historical elements of this process unfold.

SCREEN CAPTURE OF A VIRTUAL REALITY MODEL OF EXISTING DOWNTOWN ANN ARBOR. BUILDING SHAPES ARE SIMPLY EXTRUDED FROM FOOTPRINTS DIGITIZED FROM AN AERIAL.





The authors wish to thank all members of the Downtown Residential Taskforce: in addition to the two members noted above, Susan Pollay (Executive Director, Downtown Development Authority), Karen Hart (Planning Director, City of Ann Arbor), Jean Carlberg (City Council), Wendy Woods (City Council), Steve Thorp (Chair, Planning Commission), Frances Todoro (Mayor's Office), Robert Gillett, and William D. Kinley. Their thoughtful comments have helped, in various ways, to shape selected images (and are so noted when that influence was direct). Brian Barrick and Peter Pollack, both of Pollack Designs, followed our work with interest, as did Ray Detter, DDA Citizens Advisory Committee (we thank Ray for his eagle eye on building inclusion/exclusion issues). They also thank Merle Johnson of the City of Ann Arbor

ITS Department and Chandra Hurd of the City of Ann Arbor Planning Department: the former for his generosity in sharing aerials and maps from City of Ann Arbor files and the latter for sharing her expertise in analyzing city data and in checking selected files present on this site. Donald T. Uchman, Coordinator of Space Graphics, Space Information and Planning, Plant Extension--AEC, The University of Michigan, generously shared official University map files on locations and sizes of buildings. Finally, they thank an anonymous referee for his/her constructive comment. Remaining errors are ours alone.

The first author wishes to thank, in addition, the ongoing advice and support associated with various projects related to this one from the 3D Laboratory of the Media Union of The University of Michigan, Prof. Peter Beier, Ph.D., Director.

## Bibliography

- Adams, Paul C. 1998. "Network topologies and virtual place." *Annals of the Association of American Geographers*, vol. 88, no. 1 (March): 88-106.
- Arlinghaus, S. L. Summer 2003. Ann Arbor, Michigan: Virtual Downtown Experiments. Solstice: An Electronic Journal of Geography and Mathematics. Vol. XIV, No. 1, <http://www-personal.umich.edu/~copyright/image/solstice/sum03/sandy/downtown.html>
- Arlinghaus, S. L. Winter 2003. Ann Arbor, Michigan: Virtual Downtown Experiments, Part II. Solstice: An Electronic Journal of Geography and Mathematics. Vol. XIV, No. 2, <http://www-personal.umich.edu/~copyright/image/solstice/win03/mappingheight.html>
- Arlinghaus, S. L.; Arlinghaus, W. C.; and Harary, F. 2002. *Graph Theory and Geography: an Interactive View eBook*. New York: John Wiley and Sons.
- Arlinghaus, S. L. and Arlinghaus, W. C. 2003, in progress. *Spatial Synthesis*. (Possible e-publication ...)
- Batty, Michael and Yichun Xie. 1994. "From cells to cities." *Environment and Planning B: Planning and Design*, vol. 21, "Celebration Issue": 531-548.
- Batty, Michael. 1994. A chronicle of scientific planning: The anglo-American modeling experience. *Journal of the American Planning Association*, 60, 7-16.
- Batty, Michael. 1994. "Using GIS for visual simulation modeling." *GIS World*, vol. 7, no. 10. Page numbers needed.
- Batty, Michael. 1992. "Urban modeling in computer-graphic and geographic information system environments." *Environment and Planning B: Planning and Design*, vol. 19: 663-688.
- Bay, Alan. 1994. From map to model: the development of an urban information system. *Design Studies*, 15 (3), 366-384.
- Beier, Peter. 2003. Modification of files of a downtown Ann Arbor virtual reality scene: [http://www.engin.umich.edu/class/eng477/projectsf03/MAP/vrml/downtown\\_annarbor.wrl](http://www.engin.umich.edu/class/eng477/projectsf03/MAP/vrml/downtown_annarbor.wrl)
- Birta, Louis G. and Tuncer I. Oren. 1995. "Simulation modeling for environmental problems: a review of the current state." *Simulation*, vol. 64 (April): 280-282.
- Bishop, I.; Dave, B. 2001. *Beyond the Moving Camera: Systems Development for Interactive Immersive Exploration of Urban Environments*, Paper for Computers in Urban Planning and Urban Management
- Bishop, Ian; Spring, D.; John W.; and, Potter, R. 1995. Extending the geographic information base into the third dimension for use in the urban environment. *Journal of the Urban and Regional Information Systems Association*, 7 (1), 20-25.
- Borkin, Harold and Turner, James A. 1978. "The Development of Three-Dimensional Spatial Modeling Techniques for the Construction Planning of Nuclear Power Plants," *SIGGRAPH*, McIntosh
- Bosselman, Peter and K. H. Craik. 1987. Perceptual simulations of environments. In Bechtel, R. B., et al. eds, *Methods in Environmental and Behavioral Research*, (162-190), New York: Van Nostrand and Reinhold and Company.
- Bowman, D., Davis, E., Badre, A., & Hodges, L. 1999. *Maintaining Spatial Orientation during Travel in An Immersive Virtual Environment*. *Presence: Teleoperators and Virtual Environments*, 8(6), 618-631.
- Brail, R. K. 1990. "Integrating urban information systems and spatial

- models." *Environment and Planning B*, 17: 417-427.
- Branch, Melville C. 1997. *Simulation, Planning and Society*. New York: Praeger.
  - Bressi, Todd. 1995. The real thing? We're getting there. *Planning*, 61 (7) July, 16-20.
  - Britton, Harris. 1985. Urban simulations models in regional science. *Journal of Regional Science*, 25 (4), 545-567.
  - Chirapiwat, Thana. 2001. Visualization of Geographic Information using VRML. <http://www-personal.engin.umich.edu/~tnac/vrml/GISVisualization>
  - Couclelis, Helen. 1997. From cellular automata to urban models: new principles for model development and implementation. *Environment and Planning B*, vol. 24, no. 2: 165-174.
  - Cruz-Neira, C., Sandin, D. J., Fanti, T. A. D., & Hart, J. C. 1992. The Cave: Audio Visual Experience Automatic Virtual Environment. *Communications of the ACM*, V.35, 64-72.
  - Daniel, T. C., & Vining, J. 1983. Methodological Issues in the Assessment of Landscape Quality. In I. Altman & J. F. Wohlwill (Eds.), *Behavior and the Natural Environment* (pp. 39-84). New York: Plenum.
  - Decision Board, 2003. <http://www.decisionboard.org/academic/zzzsubject11.asp>
  - Decker, John. 1993. Simulation methodologies for observing large-scale urban structures. *Landscape and Urban Planning*, 26, 231-250.
  - Disaster Research, December, 2003. GIS and Hazards. <http://hazards.lsu.edu>
  - Doyle, Simon; Dodge, Martin; and Smith, Andy. 1998. Potiental of web-based mapping and virtual reality technologies for modeling urban environments. *Computers, Environment and Urban Systems*, vol. 22, no. 2 (March): 137-155.
  - Erikson, C., and W. Hundley. 1996. Advancements in related technologies bring virtual reality to GIS. In *Proceedings of the High-Fidelity Simulation for Training, Test Support, Mission Rehearsal, and Civilian Applications*, SPIE: 14-18.
  - Fedra, K. 1999. "Integrating monitoring, GIS and simulation models: Urban environmental management. *Geomatics Info Magazine*, vol. 13, no. 7: 28-31.
  - Forrester, John. 1989. *Planning in the Face of Power*. Berkeley: University of California Press.
  - Frueh, Christian (Prof. Avidah Zakhori). 2003. Fast, Automated 3D Model Reconstruction for Urban Environments. <http://www-video.eecs.berkeley.edu/~frueh>
  - Goodchild, Michael F. 1987. A spatial analytical perspective on geographic information systems. *International Journal of Geographical Information Systems*, 1 (4) October-December, 327-334.
  - Haala, Norbert and Claus Brenner. 1999. "Extraction of buildings and trees in urban environments." *Journal of Photogrammetric Engineering and Remote Sensing*, vol. 54, no. 2: 130-137.
  - Han, Seung-Hoon, 2003. Ph.D. Dissertation, December, 2003. "A Working Prototype of Distributed Collaborative Architectural Design System." University of Michigan, College of Architecture and Urban Planning.
  - Hardie, Graeme J. 1988. Community participation based on three-dimensional simulation models. *Design Studies*, 9 (1) January, 56-61.
  - Hazelton, N. W. J., Leahy, F. J., and Williamson, I. P. 1992. Integrating dynamic modeling and geographic information systems. *Journal of the Urban and Regional Information Systems Association*, 4 (2), 47-58.
  - Hearnshaw, H. M. and Unwin, D. J. eds. 1994. *Visualization in Geographical Information Systems*. New York: John Wiley and Sons.
  - Huang, Bo and Hui Lin. 1999. GeoVR: a web-based tool for virtual reality presentation from 2D GIS data. *Computers and Geosciences*, vol. 25, no. 10 (December): 1167-75.
  - Hutchinson, Bruce and Batty, Michael. 1986. *Advances in Urban Systems Modeling*. New York, Elsevier Science Publishing Co.
  - Jepson, William. (1992). UCLA Urban Simulator. <http://www.research.ucla.edu/chal/20.htm>
  - Jiang, B.; Claramunt, C.; and Batty, M. 1999. Geometric accessibility and geographic information: Extending desktop GIS to space syntax. *Computers, Environment and Urban Systems*, vol. 23, no. 2: 127-146.
  - Johnson, Glenn O. 1992. GIS applications in emergency management. *Journal of the Urban and Regional Information Systems Association*, 4 (1), 66-72.
  - Kaiser, E. J. and Godschalk, D. R. 1995. Twentieth century land use planning : A stalwart family tree. *Journal of the American Planning Association*, 61, (3)

- Summer, 365-385.
- Klosterman, Richard E. 1994. Large-scale urban models: Retrospect and prospect. *Journal of the American Planning Association*, vol. 60: 3-6.
  - Kreuseler, Matthias. 2000. Visualization of geographically related multidimensional data in virtual 3D scenes. *Computers and Geosciences*, vol. 26, no. 1 (February): 101-108.
  - Kwon, Taejung; Lazzaro, Adrien; Oppenheim, Paul J.; and Rosenblum, Aaron. Winter, 2003. Ann Arbor, Michigan: Virtual Downtown Experiments, Part III. Solstice: An Electronic Journal of Geography and Mathematics. <http://www-personal.umich.edu/~copyrght/image/solstice/win03/MAP/index.html>
  - Landis, John and Zhang, M. 1998. The second generation of the California urban futures model: Part 1: model logic and theory. *Environment and planning B: Planning and Design*, vol. 25, no. 5: 657-666.
  - Lange, Echart. 1994. Integration of computerized visual simulation and visual assessment in environmental planning. *Landscape and Urban Planning*, 30, 99-112.
  - Liggett, R., & Jepson, W. 1995. An integrated environment for urban simulation. *Environment and Planning B*, 22,291-305.
  - Loeb, Arthur L. 1976. *Space Structures: Their Harmony and Counterpoint*. Reading, MA: Addison-Wesley
  - Longley, Paul and Batty, Michael (eds.). 1996. *Spatial Analysis: Modelling in a GIS Environment*. New York: John Wiley and Sons.
  - Ma, Y.; Soatto, S.; Kosecka, J.; and Shastry, S. S. 2004. *An Invitation to 3-D Vision: From Images to Geometric Models*. New York, Springer Verlag, Series in Interdisciplinary Applied Mathematics.
  - Marans, R. W. and Stokols, D. 1993. *Environmental simulation: Research and policy issues*. New York: Plenum Press.
  - Michigan Society of Planning. 2003 version. *Community Planning Principles*. Michigan Society of Planning, 219 S. Main Street, Ann Arbor, MI 48104, <http://www.planningmi.org/resources/principles.htm>
  - Molnar, D. J. 1986. SCEEN: An Interactive Computer Graphics Design System for Real-time Environmental Simulation. *Landscape Journal*, 5,128-134.
  - Nadeau, D. R. 1999. Building Virtual Worlds with VRML. *IEEE Computer Graphics and Applications*, March/April 1999,18-29.
  - Naud, M. *LandView III, Manual for Windows*. Unpublished: distributed at conferences.
  - Nystuen, J. D. 1967. Boundary shapes and boundary problems. *Peace Research Society, Papers, VII, Chicago Conference*.
  - Nystuen, J. D. 1963. "Identification of Some Fundamental Spatial Concepts," *Papers, Michigan Academy of Letters, Sciences, and Arts, v. 48(1963): 373-384*.
  - Nystuen, J. D. 1961. with Michael F. Dacey, "A Graph Theory Interpretation of Nodal Regions," *Papers and Proceedings, Regional Science Association, v. 7 : 29-42*.
  - Nystuen, J. D. 2002. "Thünen Society, North American Division," *Solstice: An Electronic Journal of Geography and Mathematics, Volume XIII, Number 1*, <http://www.InstituteOfMathematicalGeography.org/>
  - Nystuen, J. D. "What's at Home: Shelter for the Poor in Low Income Cities," *Solstice: An Electronic Journal of Geography and Mathematics, vol. XI no. 2* <http://www.InstituteOfMathematicalGeography.org/>
  - O'Neill, M. J. 1991. Evaluation of a conceptual model of architectural legibility. *Environment and Behavior*, 23,259-284.
  - Palmer, Thomas C. Jr. Feb. 16, 2004 "Selling in 360 degrees," *Boston Globe*. [http://www.boston.com/business/articles/2004/02/16/selling\\_in\\_360\\_degrees/](http://www.boston.com/business/articles/2004/02/16/selling_in_360_degrees/)
  - Ranzinger, M. and Gleixner, G. 1995. Changing the city: datasets and applications for 3D urban planning. *GIS Europe*, vol. 4, no. 2: 28-30.
  - Raper, J. (Ed.) 1989. *Three Dimensional Applications in Geographical Information Systems*. London, New York: Taylor and Francis.
  - Rycus, M. J. 2003. "Object-Oriented Programming and Chaos Modeling in Planning," Mitchell J. Rycus, in, *The Planner's Use of Information*, Dandekar, H. C., Ed., 2nd. Edition; Planners Press, American Planning Association, Chicago, IL; pp 152-153.
  - Rycus, M. J. August, 2003. "Security Planning with Risk Assessment Models," White Paper prepared for Straec Technologies, ([www.straec.com](http://www.straec.com)).
  - Rycus, M. J. 2000. "Crime Reduction Strategies for Planning Departments" M. J. Rycus. *Michigan Planner; The Michigan Society of Planning Officials; Vol. 4, No.*

- 8; pp 1,6-7.
- Rycus, M. J. 1995-96 (Winter). "The Role of Urban Planning in Crime Reduction," City Planning and Management News, pp 3-4.
- Rycus, M. J. 1991. "Urban Terrorism: A Comparative Study," Journal of Architecture and Planning Research, 8:1-14..
- San Diego 2003. GeoWorld. [http://www.geoplace.com/gw/2001/0110/0110dv\\_1.asp](http://www.geoplace.com/gw/2001/0110/0110dv_1.asp)
- Shiffer, M. J. 1992. Toward a Collaborative Planning System. Environment and Behavior B: Planning and Design. 19, 709-722.
- SimCity, <http://www.simcity.com/>
- Simpson, David M. 2001. Virtual reality and urban simulation in planning: A literature review and topical bibliography. Journal of Planning Literature. Vo. 15, No. 3, Feb. 2001: 359-376.
- Smardon, et al. eds., 1999. Foundations for Visual Project Analysis, 115-139, New York: John Wiley and Sons.
- [http://www.giscafe.com/magazine/index.php?run\\_date=01-Sep-2003&newsletter=1](http://www.giscafe.com/magazine/index.php?run_date=01-Sep-2003&newsletter=1)
- Stokols, Daniel. 1977. Perspectives on Environment and Behavior: Theory, Research, and Applications. New York: Plenum.
- Thrall, Grant Ian, Ruiz, M., Sidman, C., and Elshaw-Thrall, S. 1993. Using GIS tools to analyze and visualize spatial phenomena. Geo Info Systems, 3 (5) May, 59-65.
- Turner, James. 2003. Syntax2D User's Manual. The University of Michigan.
- University of Michigan Record, November 17, 2003. Grant funds disaster simulation training: Center will prepare emergency workers for attacks. Jared Wadley, byline.
- Urdang, E. and Stuart, R. 1992. Orientation enhancement through integrated virtual reality and geographic information systems. In Proceedings of the Virtual Reality and Persons with Disabilities, CSUN: 55-62.
- van Veen, H. A., Distler, H. K., Braun, S. J., & Bulthoff, H. H. 1998. Navigating through a virtual city: Using virtual reality technology to study human action and perception. Future Generation Computer Systems, 14, 231-242.
- Verbree, E., van Maren, G., Germs, R., Jansen, F., & Kraak, M.-J. 1999. Interaction in virtual world views- linking 3D GIS with VR. International Journal of Geographical Information Science, 13(4), 385-396.
- Walzer, Norman. 1996. Community Strategic Visioning Programs. Westport, CT: Praeger Publishers.
- Yeh, A. G. O. and Batty, M. 1990. Applications of geographic information systems in urban and regional planning. Environment and Planning B: Planning and Design, vol. 17 (4): 369-374.
- Zube, E. H. and Simcox, D. E. 1993. Landscape Simulation: Review and Potential. In Marans, Robert W. and Stokols, Daniel, eds., Environmental Simulation: Research and Policy Issues (253-278), New York: Plenum Press.

Bibliography (from a "working" bibliography used in conjunction with grant application material generated for a proposal through TCAUP, UM)

---

*Solstice: An Electronic Journal of Geography and Mathematics, Institute of  
Mathematical Geography, Ann Arbor, Michigan.*  
Volume XV, Number 1.  
<http://www.InstituteOfMathematicalGeography.org/>

---

## Visualizing Accessibility II: Access to Food

*Marc Schlossberg*

*Assistant Professor*

*Planning, Public Policy, and Management*

*University of Oregon*

[schlossb@uoregon.edu](mailto:schlossb@uoregon.edu)

Food security is emerging as an important aspect of community and social planning, reflected in part by a recent special issue on Community Food Systems of the *Journal of Planning Education and Research* (JPER). As noted by Campbell (2004), food systems involve many stakeholders with differing values across space and time. One particular element of this larger food security issue revolves around transportation access to local food retailers. Such access is particularly important for the poor and other transportation disadvantaged who may lack mobility options (Clifton 2004). Thus, one important component of a Community Food Assessment system (Pothukuchi 2004) is to investigate and understand the spatial relationship of where individuals live and their spatial proximity to primary food outlets.

From a planning perspective, locating food outlets within neighborhoods that are easily reached through walking is often a desirous outcome. Bernick and Cervero (1997) found that people who live in pedestrian oriented environments were more likely to go by foot to the market. Handy (1995) found that residents that live in “traditional neighborhoods” have also been found to make two to four more walk/bicycle trips-per-week to neighborhood stores than those living in nearby, automobile oriented environments. And recently, Krizek (2003) found that people who live in areas with good “neighborhood accessibility” are more likely to walk and use transit than are those who live in more traditional auto oriented environments.

Markets that are within walking distance to all residents allow for equity of access; car ownership should not be the prerequisite to purchase food. The physical exercise associated with walking to a local market is an additional small way to combat growing societal waistlines. There may be, as well, enhanced social capital building opportunities when people travel through neighborhoods by foot to local food sites.

The following maps provide a visual and spatial approach to understanding access to food outlets for residents of the City of Eugene, Oregon. A description and discussion is presented under each map. Visualizing data in this way can be helpful to community planning endeavors; the visual approach transforms the abstract issue of transportation access to food into concrete understanding. Some of the maps below (Figures 2, 3, 5, and 6) were made for a food summit, hosted by the nonprofit agency Food for Lane County. They were designed to add one more piece of data and understanding to a county-wide discourse on addressing various food issues within Lane County, Oregon.

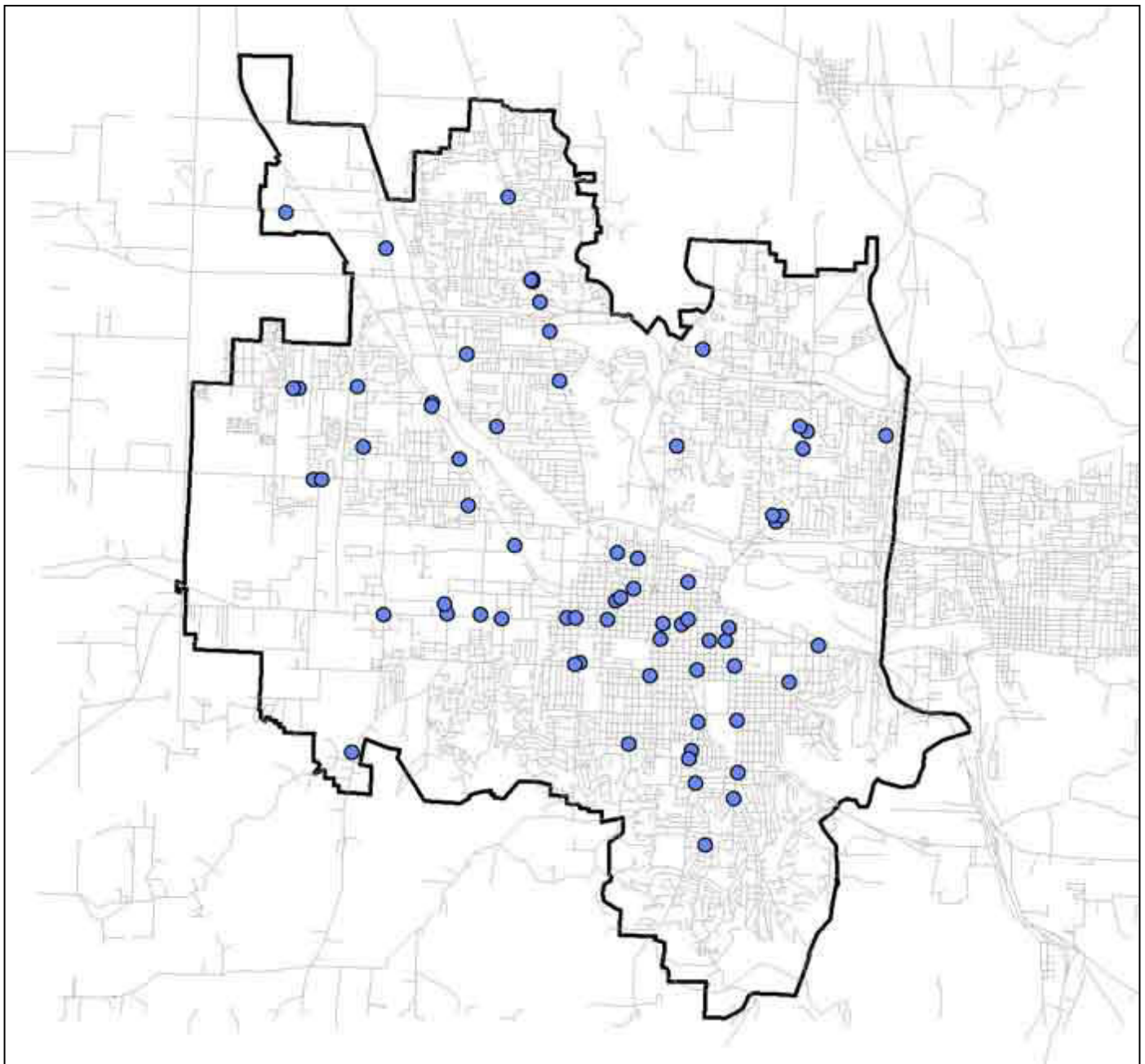


**Figure 1.** Stores and Streets.

The map in Figure 1 shows the location of sixty-nine different food markets. The underlying street network is displayed as well, providing an initial visual understanding of the urban form throughout the city. Where there is a concentration of stores in the center and center-south area, there is also a fairly tight gridded street network, representing a traditional downtown and neighborhood area in close proximity to the University of Oregon.



**Figure 2.** Food Markets by Type.

The map in Figure 2 partitions food outlets by type of establishment. In this case, retail stores have been divided into four primary categories: convenience stores, ethnic markets, neighborhood markets, and supermarkets. Both convenience stores and neighborhood markets are often located in close proximity to residential locations, but neighborhood markets are characterized by offering higher quality foods of a greater variety, including fresh produce. Although the map (Figure 2) does delineate markets by type, viewing all types at the same time while simultaneously trying to get a sense of one's accessibility to the market is difficult. The series of maps below, therefore, represents accessibility by market type.

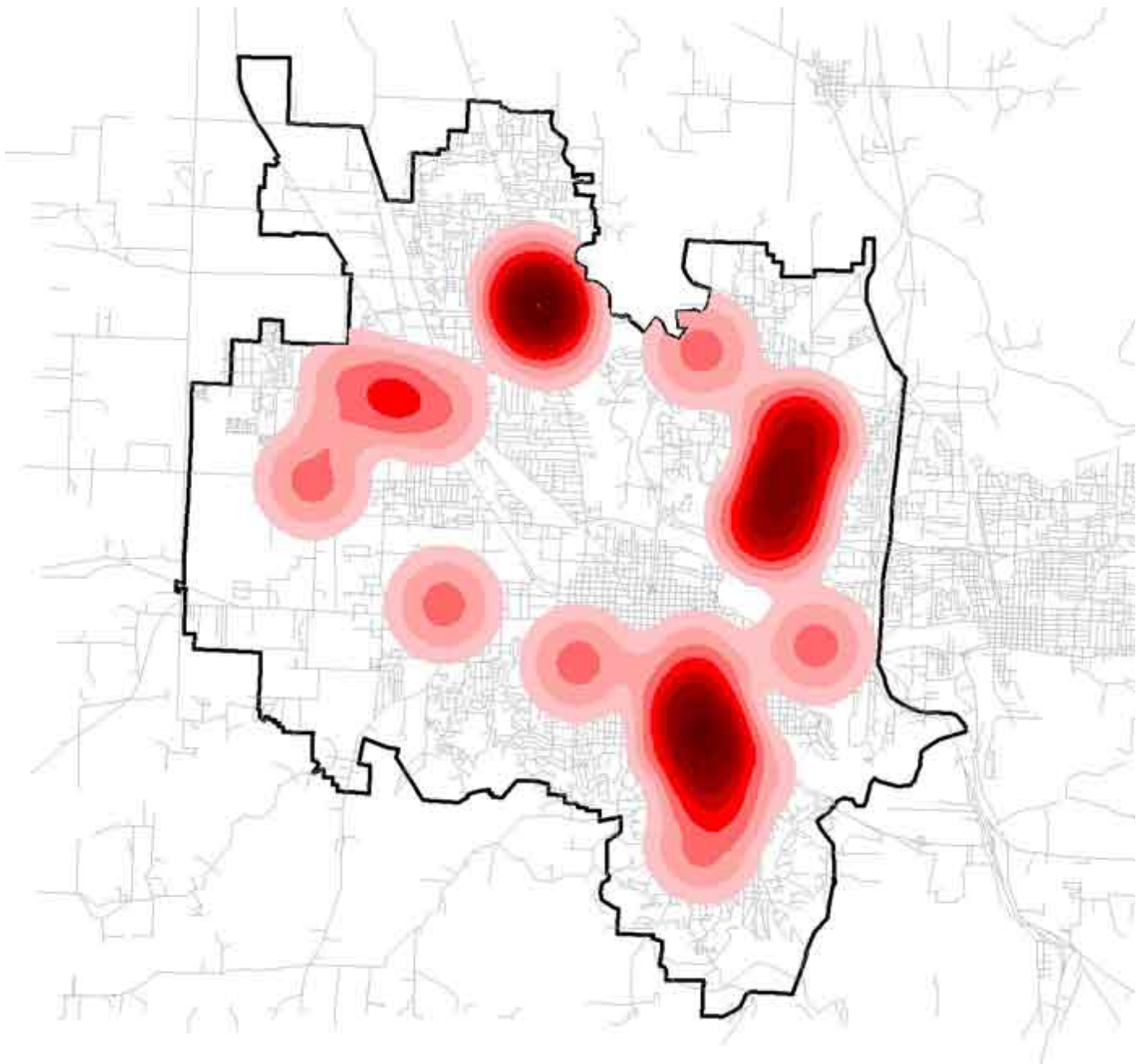


**Figure 3.** Access to Supermarkets.

In the map in Figure 3, the density of supermarkets is displayed throughout the Eugene area. A 1-mile distance has been used as a buffer; the outer edge of the most distant and lightest band of color (light pink) is one mile from the nearest supermarket. Medium colors represent areas that have good access to a single store, while the darkest reds represent areas in Eugene that have access to multiple supermarkets - places with superb supermarket access.

It is interesting to note the general pattern of supermarket access as well. There is a general band of markets that encircles the geographic center of Eugene. This center, as defined by the map in Figure 3, actually includes two distinct areas. One area is a traditional downtown composed primarily of commercial establishments (e.g. offices, restaurants, stores); the other area is largely industrial. Both contain land use types in which one would not expect to find supermarkets. The following maps show where there are areas of medium residential density.

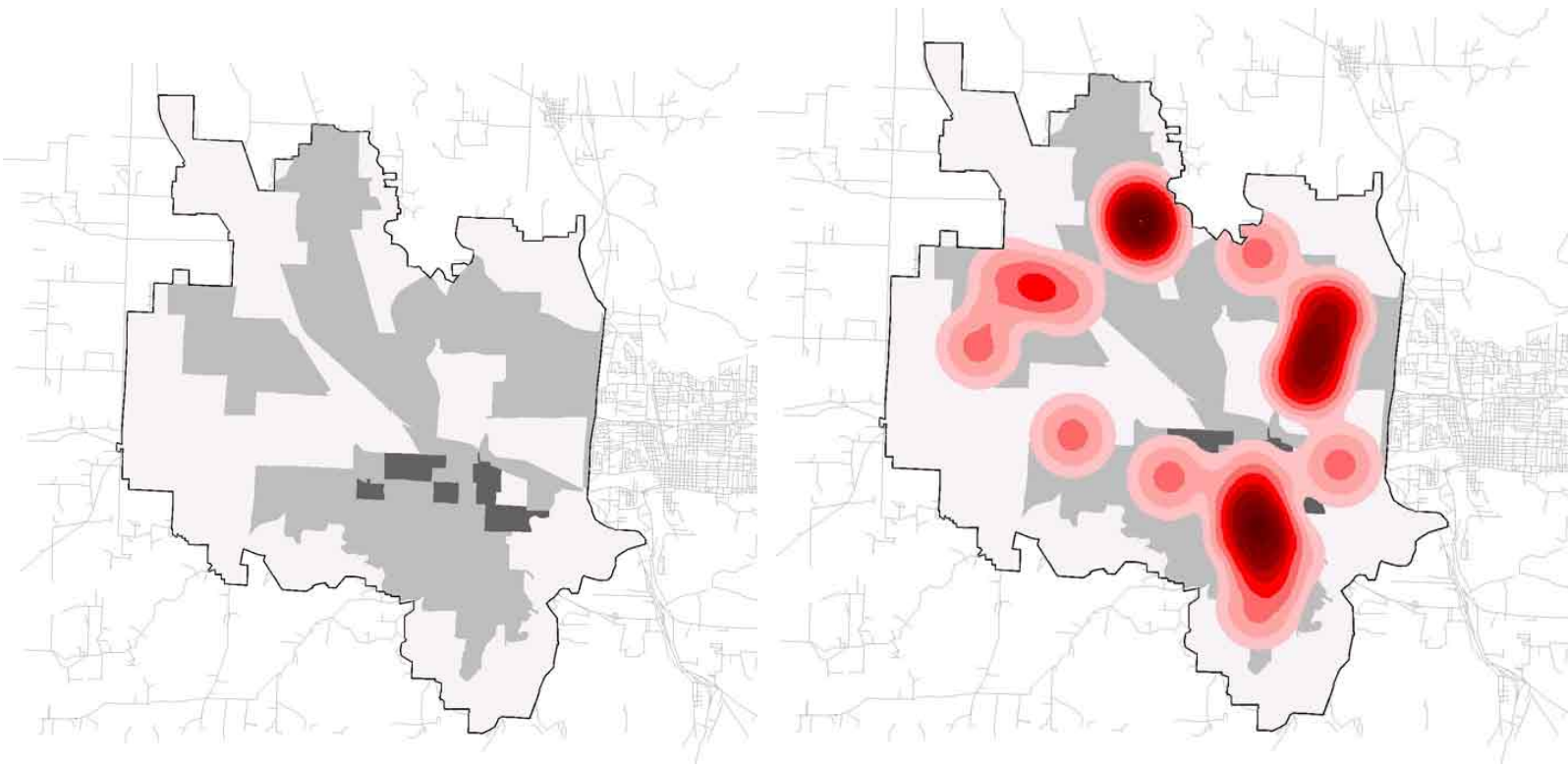


**Figure 4a and b.** Population Density and Population Density with Overlay of Supermarket Accessibility.

The map in Figure 4a represents population density, with the darkest colors representing neighborhoods generally surrounding the University of Oregon - a location with a high density of living in general (for Eugene), but with high concentrations of students in particular. The map on the right overlays the supermarket access map and the population density map in order to identify potential spatial mismatches. While the two sets of data generally align, it is evident that there are a number of neighborhoods of medium population density that are not served well by larger supermarkets. Using maps such as these as a base, a more thorough socio-demographic analysis might be conducted to identify and compare populations that are and are not served with supermarket access.

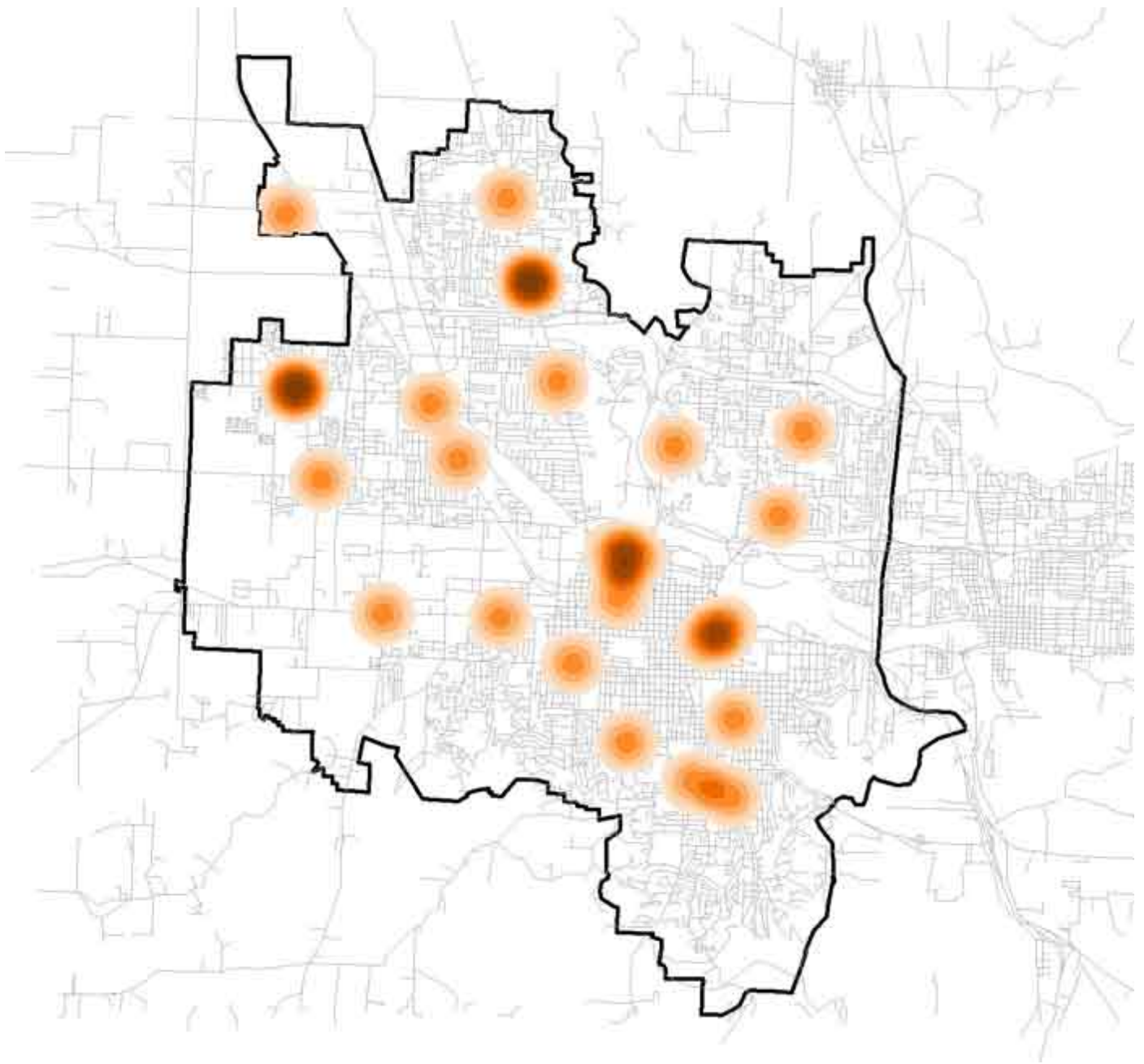


**Figure 5.** Access to Convenience Stores.

The map in Figure 5 shows access to convenience stores. In this case, distances from stores is calculated at a quarter mile - a distance many planners use when thinking about pedestrian accessibility. In this map, there are some areas with concentrations of convenience stores, but in general such stores are relatively isolated from one another and spread throughout the city.

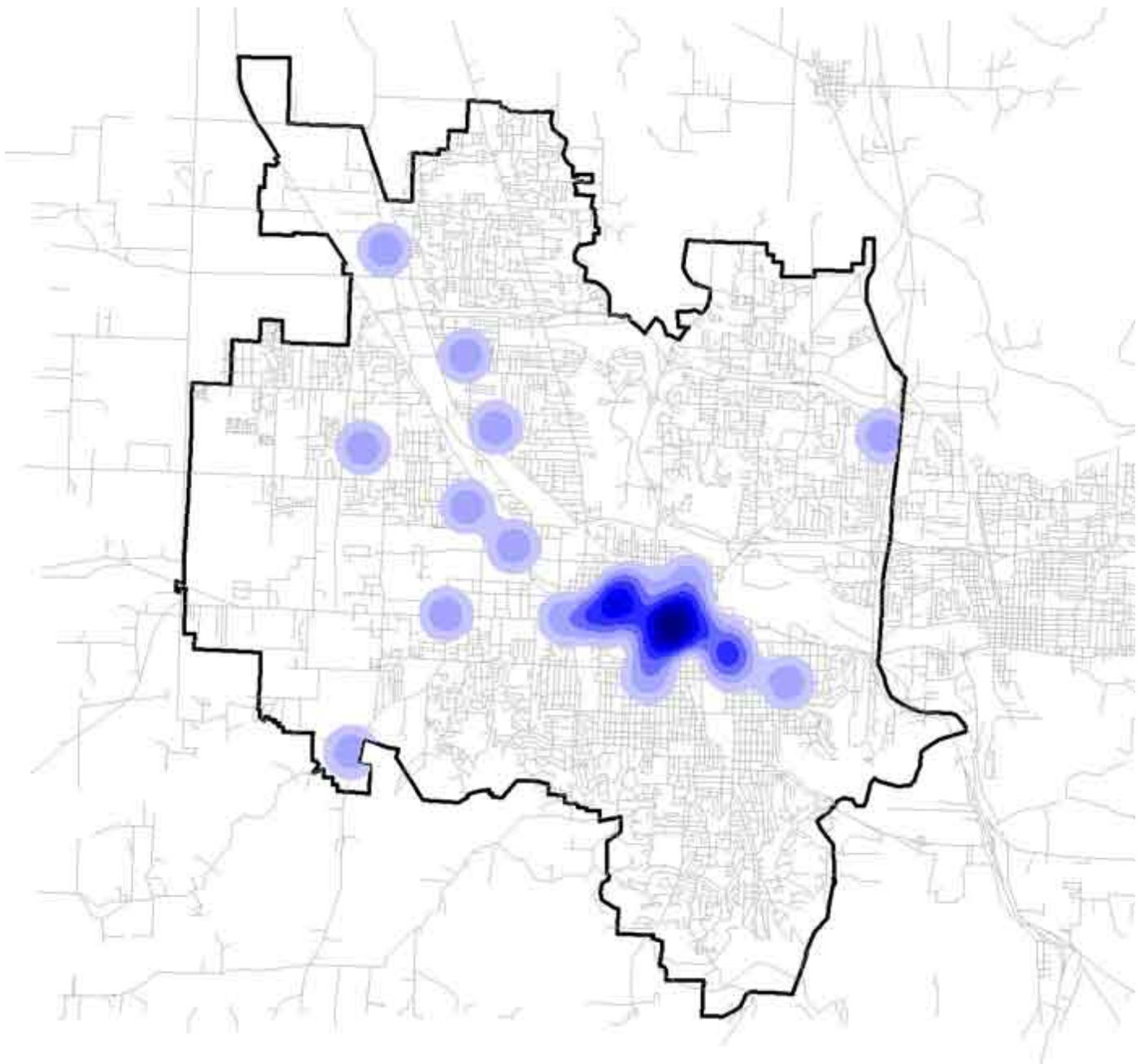


**Figure 6.** Concentration of Neighborhood Food Stores.

The map in Figure 6 shows the spatial concentration of neighborhood food stores (using a 1/4 mile radius from the sites) - perhaps the most important type of establishment in terms of easy, independent access to food. The pattern shows a distinct concentration of neighborhood markets in the center of the city, with isolated stores existing sporadically throughout the rest of the city. Thus, it is clear that one primary neighborhood has an abundance of local neighborhood food choices, while most neighborhoods lack such an option. From a planning perspective, this map (Figure 6) is instructive. If planners want more pedestrian movement to reach essential goods and services, and if neighborhood based food outlets potentially represent the most just form of food distribution (especially for those who by income, age, or impairment cannot drive), then this particular map provides both a troubling image and an opportunity for change. Again, as in Figure 3, the area of most intensity in Figure 6 is an old traditional neighborhood that has been built for a hundred years. Other areas within the city are generally newer, characterized by more suburban development, mini-malls, and opportunities for big-box retailing - including supermarkets. Neighborhood markets, thus, have in essence been zoned out of such areas. Planners and policy makers might use such a map to target land use and zoning policies to encourage pedestrian access to quality foods in currently underserved locations.

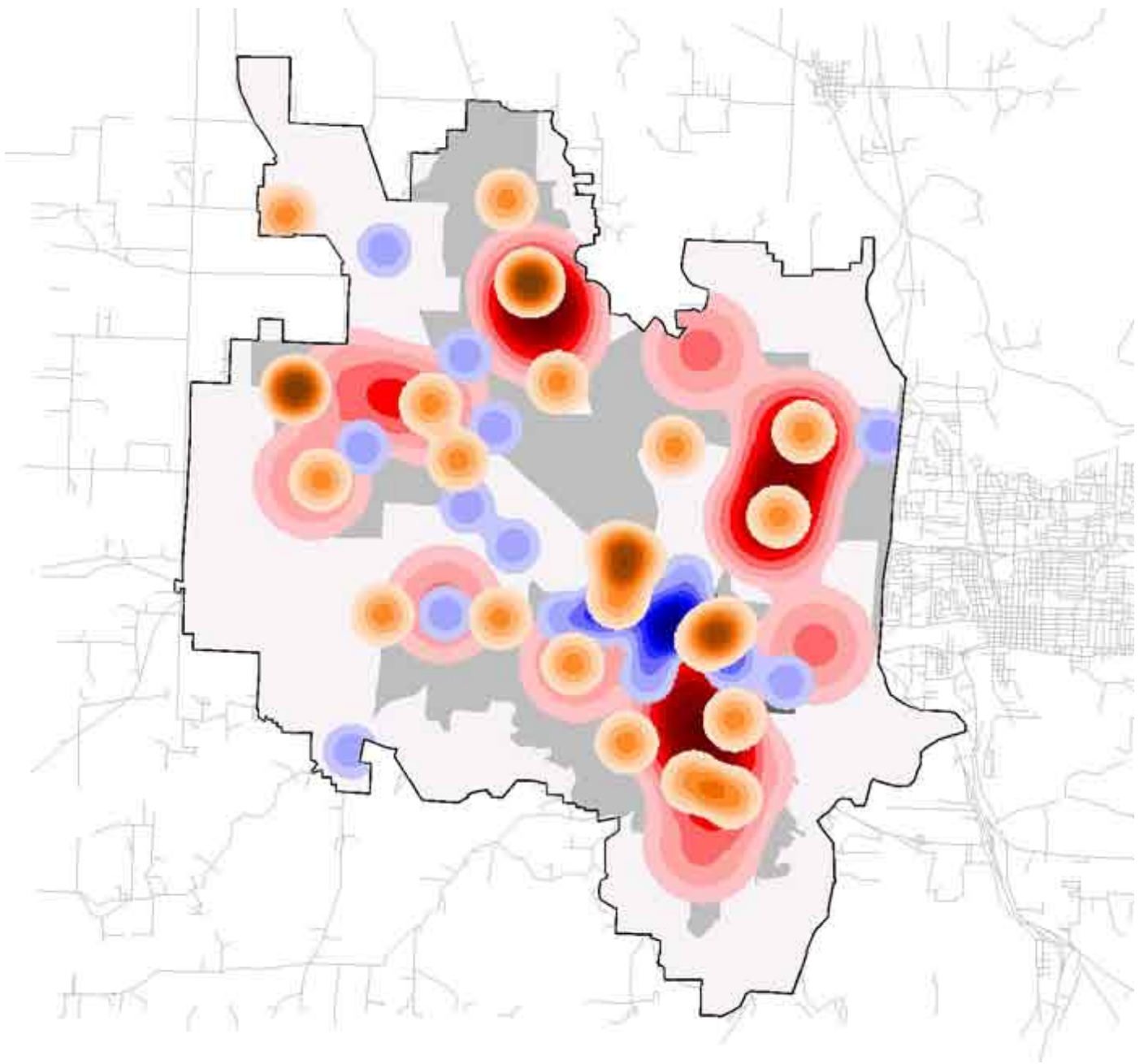


**Figure 7.** Combined Access Pattern.

The map in Figure 7 combines the access maps of the supermarkets, convenience stores, and neighborhood markets, overlaid on the population density map. Thus, one can visualize the pattern of general accessibility to food for residents of Eugene. This map suggests that most Eugene residents have reasonable access to some type of food retail market (independent of type or quality).

Spatial analysis combined with the visualization of food outlets offers planners, community activists, public health officials, and those generally concerned with equitable access to food a means to understand the spatial extent of retail food distribution in their community. Mapping software that interacts with an underlying database (Geographic Information System, GIS, software) can provide a powerful tool for facilitating the community dialogue that will be necessary to enhance food security in communities across the country; these maps represent one approach to moving that dialogue forward.

## References

Bernick, M. and R. Cervero (1997). *Transit Villages in the 21st Century*. New York, McGraw-Hill.

Campbell, M. C. (2004). "Building a Common Table: The Role for Planning in Community Food Systems." *Journal of Planning Education and Research* 23(4): 341-355.

Clifton, K. J. (2004). "Mobility Strategies and Food Shopping for Low-Income Families: A Case Study." *Journal of Planning Education and Research* 23(4): 402-413.

Handy, S. and University of California (System) Transportation Center (1995). Regional versus local accessibility : neo-traditional development and its implications for non-work travel. Berkeley, University of California Transportation Center.

Krizek, K. J. (2003). "Residential Relocation and Changes in Urban Travel: Does Neighborhood-Scale Urban Form Matter?" *Journal of the American Planning Association* 69(3): 265-281.

Pothukuchi, K. (2004). "Community Food Assessment: A First Step in Planning for Community Food Security." *Journal of Planning Education and Research* 23(4): 356-377.

## Related Credits and Issues

- Software: ESRI ArcView 3.2, ESRI Spatial Analyst
- Maps used for Food for Lane County: Figures 2, 3, 5, and 6 - note that the maps for the nonprofit were formatted slightly differently (in a more traditional layout with titles and scale bars and such). Also, the maps were not commissioned by the nonprofit; they were a public service done for their food summit. There are no ownership issues with the images.
- Food site data: derived from Yahoo! yellow pages
- Street and city boundary data: Lane Council of Governments
- Projection: 1927 State Plane, Oregon South

---

---

*Solstice: An Electronic Journal of Geography and Mathematics, Institute of Mathematical Geography, Ann Arbor, Michigan.*  
Volume XV, Number 1.

<http://www.InstituteOfMathematicalGeography.org/>

---

---



**Figure 1:** Snow waves site 1, view east.



**Figure 2:** Snow waves site 1, beginning of experiment at 9:15 LT, 20 Feb. 2004.

---

## Energy Flow: Spatial and Temporal Patterns

Peter A. Martin\*

Department of Geography  
Oregon State University

---

### INTRODUCTION

"The flow of energy through a system tends to organize that system" (Fuller, 1). This organization reveals itself by the appearance and propagation of spatial and temporal patterns on the system surface. For example, stream flow may separate and distribute alluvium according to its density. Wind blowing over featureless water may engender a rich field of periodicity in waves and aligned streaks of foam. A more prosaic example of "organization" arises in the generation of washboard on an unpaved road with the passage of traffic.

The tendency toward organization or pattern seems to be "in the cards" (see, eg. 2), and operates across a great range of scales (see, eg., 3), which may account for the fractal, or scale-wise self-similar, character of nature. We suggest that, by adopting the expectation that organization should accompany the flow of energy, one might anticipate the discovery of patterns; moreover, one might conversely take patterns to be the evidence of the flow of energy, and look for other accompanying patterns.

### DISCUSSION OF OBSERVATION AND EXPERIMENT

The case-in-point flow of energy here is the



**Figure 3:** Snow waves site 2, view west.



**Figure 4:** Snow waves site 2, beginning of experiment at 9:15 LT, 20 Feb. 2004.

waxing insolation as we move from winter solstice toward summer solstice. The observed pattern was that of waves in the surface of melting snow. The wave crests tended to be aligned roughly east-west, amplitude of the order 1cm, wavelength of the order 10cm. The conjecture was that these waves might be driven by the sun, and that they might be propagating northward because of their self-effect: intensified melting on their south faces, and protection of their north faces by their own aspect. (This propagation would be an accompanying pattern not immediately apparent to the senses because of the temporal scale.)

To gauge possible wave propagation, two 1/8" wood dowels were stuck through each of two waves and into the earth below, one at a crest and one at an adjacent trough. (See Figures 1-4.) The relative positions of the waves and dowels were observed 24 hours later. (See Figures 5-6.)

Advancement of the snow waves was apparent in both cases. The propagation was more apparent with reference to the crests than with reference to the troughs, but amounted to approximately 3cm in both cases. The snow depth at the time the dowels were placed (9:15 local time) was approximately 23cm, and the snow depth at the second observation, 24 hours later, was approximately 20cm. It was apparent that the presence of the dowels induced increased melting (so that the dowels did not remain perfectly upright). The effect of the dowels on the snow waves was small.

## CONCLUSION

This rather whimsical research experiment arose because of the flow of information (which is



**Figure 5:** Snow waves site 1, after 24 hours, at 9:15 LT, 21 Feb. 2004. The steel ruler is 12 inches long.



**Figure 6:** Snow waves site 2, after 24 hours, at 9:15 LT, 21 Feb. 2004. The steel ruler is 12 inches long.

akin to energy) through a system predisposed by its nature to exhibit organization. That is, the system (the mind of the observer) was predisposed by its nature to exhibit organization, given the flow of information.

More to the point of geography: we might expect that, wherever there is spatial pattern, there might be temporal propagation. Stationary waves are usually associated with resonance, a phenomenon that is characteristic of a bounded system. Further examples of temporal patterns that might be suggested by their accompanying spatial patterns include the advancement of stream meanders, and the spreading of the sea floor.

Readers are invited to speculate on the temporal aspect of the frost pattern shown in Figure 7 (send your comments to co-author Martin, [martinp@geo.orst.edu](mailto:martinp@geo.orst.edu)). The pattern in Figure 7 appeared overnight on the glass face of a closed box approximately 100cm wide by 150cm high and inclined approximately 30 degrees from the horizontal. It was a calm night; one educated guess is that the energy flowing through this system is the heat of fusion of the growing pattern itself, generating exquisitely scaled air currents!

## REFERENCES

1. Fuller, R. Buckminster. 1979. *Synergetics 2: Explorations in the Geometry of Thinking*. New York: Macmillan.
2. Kauffman, Stuart. 1995. *At Home in the Universe: The Search for Laws of Self-organization and Complexity*. New York:



**Figure 7:** Frost pattern on glass surface, dimensions 100cm wide by 150cm high.

Oxford Univ. Press.

3. Stevens, Peter S. 1974. *Patterns in Nature*.  
New York: Dutton.

---

Mr. Martin is working on his Master's Thesis in  
Geography.

**Copyright, Institute of Mathematical Geography and the author, 2004, All rights reserved.**

*Solstice: An Electronic Journal of Geography and Mathematics, Institute of Mathematical Geography, Ann Arbor, Michigan.*

**Volume XV, Number 1.**

<http://www.InstituteOfMathematicalGeography.org/>



## Winter Windows: Ice Largo Photography of Alma S. Lach

Click [here](#) to start music of Antonio Vivaldi, 1678-1741, and listen to the Largo from The Seasons: Winter,

Digital Musician, G. Pollen, midi file downloaded free from The Classical Music Archives.

Minimize the window on top (containing the music player), if one comes up.

Then, as you listen, click on the buttons to the left to enjoy photographic images of nature's winter spectacle.

What do you see in these images? Share your thoughts with the artist:  
[alma@almalach.com](mailto:alma@almalach.com)

File creation: IMAge

Seung-Hoon Han

Spatial Analysis of  
Subway Zones in  
Boston,  
Massachusetts

[Introduction](#)

[Study Area](#)

[Analysis I \(Subway  
Zones\)](#)

[Analysis II \(Points of  
Interest\)](#)

[Analysis III  
\(Downtown Crossing\)](#)

[Resources](#)

# Spatial Analysis of Subway Zones in Boston, Massachusetts

Seung-Hoon Han

Based on material created as a graduate student in Architecture, The University of Michigan. The author's undergraduate degree is from Harvard College.

---

**In this article, the graphics tell the story; please be sure to click on images when asked to do so!**

---

## Abstract

This project creates an information system offering pedestrians in Boston a way to use the web to consider what is near the Boston Subway (MBTA). Geographic Information Systems' (GIS) software (from ESRI) and web presentation tools were used to visualize points of interest and demographics within 0.5 and 1 mile buffer zones of the MBTA. At a deeper level, proximity to the Boston Subway is used to create zones within which U.S. Census data is employed to consider housing patterns in relation to ethnic groups. The evidence of maps from this latter activity may help to guide further research on a variety of frontiers.

Demographic data for this study was acquired from the U.S. Bureau of Census's TIGER files. These data come in a format easily downloaded as shape files for ArcView from the ESRI Web pages (<http://www.esri.com/>).

Data on subway systems and facility locations (points of interest) were retrieved from the MBTA (Massachusetts Bay Transportation Authority) pages on the Web (<http://www.mbtta.com/>). The author created datasets to be extracted into street layers for a geo-matching process. The material in this article is based on a website prepared by the author as a student in Urban Planning 507, The University of Michigan, January through April, 2001, at which time animated maps were quite unusual. Some of the author's other efforts at that time involved experiments in the use of ColdFusion to make clickable maps. His continuing interests in

both architecture and urban planning involve employing state-of-the-art technology.

---

## SUBWAY ZONES IN BOSTON, MASSACHUSETTS / ABSTRACT

The author wishes to thank the Editor and an Anonymous Reviewer for constructive comments and editorial help.

## A Golfer's Resource: Huron Hills Golf Course, Ann Arbor, Michigan

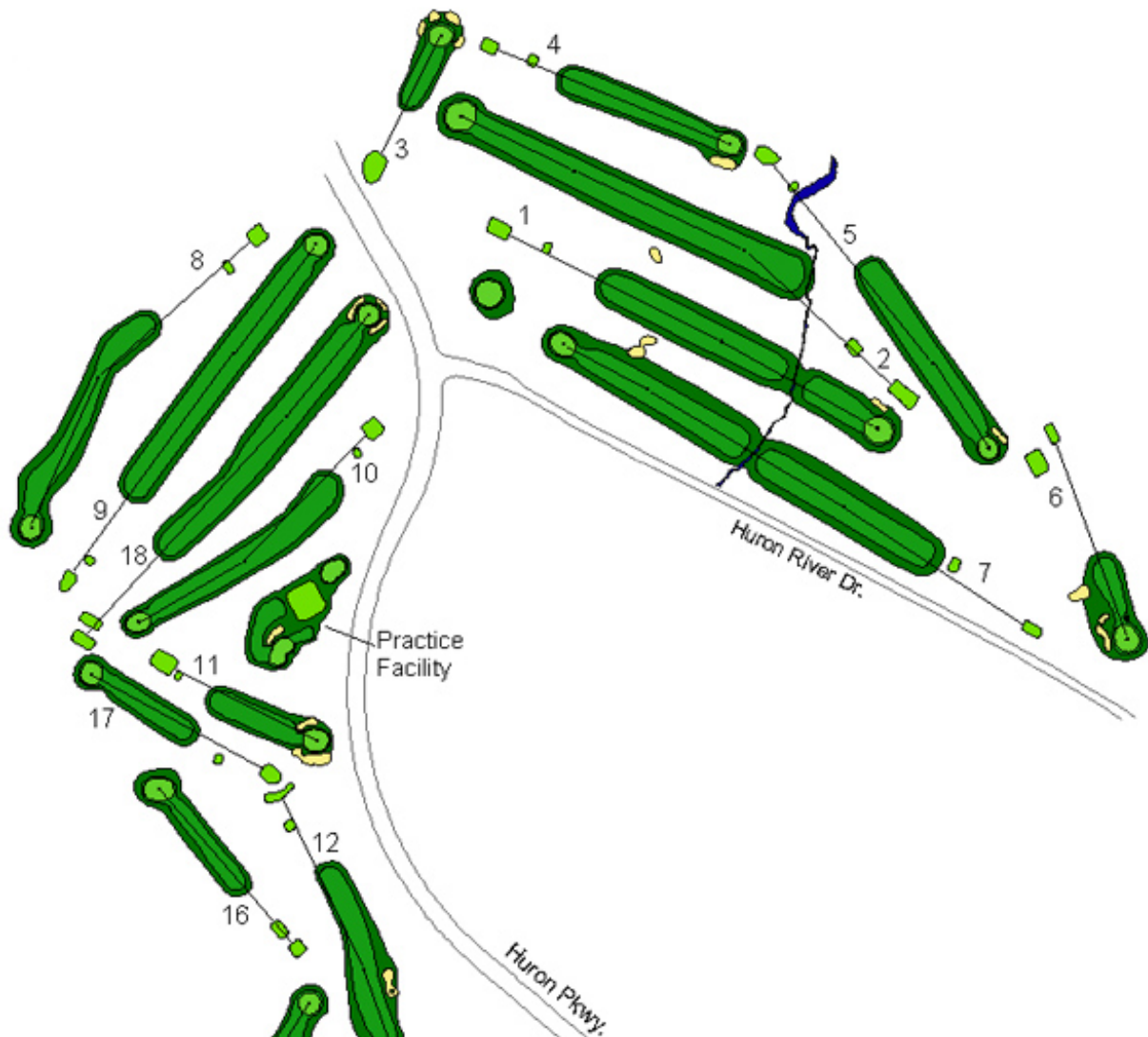
Andrew Walton, B.A. May, 2004

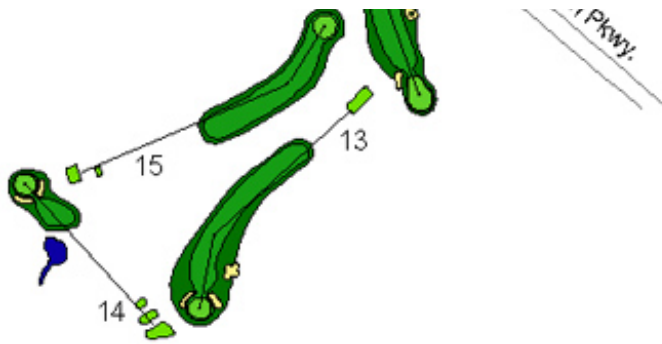
The University of Michigan

Huron Hills golf course is a [City of Ann Arbor](#) public course. It is located partially on the floodplain of the Huron River and partially on the slopes leading from that valley to nearby residential areas. The slopes are heavily wooded. Those familiar with Ann Arbor know it from seeing it on the south side of the Huron River as they travel north on Huron Parkway. The course was established in 1922 and the original architect was Thomas Bendelow.

The following virtual links offer a tour of the golf course "links." Study the photographic evidence (obtained by the author in the Fall of 2003; photographs retouched, where necessary, in Adobe Photoshop 7.0) of the course prior to play; get advice on each hole from the author, the City of Ann Arbor Men's Champion in 2002 and member of The University of Michigan golf team [Ed.]. Small photographs are linked to larger ones; click on the small photograph to link to a larger version of the same image.

The map below, digitized by the author in ArcView GIS (version 3.2, ESRI trademark) from City of Ann Arbor aeriels and from field evidence, shows the pattern and shape of elements of the golf course far more accurately than does the cover on the [linked scorecard](#). Click on part of this map to begin your tour. It serves as a visual table of content to the course. Click on individual holes for more information.





This [linked](#) image of the course has hung in the course clubhouse for many years. This image of Huron Hills is outdated and also has errors regarding course elements. A new wall-sized course map, derived from the clickable image above, now hangs in the clubhouse. One advantage to having a computerized image is that it is easy to change as the golf course changes. The old can be merged with the new, as in this [link](#).

Much of the beauty and the challenge of this course comes from its rolling surface. This [linked](#) image, a Triangulated Irregular Network (TIN), represents the topographic surface on which the Huron Hills course sits (it was made using the City contour map as a base in ESRI software). The white lines in the image represent the roads in the area. The roads serve as a guide in placing the golf course within this picture. The contour of the golf course is undulating, especially the back nine, (the lower left corner). The change in color signifies a change in elevation of 15 feet.

Images that are TINs are useful as a base over which to drape other images. The next [linked](#) image was made by extruding the TIN in 3D Analyst Extension to ArcView GIS (ESRI trademark), draping the City aerial flown in 2002 over the TIN, and finally superimposing the GIS layers from the map above in order to show location of golf course holes in relation both to the topography and to the broader urban setting depicted in the aerial. The final [link](#) shows an animation of this draped image, from various vantage points (click the reload button to restart the animation). The golfer thus has a bird's eye view of the terrain as well as the capability to fly over it in a circle and study the lay of the land from various angles.

**Software used:** ESRI: ArcView GIS, v. 3.2, Spatial Analyst Extension, and 3D Analyst Extension; Macromedia, Dreamweaver MX; Adobe Photoshop 7.0 and ImageReady 7.0.

**Acknowledgement:** Thanks to Merle Johnson of the City of Ann Arbor for supplying aerials and base maps of the region of this study. Also to Colin Smith, Facility Supervisor of [Huron Hills Golf Course](#), City of Ann Arbor Parks and Recreation Department.

**Editor's note:** Mr. Walton will be leaving for Scotland, to study for an advanced degree in [golf course architecture](#): an MSc, School of Landscape Architecture, Edinburgh School of Art, Heriot-Watt University, Edinburgh, Scotland. Look for golf courses designed by Andrew Walton, in the future!

---

## Mail

---

Regarding your siren location web material, there is some work in this area that may be of interest:  
Current, John and Morton O'Kelly. 1992. "Locating emergency warning sirens." *Decision Sciences*, 23, 221-234.

Murray, Alan T. and Morton E. O'Kelly. 2002. "Assessing representation error in point-based coverage modeling." *Journal of Geographical Systems*, 4, 171-191.

...

Regards,  
Alan Murray

---

From Marc Schlossberg:

...I have 2 web sites for you:

1. <http://www.fundrace.org/index.html> - this is a geographic-based query and some mapping) of campaign contributions.
2. [www.keyhole.com](http://www.keyhole.com) - you MUST download the trial software of this !!!!! 3D global, high resolution exploration of the entire earth. Expect to waste every minute of the 7 day trial playing with this program and showing it to others. If you haven't seen it, you have to check it out !

---

Quoting "Antonakos, Cathy (Ann Arbor)" <Cathy.Antonakos@med.va.gov>:

Sandy, I heard the sirens last night. I had taken a look at your siren map (Solstice?) and realized I was previously in a spot where they could not be heard! Lo and behold, I was thinking of you and John last night, and how much I have appreciated both of you -- how much I have learned from you. I am so much more fortunate than others who have not had such good mentors. And then -- the sirens went off!! I thought you would like to know that not only did your study provide evidence that they could be heard, but now an Ann Arbor resident is saying so!

---

Quoting Frank Witlox:

By the way, I very much liked your paper on the Christaller networks (the spatial synthesis sampler). It is always difficult to explain to students how the  $k=3$ ,  $k=4$  and especially  $k=7$  works. Now I have the

solution: point to your paper in Solstice.

---

---

idle thinking: "snail mail" = "escargot-to-go" [ed.]

---